SYNTHESIS, CHARACTERIZATION AND BIOLOGICAL ACTIVITY OF SOME CLUSTER AND MONONUCLEAR OSMIUM COMPLEXES WITH P- DONOR LIGANDS

by

JUBREY MOSIMA MONARENG

Submitted in accordance with the requirements for
the degree of

MASTER OF SCIENCE

In the subject

CHEMISTRY

At the

University of South Africa

Supervisor: Dr. H. S Clayton

February 2017

DECLARATION

Student number: 44173083

I, Jubrey Mosima Monareng, declare that "**SYNTHESIS, CHARACTERIZATION AND BIOLOGICAL ACTIVITY OF SOME CLUSTER AND MONONUCLEAR OSMIUM COMPLEXES WITH P-DONOR LIGANDS**" is my own work and that all sources that I have used or quoted have been indicated and acknowledged by means of complete references.

_____ _____

SIGNATURE DATE

(Miss)

CONFERENCES

Osmium carbonyl complexes: Synthesis, Characterization and potential application in medicinal chemistry.

J. M Monareng and H. S Clayton

2015 SACI Convention

DEDICATIONS

This dissertation is dedicated to my beloved late grandparents. Thank you for being the best. Miss you always. To my parents (Anna and Jan Monareng), not only did they give me life but they instilled in me the values of kindness, generosity, hard work and self-respect. I love you to bits. A special thanks to my uncles (Mante Lechokgotha, David Lechokgotha and Hector Molele) whom have supported me throughout my undergraduate and being my rock when I needed them. To them I will forever be grateful. I would like to express my deepest gratitude to Jomey and Willie Dreyer for their unwavering support and guidance over the years.

ABSTRACT

Routes to mononuclear Os(II) and Os(0) cluster complexes containing P-donor ligands (PR_3, P–P) were studied using the osmium salts $Y_2[OsX_6]$ (Y = NH_4, K; X = Cl, Br, I) as precursors.

Carbonylation of the precursors and then subsequent reaction with tertiary phosphines afford neutral complexes of the type *cis*,*cis*,*trans*-$[OsX_2(CO)_2(PR_3)_2]$ (X = Cl, Br, I, PR_3 = tertiary phosphine), which were characterized by combination of infrared and Raman spectroscopy, NMR (^1H, ^{13}C, ^{31}P) spectroscopy and elemental analysis. The compounds *cis*,*cis*,*trans*-$[OsBr_2(CO)_2\{Ph_2P(CH_2C_6H_5)\}_2]$ (**2b**), *cis*,*cis*,*trans*-$[OsBr_2(CO)_2\{P(CH_2C_6H_5)\}_3]$ (**3b**) and *cis*,*cis*,*trans*-$[OsBr_2(CO)_2\{P(C_6H_{11})\}_2]$ (**4b**) have been further characterized by single crystal X-ray diffraction. Thermogravimetric analysis of these complexes shows multiple stages of decomposition that can be directly related to the loss of ligands.

Microwave-promoted reaction of the osmium salt precursor with bidentate phosphine ligands affords the neutral complexes $[OsX_2(P–P)_2]$ (X = Cl, Br, I; P–P = bidentate phosphine ligand). A stepwise substitution pathway has been suggested resulting in the formation of compounds *cis*/*trans*-$[OsX_2(P–P)_2]$ in which the ligands display different reactivity. The size of the bidentate phosphine ligand determines the stereochemistry of the product complex. Reaction with short ligands such as dppm selectively yield the *cis*-$[OsX_2(P–P)_2]$ isomers. Whilst reaction with dppe and dppp under the same conditions gives the *trans*-$[OsX_2(P–P)_2]$ isomers. Steric bulkiness of the ligands influences the stereochemistry. The *cis*-$[OsX_2(P–P)_2]$ isomers are thermally stable with onset of decomposition at temperatures above 300 °C. In contrast, the *trans*-$[OsX_2(P–P)_2]$ isomers were found to be thermally less stable and found to decompose in the range 195 – 251 °C.

Microwave irradiation of $[Os_3(CO)_{12}]$ in the presence of PPh_3 in acetonitrile solution gave a mixture of disubstituted and trisubstituted phosphine cluster complexes which have been characterized by IR, Raman, ^1H and ^{31}P (where applicable) NMR spectroscopies. Variation of solvents influences substitution and give a mixture of monosubstituted and disubstituted phosphine cluster.

Complexes of the type $[OsX_2(P{-}P)_2]$ exhibited both anticancer and antimicrobial activity. In some instances the activity was comparable to that of the reference drugs. The complexes *cis,cis,trans*-$[OsX_2(CO)_2(PR_3)_2]$ and phosphine substituted derivatives of $[Os_3(CO)_{12}]$ exhibited moderate antibacterial activity against Gram-negative bacterial strains and some fungal strains under study.

Table of Contents

List of figures

List of tables

List of schemes

List of chart

List of abbreviations and symbols

Å	Angstrom
°	Degree
Asym	Asymmetric
COT	1,3,5,7-cyclooctatetraene
DCE	Dichloroethane
DCM	Dichloromethane
dppe	1,2-bis(diphenylphosphino)ethane
dppm	1,1-bis(diphenylphosphino)methane
dppp	1,3-bis(diphenylphosphino)propane
DMSO	Dimethyl sulfoxide
DNA	Deoxyribonucleic acid
FT-IR	Fourier Transform Infrared
IC_{50}	50% of cell growth inhibition
INT	2-(4-iodophenyl)-3-(4-nitrophenyl)-5-phenyl-2H-tetrazolium
K	Kelvin
MIC	Minimum Inhibitory Concentration
MW	Microwave
MTT	3-(4,5-Dimethylthiazol-2-yl)-2,5-diphenyl tetrazolium bromide
NMR	Nuclear Magnetic Resonance
PR_3	Two electron donor tertiary phosphine
P–P	Bidentate phosphine ligand
SRB	Sulforhodamine B
Sym	Symmetric
TGA	Thermogravimetric Analysis
TLC	Thin Layer Chromatography

ACKNOWLEDGEMENTS

I wish to extend my sincere gratitude to my advisor Dr. H. S Clayton for the continuous support, guidance and encouragement throughout of my MSc study and related research, for his immense knowledge, motivation and patience.

Furthermore, I wish to thank other people who have a share in both the progress of this work and in the making of this Thesis.

- Dr B. Van der Westhuisen, lecturer at the University of South Africa and also my mentor, for her assistance and also for the hard questions which motivated me to invest and widen my research.
- Prof A. Lemmerer, University of the Witwatersrand, for data collection and structure determinations (X-ray crystal structures).
- Agricultural Research Council (ARC)- Institute for providing microanalytical service.
- Council for Scientific and Industrial Research (CSIR) for invaluable anticancer assay services.
- Dr. T. Makhafola, University of South Africa, for antimicrobial assay services and insightful knowledge.
- My family and friends for supporting me spiritually and emotionally throughout writing this thesis and my life in general.

I would like to acknowledge the Anglo Platinum research laboratories for donating the potassium osmate, without which this Thesis would not have been possible. Also would like to thank the University of South Africa for granting me the opportunity to undertake my investigations at their research laboratories. The financial assistance of the National Research Foundation (NRF) towards this research is hereby acknowledged. Opinions expressed and conclusions arrived at, are those of the author and are not necessarily to be attributed to the NRF

Chapter 1

General introduction

1.1 Bioinorganic chemistry

Bioinorganic chemistry describes the role of inorganic substances in biological systems. This field encompasses a variety of disciplines including inorganic chemistry, biochemistry, molecular biology and medicine. Bioinorganic chemistry includes the study of both naturally occurring as well as synthetically introduced transition metals in medicine. Natural bioinorganic molecules include urease, an enzyme that catalyses the hydrolysis of urea to carbon monoxide and ammonia. Based on the X-ray crystal structure of this enzyme, the active centre contains two nickel ions.[1,2] Metal ions play a vital role in various biological processes. Some of the complexes are particular on the type of metal and a specific oxidation state to execute the necessary catalytic function.

Vitamin B_{12}, also called cobalamin, and its coenzymes are naturally occuring cobalt-containing compounds (Figure 1.1). Cobalamin is involved in the metabolism of every cell of the human body and plays a key role in processes such as fatty acid and amino acid metabolism.[3] In many biological reactions metal ions are often found at the catalytic centre (active site) of enzymes. The metal ion can modify electron flow in a substrate or enzyme, thus effectively controlling an enzyme-catalyzed reaction. Many biological reactions involve water and examples of hydrolase enzymes are metallophosphatases and metalloproteinases which catalyse hydrolysis reactions.

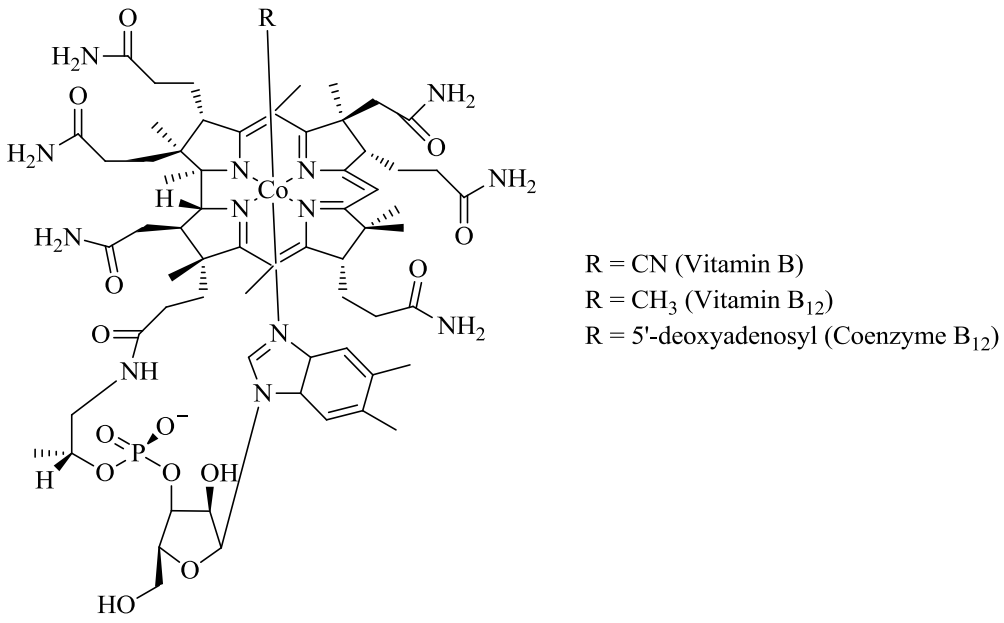

Figure 1.1: Chemical structure of Vitamin B_{12} and related compounds.

Inorganic compounds have been used in medicine, for treatment of various diseases and ailments for centuries. Introduction of metals into biological systems may be either for diagnostic or therapeutic purposes, although in many cases the two overlap. As early as 1910 Paul Ehrlich reported on the use of metals in medicine. He introduced the organoarsenic compound 3-amino-4-hydroxyphenylarsenic(I) (Salvarsan) for treatment of syphilis, a disease caused by the spirochaete bacterium *Treponema pallidum*. This work demonstrated the relevance of the use of metals in medicine.[4] Rosenberg's discovery of the anticancer activity of *Cisplatin*,[5] *cis*-$[PtCl_2(NH_3)_2]$ in 1965, further fuelled interest in using transition metals in medicine.

Bioinorganic complexes have found application in a wide variety of areas namely, photodynamic therapy, biocatalysis and pharmaceuticals.[6-8] The work in this thesis involves the application of bioinorganic compounds as pharmaceuticals, particularly as anticancer and antimicrobial agents.

1.2 Bioinorganic compounds in pharmaceuticals

Various bioinorganic complexes have been explored as pharmaceuticals that include antibacterial, antifungal and anticancer drugs. Metal complexes have properties that tend to offer advantages over organic molecules. The complexes diverse coordination numbers as well as coordination geometries offer novel mechanisms of action not available to organic compounds.

1.2.1 Bioinorganic complexes as antibacterial agents

Bioinorganic compounds have shown a lot of success in the area of antimicrobial drugs. The growing interest in inorganic compounds is owed to increasing resistance of the pathogens against organic drugs. The accidental discovery of Penicillin (Figure 1.2) by Alexander Fleming in 1928 marked the beginning of antimicrobial research, although clinical use of penicillin was only later reported in the 1940s.[9] Within a few years of therapeutic use there were reports on resistance against these organic antibiotics.[10]

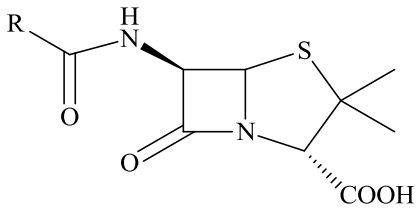

Figure 1.2: Penicillin, with a β-lactam antibiotic core structure, where R is a variable group.

Meticillin, a β-lactam antibiotic of the penicillin class, was introduced in 1959 to address penicillin-resistance. Again within a few years this β-lactam suffered resistance against the Gram positive bacteria *Staphylococcus aureus*. Over the years this bacterial strain developed multiple-antibiotic resistance against several classes of antibiotics.[11] Another class of

antibiotics such as gentamycin, erythromycin and neomycin were later shown to be susceptible to resistance. The *Staphylococcus aureus* bacterial strain was also reported to develop resistance against a fluoroquinoline antibiotic, ciprofloxacin.[12] To combat the multi-resistance of *Staphylococcus aureus* Vancomycin, a glycopeptides antibiotic that has been used for the past two decades. *Staphylococcus aureus* was also later reported to have developed resistance against this antibiotic.[13] This shows that pathogens routinely develop resistance against purely organic antibiotics. Hence, there is a need to develop new antibiotics with novel modes of action to control virulence of multidrug resistant pathogens.

Combination of an organic moiety and a metal is one of the strategies used in overcoming resistance. The metal can offer a novel mechanism of action not available for a purely organic molecule. A number of papers on the metal modification of organic structures have been reported in literature.[14-17] The majority of these complexes were found to possess higher biological activity than the parent organic drug. An example includes the antimalarial candidate Ferroquine, a derivative of chloroquine (Scheme 1.1). Ferroquine has been reported to overcome chloroquine-resistance against *Plasmodium falciparum* (Dd2).[15]

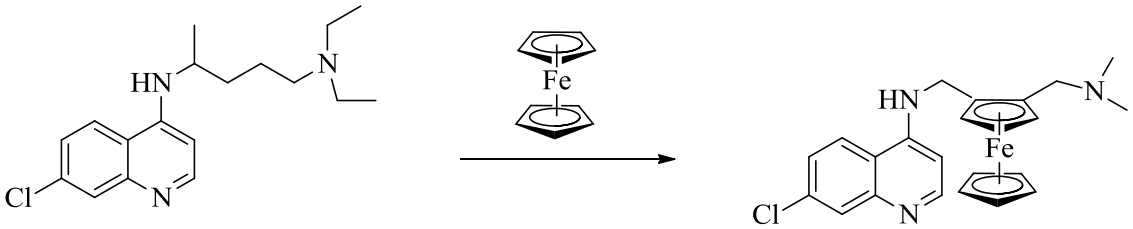

Chloroquine Ferroquine

Scheme 1.1: Synthesis of Ferroquine.

Similarly, the efficacy of the organic drug Pentamidine has decreased due to increased bacterial resistance. To try and overcome drug resistance the existing antimicrobial drug has been complexed with several different metal centres and activity evaluated against

Leishmania donovani DD8 promastigotes. Of these the organo-iridium derivative, Ir-(COT)-pentamidine alizarin red (Figure 1.3), was found to have a higher therapeutic index than pentamidine against the parasitic disease leishmanias.[17]

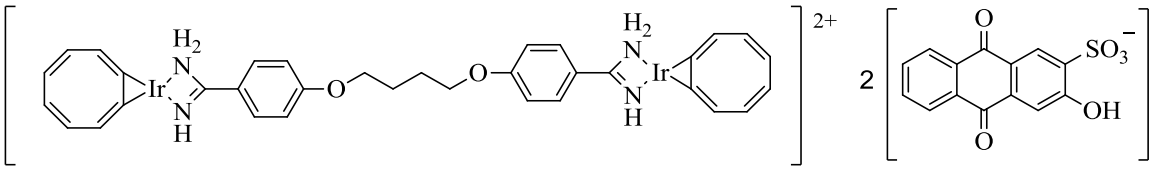

Figure 1.3: Chemical structure of Ir-(COT)pentamidine alizarin red.

Multinuclearity have also shown to be an innovative strategy in improving biological activity with respect to the mononuclear compounds. This is attributed to increased stability, lipophilicity and/or solubility of the organometallic scaffolds. The work by Prof G. Smith and colleagues show the synthesis of dinuclear Ru(II) arene compounds complexed with aryl ether moieties (Scheme 1.2).[18,19] Complexation leads to enhanced synergistic biological effect. The ligands stabilize the metal framework and allow delivery of the intact complex to the pharmacological target. These complexes showed increased inhibitory effects against the human protozoal parasite compared to the dimer as well as the free ligand.

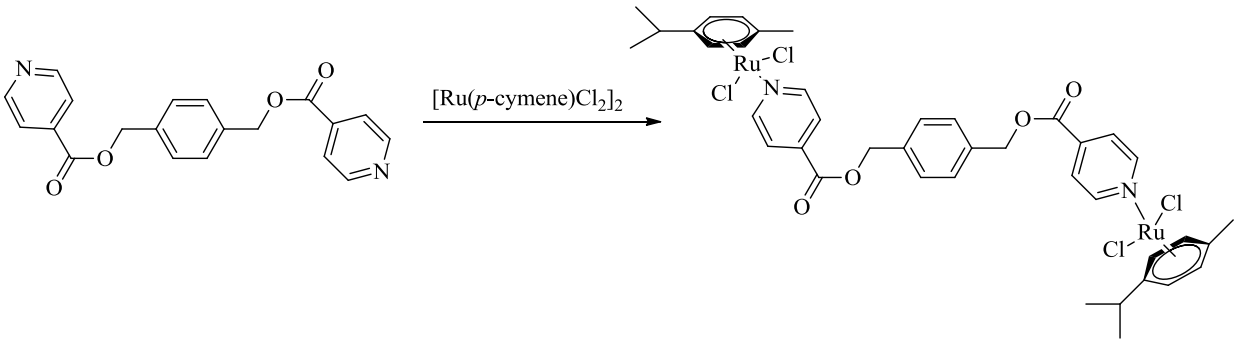

Scheme 1.2: Dinuclear Ru(II) arene complex.

1.2.2 Bioinorganic complexes as antifungal agents

The development of antifungal agents has failed to keep up with that of antibacterial agents. This is a consequence of the distinction between structures of the two organisms involved. Bacteria are prokaryotes and hence offer different structural and metabolic targets different from the host. In contrast, fungi are eukaryotes and as a result most agents toxic to fungi are also toxic to the host. In addition, because fungi generally are slow growing and often in multicellular forms, they are more difficult to quantify than bacteria.

Regardless of these limitations, numerous advances have been made in developing new antifungal agents. Many antifungal agents that are currently in use are organic based and have limitations which include undesirable toxic effects. Continued use of these agents had led to development of drug resistance which leads to failure of the treatment.

To overcome this resistance the organic molecules are modified by incorporating metal ions. Various metal containing antifungal agents have been prepared and the activity evaluated. The silver sulfadiazine, a coordination complex formed by reacting sulfadiazine with inorganic silver salt such as silver nitrate (Scheme 1.2)[20], is an effective antifungal agent. Its activity is owed to combination of both silver and the sulfadiazine. The silver ion is thought to bind to DNA of the organism and the sulphonamide interferes with metabolic pathway of the microbe. This compound is active against *Candida albicans* and *Staphylococcus aureus* strains. Silver sulfadiazine is used as a topical cream to prevent and treat infections among burned patients.[21]

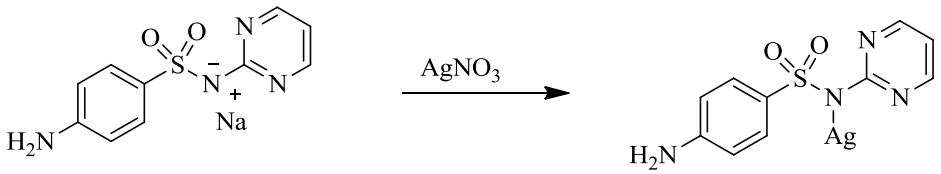

Scheme 1.3: Preparation of silver sulfadiazine.

Incorporation of metal ions into organic molecule has proved effective in antifungal agents. The Cu(II) and Au(I) complexes of clotrimazole and ketoconazole exhibited higher inhibitory activity than the parent compound against cultures of *Trypanosama cruzi*.[22] The ruthenium clotrimazole complex also showed enhanced efficacy against *Trypanosome cruzi* relative to the ligand.[23] Metal complexes containing a thiadiazine core have been demonstrated to possess antifungal properties. It is well established that the thiadiazine-thione moiety exhibits antifungal activity through the production of isothiocyanate and dithiocarbamic acids.[24]

1.2.3 Bioinorganic complexes as anticancer agents

Although the use of bioinorganic complexes is not limited to anticancer agents, it nonetheless represents the most intensely researched area of application. Examples of metal-based anticancer agents include the platinum compound *Cisplatin* and its derivatives as well as ruthenium and osmium arene complexes and also triosmium carbonyl cluster complexes. These complexes have shown different modes of activity.

1.2.3.1 Cisplatin and related platinum compounds

Cisplatin is a tetracoordinated platinum(II) complex, $[Pt(NH_3)_2Cl_2]$, which adopts a square planar geometry (Scheme 1.3, complex A). This bioinorganic complex is a leading anticancer agent and it is has been shown to derive its antitumour effect by interaction with DNA.[25,26] It

was first synthesized in 1844 by Peyrone[27] yet its anticancer activity was only discovered in the 1960s by Rosenberg and was approved for clinical use in 1978.[8]

Cisplatin is administered intravenously. The high concentration of chloride in the blood prevents activation of the complex and it remains intact. Intracellular chloride concentration is less than extracellular levels. In the cell the complex is activated with Pt(II)–Cl bond cleavage.[28] One of the two chlorido ligands, in a process called aquation, is cleaved. The lost chlorido ligand is substituted by an aqua ligand forming an active positively charged species $[Pt(NH_3)_2Cl(H_2O)]^+$ (Scheme 1.3, complex B).[29] The active species is then attracted to the negatively charged end of the DNA forming a platinum-DNA adduct (Scheme 1.3, complex D). Complex B, $[Pt(NH_3)_2Cl(H_2O)]^+$, can further be hydrolysed, losing the second chlorido ligand (Scheme 1.3, complex C). The resulting complex reacts with an adjacent base forming a 1,2 intrastrand adduct with DNA (Scheme 1.3, complex E). This DNA-*Cisplatin* adduct can stimulate a variety of cellular responses, such as apoptosis and G2 cell cycle arrest.[30-33] Proteins responsible for replication of DNA cannot recognize the distorted double-strand helix and an attempt to repair the distorted DNA is made. If that is not achieved then a signal is released for apoptosis (programmed cell death) to take place. The activity of the platinum complex is owed to the direct interaction between the platinum(II) ion and DNA.[25,26]

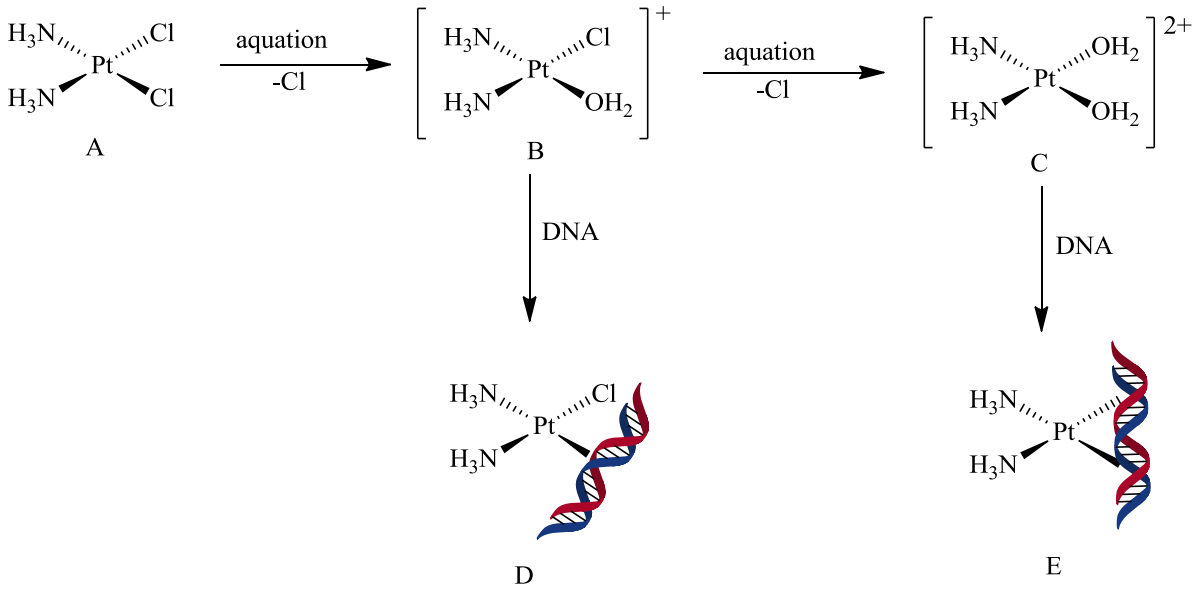

Scheme 1.4: Hydrolysis of *Cisplatin* to form *Cisplatin*-DNA adduct (D and E).[34-35]

Cisplatin has been clinically proven to combat different types of cancers including ovarian, lung, breast, prostate, esophageal, colon, testicular, head and neck as well melanoma cancer.[36] Despite its success, *Cisplatin* suffers from limitations such as major side effects and drug resistance. Its success and drawbacks has stimulated the search for other platinum based compounds with the intention to improve on its therapeutic effect. Thousands analogues of *Cisplatin* were examined and only 13 of these analogues entered clinical trails. From these only a few, *Carboplatin*, *Oxaliplatin*, *Nedaplatin*, *Heptaplatin* and *Lobaplatin*, has been successfully used to treat solid tumours (Chart 1.1).[37]

These platinum complexes suffer from severe side effects and this limits their use in the clinic. Use is also limited in many widespread tumours due to acquired or intrinsic resistance. These limitations inspired research on the design of new non-platinum compounds that are capable of widening the spectrum of activity and avoid platinum's resistance.

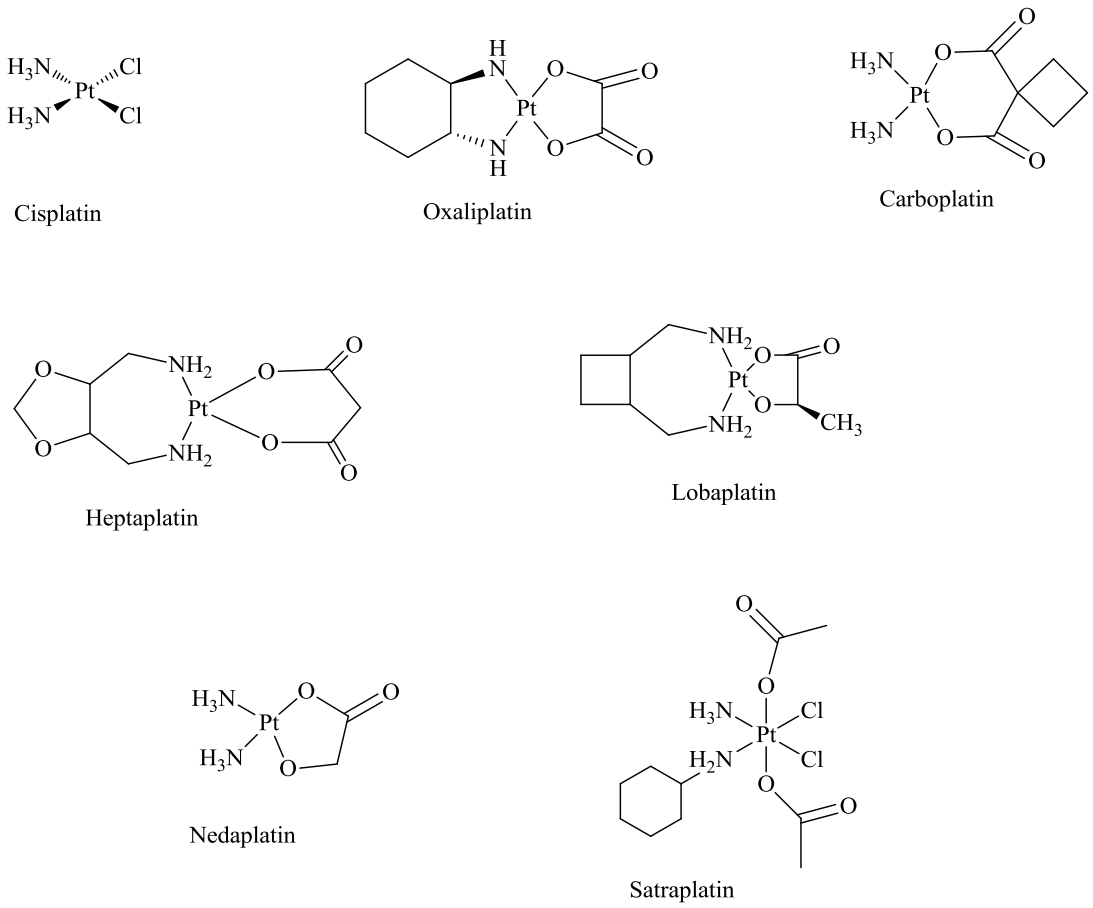

Chart 1.1: Chemical structures of selected platinum drugs.

1.2.3.2 Ruthenium complexes as anticancer agents

Ruthenium complexes possess several favourable chemical properties that indicate it may be a suitable alternative transition metal for anticancer drug design. The non-platinum transition metal complexes offer the following advantages; i) Most Ru complexes adopt an octahedral geometry. Compared to the square planar geometry of the platinum complex, the octahedral complexes offer additional coordination sites; ii) Ru can occur in various oxidation states 2+, 3+ and 4+ under physiological conditions; iii) The rate of ligand exchange is comparable to that of the platinum complexes or can be modified by introduction of ancillary ligands; iv) Ru has the ability to mimic Fe in binging to biomolecules, such as human serum albumin and transferring;[38] v) The Ru complexes have a different mechanism of action compared to the

Pt(II) complexes and this is a result of the difference in geometry between the complexes. Ru complexes predominately form inter-strand crosslinks with DNA as opposed to intra-strand cross links favoured by cisplatin.[39,40] vi) The activation-by-reduction mechanism could also be responsible for the lower general toxicity of some ruthenium containing agents.[41,42] The activation from Ru(III) to Ru(II) requires environments with low oxygen levels and these are obtained in hypoxic tumour cells, because of insufficient formation of new blood vessels and poor blood supply, as opposed to normal cells. vii) Ru complexes have a larger and different spectrum of activity.

Amongst the Ru based pharmaceuticals showing anticancer activity Ru-arene complexes have attracted greatest interest. These complexes have shown stability, water-solubility and exhibit cytotoxicities against a range of cancer cell lines,[43] including *Cisplatin*-resistant cell lines such as the human ovarian cancer cell line A2780.[44,45] The Ru(II) arene complex [(η^6-p-cymene)Ru(en)Cl)]$^+$ exhibits both *in vitro* and *in vivo* activity comparable to that of *Carboplatin*.[46,47] Similar to *Cisplatin* the Ru(II)-arene complexes selectively target specific DNA bases forming monofunctional DNA adducts.[47] When bearing an extended arene ligand such as dihydroanthracene and biphenyl DNA intercalation is a possibility.

Several ruthenium arene phosphaadamantane (RAPTA) complexes, another family of Ru(II)-arene complexes, have been reported to exhibit cytotoxicity. In aqueous solution the RAPTA complexes hydrolyses like *Cisplatin*, forming the activated aqua form of the RAPTA complex, [Ru(η^6-arene)Cl(H_2O)(PTA)]$^+$ (Scheme 1.4).[48-50] Some of the RAPTA complexes have been shown to exhibit antimetastatic activity and others were proven to exert their activity by a DNA binding mechanism.[51,52]

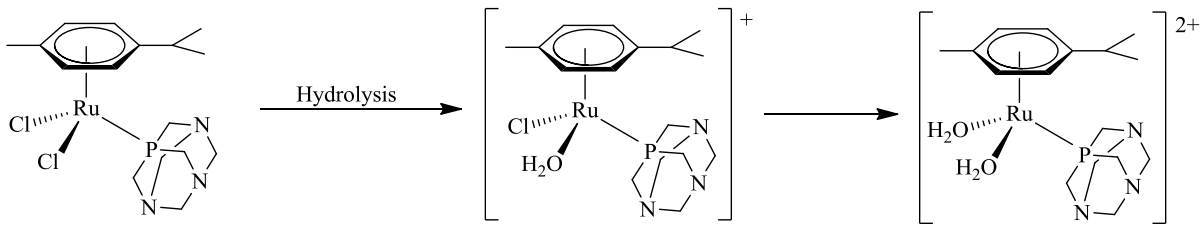

Scheme 1.5 : Activation of Ru(II)–Cl in RAPTA complexes.

Ru(III)-arene complexes have also attracted interest because of their ability to fight against metastatic cancers[53] and their high affinity to imine sites of biomolecules.[54,55] Studies on these complexes show high selectivity for tumour cells and a general low toxicity. Ru(III) complexes currently in clinical trials, include NAMI-A (*trans*-[tetrachloride(dimethylsulfoxide)(1H-imidzole) ruthenate(III)], KP1019 (Ru(III)-arene complexes; Indazolium *trans*-[tetrachloridobis(1H-indazole) ruthenate(III)] and KP1339 (sodium *trans*-[tetrachlorobis(1H-indazole) ruthenate(III)] (Chart 1.2).

These Ru(III) complexes are structurally similar, however, they have a different spectrum of activity. NAMI-A has been found to inhibit the formation of cancer metastases while KP1019 and KP1339 have shown activity against primary tumours by inducing apoptosis.[56,57] Binding of the complex KP1019 to transferrin is thought to be an important step in the activity of this complex. The KP1019 complex initially accumulates in transferrin receptors in tumour cells, where it is reduced to a Ru(II) species.[58] The reduced complex is then released from the protein in endosomes at a lower pH in the presence of biological chelators and binds to nucleotides and DNA triggering an apoptotic process.[59]

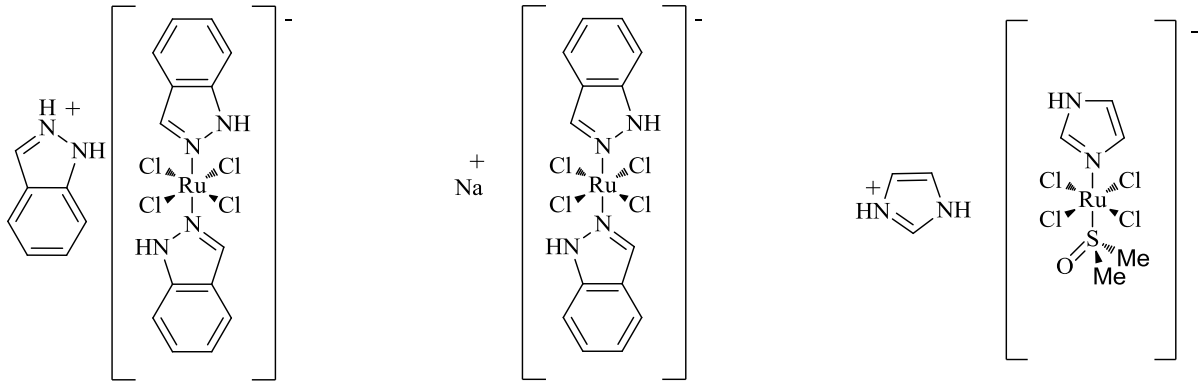

Chart 1.2: Structure of Ru(III) drugs.

NAMI-A has been shown to exhibit anti-angiogenic and anti-invasive properties.[60] Recent studies suggest that the "activation by reduction" hypothesis suggested by previous reseachers is not necessarily the reactivity pathway of the NAMI-A complex.[61] This complex is generally labile at physiological pH and activation is postulated to occur by aquation.[62-64] The aqua ligand is very labile and can be easily lost through subsequent interaction with biomolecules. In addition, recent findings excludes DNA as the primary target for NAMI-A and suggests that proteins in tumour cells are likely to be the primary target for this complex. For many years focus has been directed to the preparation of complexes that could have direct interaction with DNA. However, recent studies on Ru arene complexes suggest that targeting other biomolecules such as proteins could prove to be more effective. These ruthenium compounds have demonstrated a novel mode of action.

1.2.3.3 Osmium complexes as anticancer agents

Osmium complexes are generally more inert towards hydrolysis compared to their ruthenium analogues. Hence, more often osmium complexes are found to be biologically inactive or have a lower activity than ruthenium complexes.[65,66] However, there has been a growing

interest in the development of osmium complexes as anticancer agents. Some of the complexes under study showed promising antiproliferative activity (Chart 1.3).[67-69]

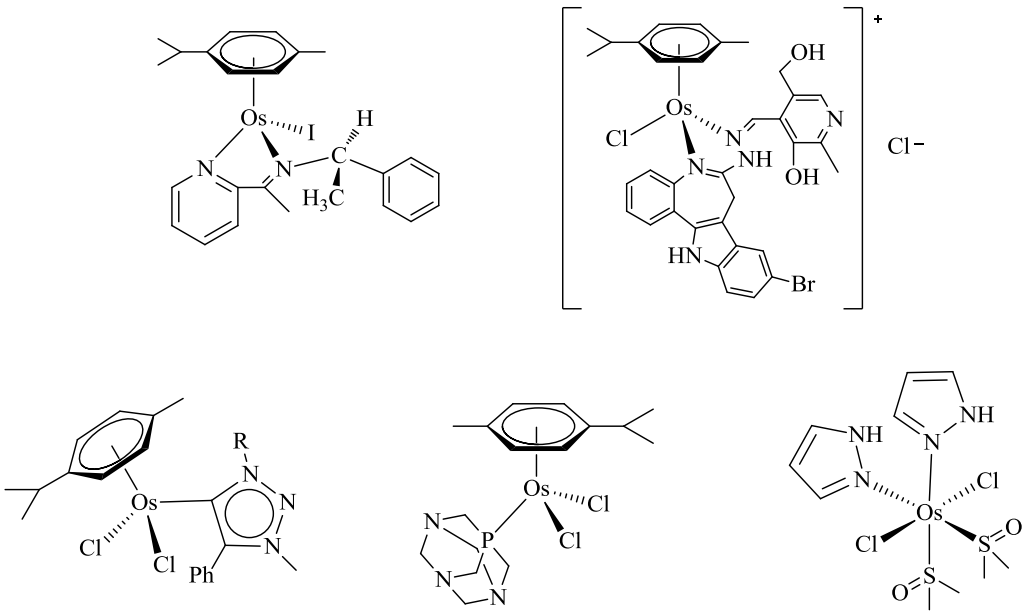

Chart 1.3: Os(II) complexes which exhibit promising anticancer activity.

Osmium offers a number of advantages over its lighter congener, ruthenium;

i. It is a third-row transition metal and its complexes are more inert compared to second and first-row transition metal complexes. For example, the rate of ligand substitution of Pt(II) complexes are commonly *ca*. 5 orders of magnitude slower that those of Pd(II) and similarly Os(II) complexes are generally found to be more inert than their lighter congener Ru(II) complexes.[65,66,70]
ii. Complexes of third row transition metals are generally more stable under physiological conditions,
iii. Accessibility of various oxidation states,
iv. From lower oxidation states stronger π-back donation occurs.

These properties suggest that Os metal complexes are interesting candidates for further investigation as alternative for synthesis of new anticancer agents.

Different approaches for the synthesis of osmium compounds with potential antitumour activity have been investigated. This gave birth to a range of osmium based compounds including mononuclear and multinuclear clusters with a variety of chemical and biological properties.[65,66,71,72] The choice of the type of coordinated ligands and coordination geometry provides an ability to fine-tune the chemical reactivity of complexes, potentially allowing control of pharmacological properties, including cell uptake, distribution, DNA binding, metabolism and toxic side effects.

a) Mononuclear osmium complexes

Investigation of osmium transition metal as potential anticancer agents started with preparation of complexes that are structurally similar to Ru complexes of known anticancer activity. Osmium analogues of NAMI-A, KP1019 and KP1339 were prepared and the anticancer activity evaluated. These complexes showed a different mode of activity and were associated with very slow rate of hydrolysis compared to the Ru analogues. However, it was revealed that the rate of hydrolysis can be controlled by choice of ligands.[65,72] The rate of hydrolysis of osmium analogue of NAMI-A was slow compared to the parent and related compounds,[73] however, high cytotoxicity was observed. This suggested that hydrolysis is not an essential prerequisite for biological activity of this class of compounds.[74] The osmium analogue of KP1019 also showed stability in aqueous media, and cytotoxicity similar to the ruthenium analogue.[75]

Various Os(II) analogues of RAPTA complexes have been prepared and their anticancer activity evaluated. Complex [Os(η^6-p-cymene)Cl_2(pta)] (Chart 1.3) showed selectivity towards cancerous cells and exhibited cytotoxicity similar to the Ru analogue.[48] However, the cationic derivative [Os(η^6-p-cymene)Cl_2(pta-Me)]$^+$ showed no selectivity and damaged both normal healthy and cancerous cells. Reactivity studies of osmium analogues of RAPTA compounds with biomolecules have been reported. A combination of theoretical and experimental data revealed that the osmium complexes bind to the DNA oligomer. Unlike *Cisplatin*, these complexes appear to be more specific in their cytotoxicity toward cancer cells relative to the healthy cells. This suggest a different binding mode is in operation or there is a different biological target for these class of complexes.[76]

b) Osmium carbonyl clusters

Organometallic osmium clusters have also shown potential as antitumour agents.[77,78] The estrogen receptor (ER) –dependent MCF-7 and ER-independent MDA-MB-231 breast cancer cell lines were treated with a series of triosmium carbonyl cluster complexes of the type [$Os_3(CO)_{12-n}(L)_n$] and their protonated analogues (L = nitriles, maltol, triphenylphosphine) and results show that the cytotoxicity of the complexes were strongly dependent on the type of coordinated ligands and solubility. Complexes containing labile ligands were significantly more active compared with complexes with nonlabile ligands.[79] The [$Os_3(CO)_{10}(CNMe)_2$] cluster has been reported to disrupt the normal functions of the cell by causing disruptions of the microtubule morphology.[79,80] It is known that proper dynamics of microtubules are required for normal functioning and therefore, their hyperstabilization by Os clusters leads to cellular dysfunction and apoptosis. This can be explained by loss of the labile CNMe ligand and creation of a vacant coordination site at the metal centre allowing binding to biomolecules.

Cationic clusters showed enhanced activity compared to neutral analogues because of increased solubility and cell permeability. These clusters induce apoptosis and exhibit cytotoxicity in the micromolar range with selectivity for cancerous cells over normal epithelial cells. Studies show the mode of action of these complexes involve biotargets that are different from hormone receptors as the clusters were more potent against an ER-independent cell line compared to ER-dependent cell line. At the molecular level the triosmium clusters interact with both intra and extracellular sulfhydryl groups.[79]

Another approach to combat against cancer is targeting biomolecules other than DNA. The group of Colangelo studied the ability of a series of water-soluble quinoline-triosmium clusters $[(\mu\text{–H})Os_3(CO)_9(L)(\mu_3\text{-}\eta^2\text{-}(Q\text{-H})]$, (where L = $[P(C_6H_4SO_3Na)_3]$ or $[P(OCH_2CH_2NMe_3I)_3]$ and Q = quinoline, 3-aminoquinoline, quinoxaline or phenanthridine) (Chart 1.3) to inhibit telomerase, a crucial enzyme for cancer progression.[77] The quinoline substituent was selected because of its well-known biological properties, especially inhibiting enzymes.[81,82] Among the clusters studied the negatively charged clusters (Chart 1.3 complex **F(i)**-**I(i)** were able to inhibit telomerase activity in the cell-free biochemical assay. However, these clusters were ineffective *in vitro* on Taq, a different DNA polymerase.[77] This suggests that these clusters are selective for telomerase.

The positively charged clusters (**F(ii)**-**I(ii)**) were found to be inactive and no further investigation was carried out on these clusters. These results suggest that the interaction of these clusters to telomerase is electrostatic. In fact, the telomerase is rich in positively charged amino acids, such as lysine and arginine and it was postulated that the negatively charged portion of the clusters interact with these amino acids.[77]

The group of Rosenberg studied the interaction of triosmium clusters with albumin.[83] The water soluble clusters $[Os_3(CO)_9(\mu\text{-}\eta^2\text{-Bz})(\mu\text{-H})L^+]$ (L^+ = $[P(OCH_2CH_2NMe_3)_3I_3]$; Bz = quinoxaline] and its negatively charged analog $[Os_3(CO)_9(\mu\text{-}\eta^2\text{-Bz})(\mu\text{-H})L^-]$ (L^- = $[P(C_6H_4SO_3)_3Na_3]$; Bz = phenanthridine, benzoquinoline, 3-amino quinoline) have been prepared and evaluated. Results show that the negatively charged clusters bind more tightly to albumin compared to their positively charged analogues. It was hypothesised that this could result from electrostatic attraction towards the positively charged amino acid groups of albumin.[83]

Osmium complexes show potential as new anticancer agents and further investigation is necessary. The reactivity of Os complexes is dependent on the coordinated ligand. The choice of the type of coordinated ligands and coordination geometry provides an ability to fine-tune the chemical reactivity of complexes, potentially allowing control of pharmacological properties, including cell uptake, distribution, DNA binding, metabolism and toxic side effects.

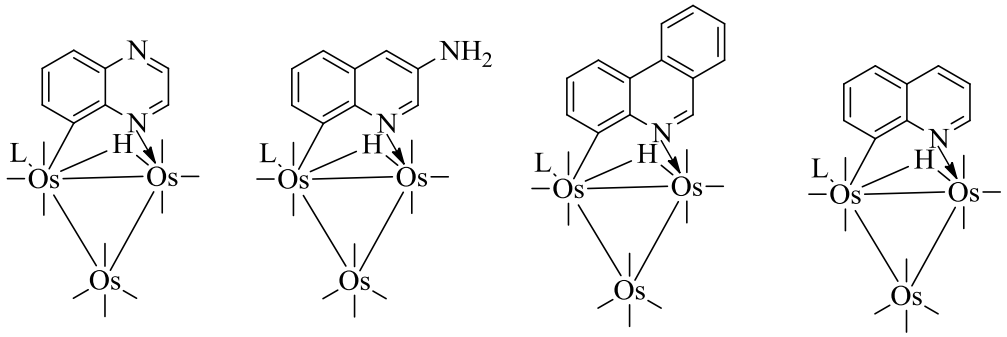

F **G** **H** **I**

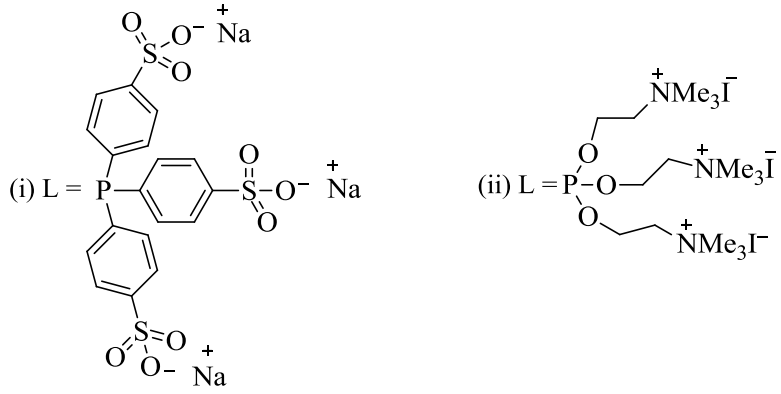

Chart 1.4: Triosmium clusters with potential inhibition of telomerase enzyme.

1.3 Aims and objectives

The overall aim of this project is to investigate aspects of the synthesis, characterization and structural features of osmium-halide complexes coordinated to different P-donor ligands. Furthermore, we will report here the biological activity, anticancer and antimicrobial, of selected complexes.

Specific aims

- Synthesis of osmium carbonyl complexes of the type $[OsX_2(CO)_2(PR_3)_2]$ from stable osmium salts $Y_2[OsX_6]^{2-}$ (Y = NH_4, K; X = Cl, Br, I) using the method demonstrate by Hales and Irving (where PR_3 = triphenylphosphine ($P(C_6H_5)_3$), benzyldiphenylphosphine ($Ph_2P(CH_2C_6H_5)$), tribenzylphosphine ($P(CH_2C_6H_5)_3$), tricyclohexylphosphine.

- Microwave-assisted preparation of coordination complexes of the type $[OsX_2(P–P)_2]$ from osmium salt $Y_2[OsX_6]^{2-}$ (where P–P = dppm, dppe, dppp, dppb).
- Preparation of osmium carbonyl cluster complexes under pressurised CO gas and further substitution using microwave heating to produce substituted cluster complexes of the type $Os_3(CO)_{12-n}(PR_3)_n$ (n = 1 – 3).
- The change in phosphine and halide ligands will address important aspects that will be investigated.
    1. Effect of change in halide and phosphine ligand on the bioactivity of the complex.
    2. Thermal stability of complexes using TGA.
    3. The effect of monodentate ligands vs bidentate ligands on the reactivity and bioactivity of the complexes.

The complexes studied have demonstrated application as catalysts, molecular electronic devices, and use in organic synthesis.[84-87] In contrast, to the best of our knowledge the use of these complexes as pharmaceuticals has remained unexplored. It is thus of interest to investigate the possibility of using these complexes for anticancer and antimicrobial purposes. The scope of the study thus involved the synthesis and characterization of complexes of the type $[OsX_2(CO)_2(PR_3)_2]$, $[OsX_2(P–P)_2]$,$[Os_3(CO)_{11}(P\text{-}P)]$ and $[Os_3(CO)_{12-n}(PR_3)_n]$ (n = 1-3) and exploration of their application as anticancer and antimicrobial agents.

1.4 References

(1) Jabri, E.; Carr, M. B.; Hausinger, R. P.; Karplus, P. A. *Science.* **1995**, *268*, 998.

(2) Karplus, P. A.; Pearson, M. A.; Hausinger, R. P. *Acc. Chem. Res.* **1997**, *30*, 330.

(3) Yamada, K. *Met. Ions. Life. Sci.* **2013**, *13*, 295.

(4) Lloyd, N. C.; Morgan, H. W.; Nicholson, B. K.; Ronimus, R. S. *Angew. Chem. Int. Ed.* **2005**, *44*, 941.

(5) Rosenberg, B.; Van Camp, L.; Krigas, T. *Nature.* **1965**, *205*, 698.

(6) Bown, S. G. *Philos. Trans. R. Soc. A-math. hys. Eng. Sci.* **2013**, *371*, 1.

(7) Yu, S.; Wang, J.; Sledziewski, J.; Madhira, V.; Takahashi, C.; Leon, M.; Dudkina, Y.; Budnikova, Y.; Vicic, D. *Molecules* **2014**, *19*, 13603.

(8) Alderden, R. A.; Hall, M. D.; Hambley, T. W. *J. Chem. Ed.* **2006**, *83*, 728.

(9) Chain, E.; Florey, H. W.; Gardner, A. D.; Heatley, N. G.; Jennings, M. A.; Orr-Ewing, J.; Sanders, A. G. *Lancet* **1940**, *2*, 226.

(10) Kirby, W. M. M. *Science.* **1944**, *99*, 452.

(11) Diep, B. A.; Gill, S. R.; Chang, R. F.; Phan, T., H; Chen, J. H.; Davidson, M. G.; Lin, F.; Lin, J.; Carleton, H. A.; Mongodin, E. F.; Sensabaugh, G. F.; Perdreau-Remington, F. *Lancet.* **2006**, *367*, 731.

(12) Harnett, N.; Brown, S.; Krishnan, C. *Antimicrob. Agents. Chemother.* **1991**, *35*, 1911.

(13) Chaudhary, M.; Anurag, P. *Int. J. Pharmacol. Scie. Rev. Res.* **2015**, *31*, 135.

(14) Hokai, Y.; Jurkowicz, B.; Fernandez-Gallardo, J.; Zakirkhodjaev, N.; Sanau, M.; Muth, T. R.; Contel, M. *J. Inorg. Biochem.* **2014**, *138*, 81.

(15) Wani, W. A.; Jameel, E.; Baig, U.; Mumtazuddin, S.; Hun, L. T. *J. Med. Chem.* **2015**, *101*, 534.

(16) Yeo, C. I.; Sim, J. H.; Khoo, C. H.; Goh, Z. P.; Ang, K. P.; Chea, Y. K.; Fairuz, Z. A.; Halim, S. N. B. A.; Ng, S. W.; Seng, H. L.; Tiekink, E. R. T. *Gold Bull.* **2013**, *46*, 145.

(17) Mbongo, N.; Loiseau, P. M.; Lawrence, F.; Bories, C.; Craciunescu, D. G.; Robert-Gero, M. *Parasitol. Res.* **1997**, *83*, 515.

(18) Chellan, P.; Land, K. M.; Shokar, A.; Au, A.; An, S. H.; Taylor, D.; Smith, P. J.; Chibale, K.; Smith, G. S. *Organometallics* **2013**, *32*, 4793.

(19) Chellan, P.; Land, K. M.; Shokar, A.; Au, A.; An, S. H.; Taylor, D.; Smith, P. J.; Riedel, T.; Dyson, P. J.; Chibale, K.; Smith, G. S. *Dalton Trans.* **2014**, *43*, 513.

(20) Cereser, K. M. *Rev. Bras. Farm.* **1995**, *76*, 58.

(21) Hegazy, A. A.; Sharaf, S. S.; El-Feky, G. S.; El-Shafei, A. *Int. J. Pharm. Pharm. Sci.* **2013**, *5*, 461.

(22) Navarro, M.; Fajardo, E. J.; Lechmann, T.; Delgado, R. A.; Atencio, R.; Silva, P.; Liva, R.; Urbina, J. A. *Inorg. Chem.* **2001**, *40*, 6879.

(23) Sanchez-Delgado, R. A.; Larzardi, K.; Rincon, L.; Urbina, J.; Hubert, A. J.; Noels, A. N. *J. Med. Chem.* **1993**, *36*, 2041.

(24) Rodriguez-Fernandez, E.; Manzano, J. L.; Benito, J. J.; Hermosa, R.; Monte, E.; Criado, J. J. *J. Inorg. Biochem.* **2005**, *99*, 1558.

(25) Fong, C. W. *Free Radical Biology and Medicine* **2016**, *95*, 216.

(26) Kartalou, M.; Essigmann, J. M. *Mutation Research* **2001**, *478*, 1.

(27) Peyrone, M. *Liebigs Annalen der Chem.* **1844**, *51*, 1.

(28) Jennerwein, M.; Andrews, P. A. *Drug Metab. Dispos.* **1995**, *23*, 178.

(29) Wang, D.; Lippard, S. J. *Nat. Rev. Drug. Discov.* **2005**, *4*, 307.

(30) Theis, S.; Roemer, K. *Oncogene* **1998**, *17*, 557.

(31) Cong, F.; Goff, S. P. *Proc. Natl. Acad. Sci. U.S.A.* **1999**, *96*, 13819.

(32) Katayama, H.; Sasai, K.; Kawai, H.; Yuan, Z. M.; J., B. *Nature Genet.* **2004**, *36*, 55.

(33) Alexander, A.; Tulub, V. E. S. *Int. J. Biol. Macromol.* **2001**, *28*, 191.

(34) Davies, M. S.; Berners-Price, S. J.; Hambley, T. W. *Inorg. Chem.* **2000**, *39*, 5603.

(35) Hambley, T. W. *J. Chem. Soc., Dalton Trans.* **2001**, 2711.

(36) Kelland, L. R. *Drugs* **2000**, *59*, 1.

(37) Liu, W.; Jiang, J.; Xu, Y.; Hou, S.; Sun, L.; Ye, Q.; Lou, L. *J. Inorg. Biochem.* **2015**, *146*, 14.

(38) Allardyce, C. S.; Dyson, P. J. *Platinum Metals Rev.* **2001**, *45*, 62.

(39) Gallori, E.; Vettori, C.; Allessio, E.; Vilchez, F. G.; Vilaplana, R.; Orioli, P.; Casini, A.; Messori, L. *Arch. Biochem. Biophys.* **2000**, *376*, 156.

(40) Fruhauf, S.; Zeller, W. J. *Cancer. Res.* **1991**, *51*, 2943.

(41) Schluga, P.; Hartinger, C. G.; Egger, A.; Reisner, E.; Galanski, M.; Jakupec, M. A.; Keppler, B. K. *Dalton Trans.* **2006**, *14*, 1796.

(42) Jakupec, M. A.; Arion, V. B.; Kapitza, S.; Reisner, E.; Eichinger, A.; Pongratz, M.; Marian, B.; Graf von Keyserlingk, N.; Keppler, B. K. *Int. J. Clin. Pharmacol. Ther.* **2005**, *43*, 595.

(43) Habtemariam, A.; Melchart, M.; Fernandez, R.; Parsons, S.; Oswald, I. D. H.; Parkin, A.; Fabbiani, F. P. A.; Davidson, J. E.; Dawson, A.; Aird, R. E.; Jodrell, D. I.; Sadler, P. J. *J. Med. Chem.* **2006**, *49*, 6858.

(44) Morris, R. E.; Aird, R. E.; Murdoch, P. D.; Chen, H.; Cummings, J.; Hughes, N. D.; Parsons, S.; Parkin, A.; Boyd, G.; Jodrell, D. I.; Sadler, P. J. *J. Med. Chem.* **2001**, *44*, 3616.

(45) Guo, M.; Sun, H.; McArdle, H. J.; Gambling, L.; Sadler, P. J. *Biochemistry* **2000**, *39*, 10023.

(46) Aird, R.; Cummings, J.; Ritchie, A.; Muir, M.; Morris, R.; Chen, H.; Sadler, P. J.; Jodrell, D. I. *Br. J. Cancer* **2002**, *86*, 1652.

(47) Novakova, O.; Kasparkova, J.; Bursova, V.; Horf, C.; Vojtiskova, M.; Chen, H.; Sadler, P. J.; Brabec, V. *Chem. Biol.* **2005**, *12*, 121.

(48) Dorcier, A.; Ang, W. H.; Bolano, S.; Gonsalvi, L.; Juillerat-Jeannerat, L.; Laurenczy, G.; Peruzzini, M.; Phillips, A. D.; Zanobini, F.; Dyson, P. J. *Organometallics* **2006**, *25*, 4090.

(49) Scolaro, C.; Chaplin, A. B.; Hartinger, C. G.; Bergamo, A.; Cocchietto, M.; Keppler, B. K.; Sava, G.; Dyson, P. J. *Dalton. Trans.* **2007**, *43*, 5065.

(50) Gossens, C.; Dorcier, A.; Dyson, P. J.; Rothlisberger, U. *Organometallics* **2007**, *26*, 3969.

(51) Ang, W. H.; Dyson, P. J. *Eur. J. Inorg. Chem.* **2006**, *20*, 4003.

(52) Yan, Y. K.; Melchart, M.; Habtemariam, A.; Sadler, P. J. *Chem. Commun.* **2005**, *38*, 4764.

(53) Sava, G.; Pacor, S.; M, C.; Mariggio, M.; Cocchietto, M.; Alessio, E.; Mestroni, G. *Drug. Invest.* **1994**, *8*, 150.

(54) Gray, H. B.; Winkler, J. R. *Annu. Rev. Biochem* **1996**, *65*.

(55) Messori, L.; Orioli, P.; Vullo, D.; Alessio, E.; Iengo, E. *Eur. J. Biochem.* **2000**, *267*, 1206.

(56) Trávníček, Z.; Matiková-Maľarová, M.; Novotná, R.; Vančo, J.; Štěpánková, K.; Suchý, P. *J. Inorg. Biochem.* **2011**, *105*, 937.

(57) Hanif, M.; Babak, M. V.; Hartinger, C. G. *Drug Discovery Today* **2014**, *19*, 1640.

(58) Hartinger, C. G.; Jakupec, M. A.; Zorbas-Seifried, S.; Groessl, M.; Egger, A.; Begger, W.; Zorbas, H.; Dyson, P. J.; Keppler, B. K. *Chem. Biodivers.* **2008**, *5*, 2140.

(59) Kratz, F.; Hartmann, M.; Keppler, B. K.; Messori, L. *J. Biol. Chem.* **1994**, *269*, 2581.

(60) Dyson, P. J.; Sava, G. *Dalton, Trans.* **2006**, 1929.

(61) Graf, N.; Lippard, S. J. *Adv. Drug Deliv. Rev.* **2012**, *64*, 993.

(62) Bratsos, I.; Jedner, S.; Gianferrara, T.; Alessio, E. *Chimia* **2007**, *61*, 692.

(63) Sava, G.; Bergamo, A.; Zorzet, S.; Gava, B.; Casarsa, C.; Cocchietto, M.; Furlani, A.; Scarcia, V.; Serli, B.; Iengo, E.; Mestroni, G. *Eur. J. Cancer* **2002**, *38*, 427.

(64) Velders, A. H.; Bergamo, A.; Alessio, E.; Zangrando, E.; Haasnoot, J. G.; Casarsa, C.; Cocchietto, M.; Zorzet, S.; Sava, G. *J. Med. Chem.* **2004**, *47*, 1110.

(65) Peacock, A. F. A.; Habtemariam, A.; Fernandez, R.; Walland, V.; Fabbiani, F. P. A.; Parsons, S.; Aird, R. E.; Jodrell, D. I.; Sadler, P. J. *J. Am. Chem. Soc.* **2006**, *128*, 1739.

(66) Peacock, A. F. A.; Melchart, M.; Deeth, R. J.; Habtemariam, A.; Parsons, S.; Sadler, P. J. *Chem. Eur. J.* **2007**, *13*, 2601.

(67) Fu, Y.; Soni, R.; Romero, M. J.; Pizarro, A. M.; Salassa, L.; Clarkson, G. J.; Hearn, J. M.; Habtemariam, A.; Wills, M.; Sadler, P. J. *Chem. Eur. J.* **2013**, *19*, 15199.

(68) Muhlgassner, G.; Bartel, C.; Schmid, W. F.; Jakupec, M. A.; Arion, V. B.; Keppler, B. K. *J. Inorg. Biochem.* **2012**, *116*, 180.

(69) Kilpin, K. J.; Crot, S.; Riedel, T.; Kitchen, J. A.; Dyson, P. J. *Dalton Trans* **2014**, *43*, 1443.

(70) Tobe, M. L.; Burgess, J. *Inorganic Reaction Mechanisms*; Addison-Wesley Longman Inc.: Essex, 1999.

(71) Peacock, A. F. A.; Habtemariam, A.; Moggach, S. A.; Prescimone, A.; Parsons, S.; Sadler, P. J. *Inorg. Chem.* **2007**, *46*, 4049.

(72) Peacock, A. F. A.; Parsons, S.; Sadler, P. J. *J. Am. Chem. Soc.* **2007**, *129*, 3348.

(73) Cebrian-Losanto, B. *Inorg. Chem.* **2007**, *46*, 5023.

(74) Egger, A.; Cebrain-Losanto, B.; Stepanenko, I. N.; Krokhin, A. A.; Eichinger, R.; Jakupec, M. A.; Arion, V. B.; Vladimir, B.; Kleppler, B. K. *Chem. Biodivers.* **2008**, *5*, 1588.

(75) Buchel, G. E. *Inorg. Chem.* **2001**, *50*, 7690.

(76) Dorcier, A.; Dyson, P. J.; Gossens, C.; Rothlisberger, U.; Scopelliti, R.; Tavernelle, I. *Organometallics* **2005**, *24*, 2114.

(77) Colangelo, D.; Ghiglia, A.-L.; Ghezzi, A.-R.; Ravera, M.; Rosenberg, E.; Spada, F.; Osella, D. *J. Inorg. Biochem.* **2005**, *99*, 505.

(78) Hartinger, C. G. *Curr. Top. Med. Chem.* **2011**, *11*, 2688.

(79) Kong, K. V.; Leong, W. K.; Lim, L. H. K. *Chem. Res. Toxicol.* **2009**, *22*, 1116.

(80) Kong, K. V.; Leong, W. K.; Ng, S. P.; Nguyen, T. H.; Lim, L. H. K. *Chem. Med. Chem.* **2008**, *3*, 1269.

(81) Hidaka, H.; Inagaki, M.; Kawamoto, S.; Sasaki, Y. *Biochemistry* **1984**, *23*, 5036.

(82) Kim, J. H.; Lee, G. E.; Kim, S. W.; Chung, I. K. *Biochem. J.* **2003**, *373*, 523.

(83) Nervi, C.; Gobetto, R.; Milone, L.; Viale, A.; Rosenberg, E.; Spada, F.; Rokhsana, D.; Fiedler, J. *J. Organomet. Chem.* **2004**, *689*, 1796.

(84) Mayer, H. A. *Chem. Rev.* **1994**, *94*, 1239.

(85) van Rijn, J. A.; Siegler, M. A.; Spek, A. L.; Bouwman, E.; Drent, E. *Organometallics* **2009**, *28*, 7006.

(86) Lindner, E.; Warad, I.; Eichele, K.; Mayor, H. A. *Inorg. Chim. Acta* **2003**, *350*, 49.

(87) Warad, I.; Lindner, E.; Eichele, K.; Mayor, H. A. *Inorg. Chim. Acta* **2004**, *357*, 1847.

Chapter 2

Os(II) dicarbonyl-dihalido-diphosphine complexes

2.1 Background

2.1.1 $[OsX_2(CO)_2(PR_3)_2]$ complexes

The chemistry of osmium containing complexes has been of interest for the past 60 years, mainly because of the wide range of chemical properties exhibited by these complexes.[1-5] These properties are directed by the coordinated ligands, structure and stereochemistry of the complex and the metal oxidation state. Heteroleptic metal(II) complexes of group 8 containing at least one halide ligand, one CO group and P-donor ligands have been of interest as catalysts,[6,7] some have shown photochemical properties[4,5,8] and the group of Dharmaraj have discussed their potential application as therapeutics.[9]

In addition to the various chemical properties offered by osmium complexes of the type $[OsX_2(CO)_2(PR_3)_2]$, continued interest is also increased by their ease of accessibility and because these complexes are highly reactive they are increasingly being used as precursors for other Os(II) derivatives.[4] Various methods can be used for preparation.

2.1.2 Preparatory methods

Various methods are known for preparation of complexes of the type $[MX_2(CO)_2(PR_3)_2]$ (where M = Os, Ru; X = Cl, Br, I; PR_3 = tertiary monophosphine). This includes carbonylation of Os(III) halides $[MCl_3]$ in alcohol media followed by coordination of appropriate phosphine ligand (Scheme 2.1, Eq. 1).[10] This route is most effective with carbonylation of $[RuCl_3]$. However, carbonylation of $[OsCl_3]$ is slow because of general poor solubility. For preparation of osmium derivatives the more soluble Os(IV) hexahalide salt,

$[OsX_6]^{2-}$, is used instead (Scheme 2.1, Eq. 2).[10] Carbonylation of phosphine-substituted metal halides such as $[MX_2(PR_3)_3]$ (Scheme 2.1, Eq. 3)[11]

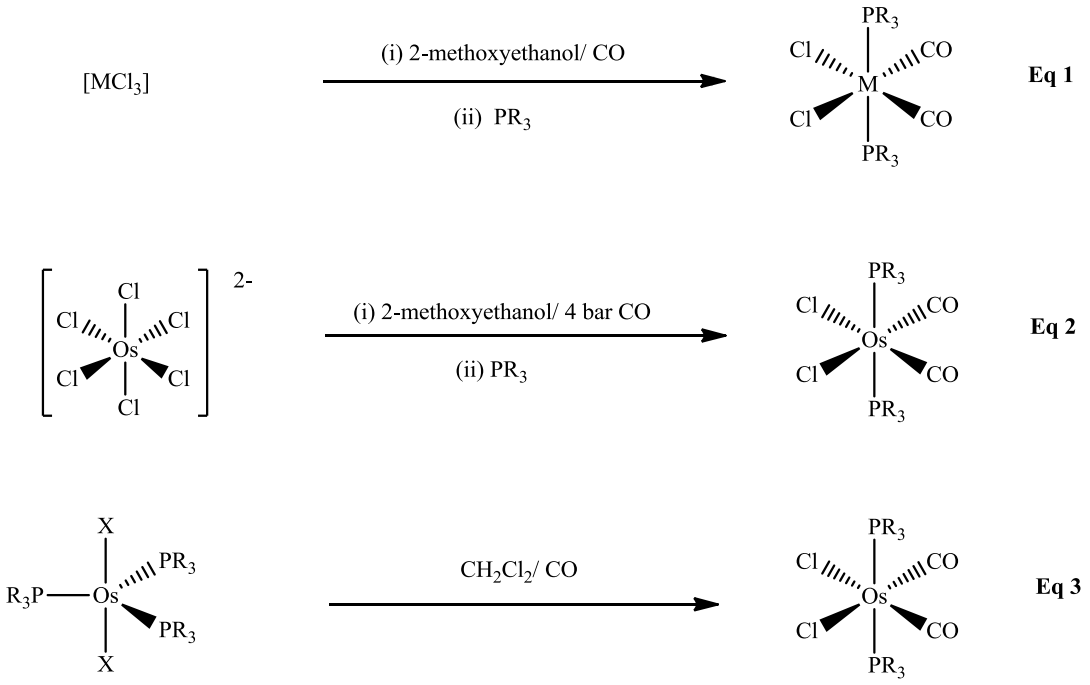

Scheme 2.1: Preparation of $[OsCl_2(CO)_2(PR_3)_2]$ *via* carbonylation.

These complexes can also be prepared *via* ligand substitution. The appropriate ligand replaces coordinated CO ligand in the neutral metal carbonyl halides complex $[Os(\mu\text{-}Cl)_2(CO)_3]_2$, breaking halide bridges (Scheme 2.2, Eq. 4).[12] Interaction of appropriate ligand with polymeric metal carbonyl halide (Scheme 2.2, Eq. 5).[13]

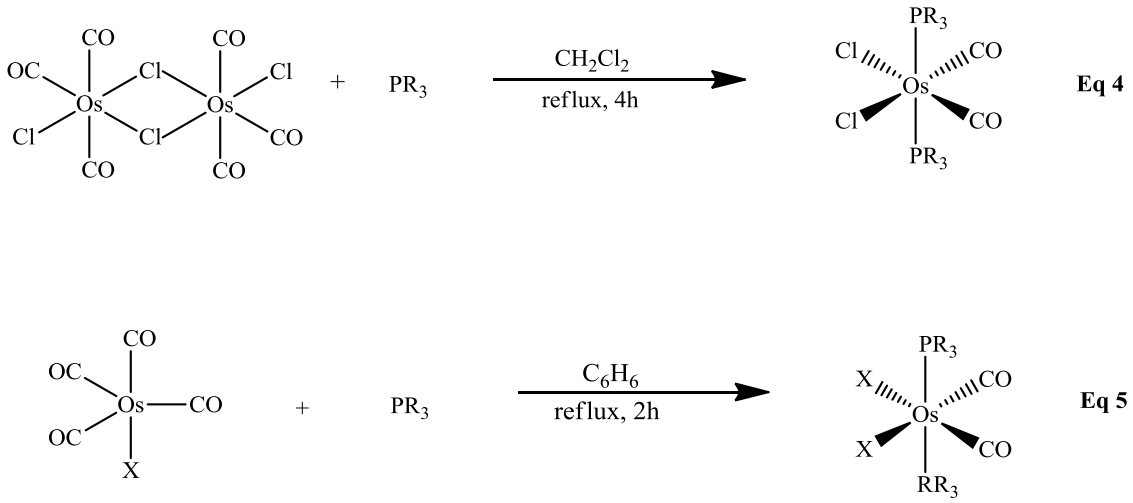

Scheme 2.2: Preparation of $[OsX_2(CO)_2(PR_3)_2]$ *via* ligand substitution.

2.1.3 Focus of this study

In this section of the study a series of $[MX_2(CO)_2(PR_3)_2]$ complexes (where M = Os; PR_3 = tertiary phosphine and X = Cl, Br, I) were synthesised. A lot of research which focused on the preparation of these complexes has been reported. However, none of the work investigated the effect of varying the R group of the tertiary phosphine and halide ligands on the spectroscopic data and biological activity of these complexes.

This class of compounds is of interest because they contain potentially labile ligands. It is this *cis*-configuration of the labile ligands (Cl, Br, I) in this type of complex where application in pharmaceuticals, particularly anticancer agents, can be found. Chart 2.1 is a representative of the 9 complexes synthesised in this chapter.

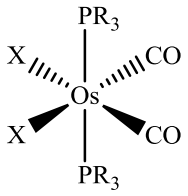

1a X = Cl, $PR_3 = P(C_6H_5)_3$
1b X = Br, $PR_3 = P(C_6H_5)_3$
1c X = I, $PR_3 = P(C_6H_5)_3$

2a X = Cl, $PR_3 = Ph_2P(CH_2C_6H_5)$
2b X = Br, $PR_3 = Ph_2P(CH_2C_6H_5)$

3a X = Cl, $PR_3 = P(CH_2C_6H_5)_3$
3b X = Br, $PR_3 = P(CH_2C_6H_5)_3$

4a X = Cl, $PR_3 = P(C_6H_{11})_3$
4b X = Br, $PR_3 = P(C_6H_{11})_3$

Chart 2.1: Os(II) carbonyl complexes synthesized.

2.2 Synthesis

Collman's approach[10] was employed in the synthesis of the desired osmium carbonyl complexes, $[OsX_2(CO)_2(PR_3)_2]$ (Scheme 2.3).

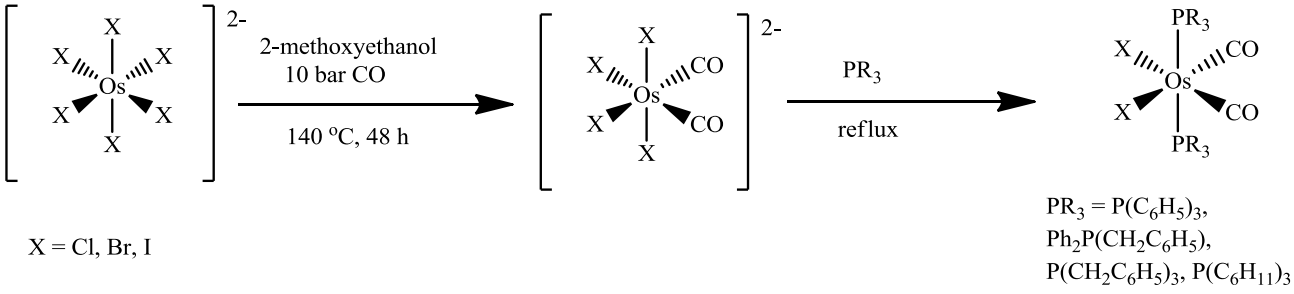

Scheme 2.3: Synthesis of complex **1a-c, 2a-4b**.

Carbonylation of the hexahalido osmate complex, $[OsX_6]^{2-}$, is accomplished by use of 2-methoxyethanol, at 140 °C for 48 h under pressurised CO gas. Upon carbonylation the two carbonyl ligands take up mutually *cis* positions *trans* to the weak π-accepting and σ-donating halide ligands. Ligands *trans* to each other use the same orbitals on the metal for bonding. Thus, if one ligand is a strong σ–donor, the ligand *trans* to it cannot donate electrons to the metal resulting in a weaker interaction with the metal. In this *cis*-position the CO ligands have a better interaction with the low-spin d^6 metal ion. Hence, *cis*-CO coordination is preferred. The *cis*-CO complex reacts with the PR_3 under refluxing conditions. In contrast to

carbonyls, phosphines are weaker π-acids and are forced to take mutually *trans* positions. Because of the bulkiness of the this ligand these positions are also sterically favoured.

An attempt to prepare the iodine compounds of $PPh_2(CH_2C_6H_5)$, $P(CH_2C_6H_5)_3$ and $P(C_6H_{11})_3$ was made however, that was without success. Carbonylation of the osmium salt K_2OsI_6 was achieved which was characterized by IR spectroscopy. Coordination of the phosphine ligands difficult to achieve which made it difficult to prepare the desired $[OsI_2(CO)_2(PR_3)_2]$ (PR_3 = $PPh_2(CH_2C_6H_5)$, $P(CH_2C_6H_5)_3$, $P(C_6H_{11})_3$). Failure to prepare these complexes could result from formation of *trans,cis,cis*-$[OsI_2(CO)_4]$] instead of the required cis,trans,cis$[OsI_4(CO)_2]$ upon carbonylation. These two would result in similar IR spectra. Hence, coordination of phosphine ligands will be difficult for the former complex.

The desired *cis,cis,trans*-$[OsX_2(CO)_2(PR_3)_2]$ complexes were formed as solids in yields ranging from 31 – 92%. The resulting products were characterized spectroscopically using FT-IR, NMR (^1H, $^{13}C\{H\}$, $^{31}P\{H\}$), Raman spectroscopy, elemental analysis and X-ray crystallography.

2.3 Results and discussions

The Os(II) carbonyl-halide-phosphine complexes **1a-c, 2a-4b** were characterized in solution using NMR spectroscopy and solid state FT-IR, Raman as well as molecular crystal structure determinations for selected complexes.

2.3.1 Infra-red spectroscopy

The stretching vibrational frequencies, $\nu_{(CO),}$ of the coordinated CO ligands in complexes **1a-c**, **2a-4b** are given in Table 2.1. The infrared spectra of complexes (**1a-c, 2a-4b**) show two bands in the $\nu_{(CO)}$ region, characteristic of mutually *cis* carbonyl ligands.[12-14]

The C–O vibration for free CO occurs at 2143 cm^{-1}. The shift in the CO stretching frequency of the coordinated CO is influenced by electron density donation from the metal to the carbon monoxide ligand *via* backbonding. A decrease in the frequency of ν_{CO} bands is characteristic of an increase in backbonding. The M–CO bond strengthens and shortens and in turn the C–O bond is weakened and becomes longer.

The *cis,cis,trans*-$[OsX_2(CO)_2(PR_3)_2]$ complexes show a significant change in $\nu_{(CO)}$ with change in PR_3. This results from the difference in the σ-donating ability of the PR_3 ligands (Figure 2.1).

Table 2.1: IR data in the carbonyl region of complex **1a-c**, **2a-4b.**

Complex			Carbonyl stretching frequencies (ν_{CO}, cm^{-1})[a] for *cis,cis,trans*-$[OsBr_2(CO)_2(PR_3)_2]$ complexes	
	PR_3	X	B_2 (Asymmetric stretch)	A_1 (Symmetric stretch)
1a	$P(C_6H_5)_3$	Cl	2043	1960
1b		Br	2042	1960
1c		I	2033	1962
2a	$Ph_2P(CH_2C_6H_5)$	Cl	2036	1962
2b		Br	2040	1970
3a	$P(CH_2C_6H_5)_3$	Cl	2034	1960
3b		Br	2023	1953
4a	$P(C_6H_{11})_3$	Cl	2010	1933
4b		Br	2012	1939

[a]Measured in solid-state.

The $\nu_{(CO)}$ decreases in the order $P(C_6H_5)_3 > Ph_2P(CH_2C_6H_5) > P(CH_2C_6H_5)_3 > P(C_6H_{11})_3$. This trend is consistent with a decrease in the σ-donor and an increase in π-acceptor ability of these ligands (Table 2.1).

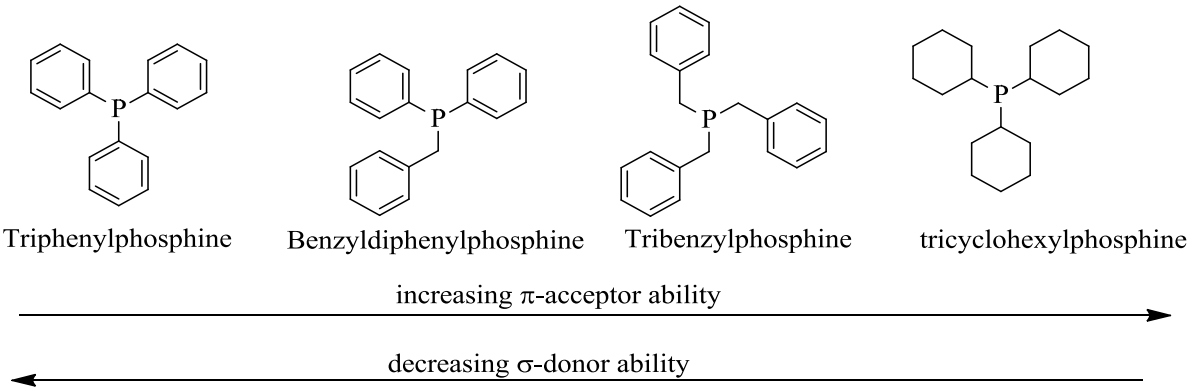

Figure 2.1: Tertiary PR_3 ligands showing the trend of decreasing σ-donor and increasing π-acceptor ability.

The CO stretching frequencies of the complexes show an decrease in the order Cl > Br > I for the asymmetric stretch in the case where the halides are changed and ligand PR_3 remains the same.[15] Although a negligible change is observed going from Cl to Br, which may result from the small difference in electronegativity between the two atoms. However, a significant decrease in the CO stretching frequency is observed moving from Br to I. The inductive effect of the halide is considered to decrease along this series and the π-bonding capabilities to increase.[16] The decrease in inductive power going from Cl to I leads to greater electron density on the metal which in turn redistributs the electron density in the M-CO π-system. This leads to an decrease in the stretching frequency. If π-bonding effect was the contributing effect then the CO stretching frequency would be expected to increase.[13] In this case the inductive power is the important contributing factor. Unfortunately, there is no clear trend in

the symmetric stretch, although for complex $[OsX_2(CO)_2(PPh_3)_2]$ (where X = Cl, Br, I) the symmetric stretch remains relatively constant.

The IR spectrum of complex **1b** is given in Figure 2.2, two bands were observed. The point group/symmetry type of the complexes assists in predicting the number of carbonyl stretching frequencies in the IR spectrum. Two bands are predicted as shown by the IR spectrum. The two bands: symmetric A_1 and asymmetric B_2 modes corresponds to C_{2v} symmetry (Figure 2.3).

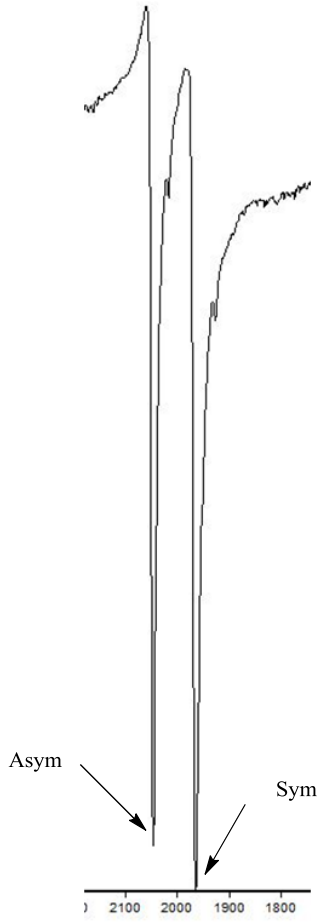

Figure 2.2: IR spectrum of complex *cis*,*cis*,*trans*-$[OsBr_2(CO)_2\{P(C_6H_5)_3\}_2]$, **1b** in carbonyl region.

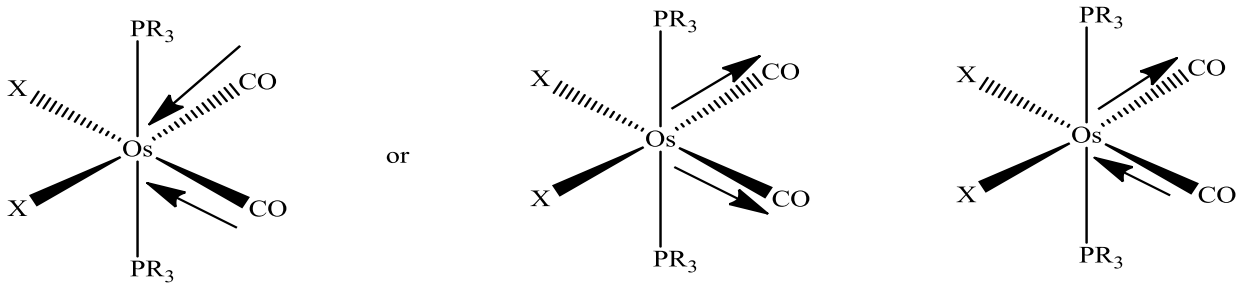

Sym Asym

Figure 2.3: IR-active normal modes observed for *cis,cis,trans*-$[OsX_2(CO)_2(PR_3)_2]$ complexes.

2.3.2 Raman spectroscopy

The Raman spectroscopy data of complex **1a-c** and **2a-4b** are given in Table 2.2. Two CO stretching vibrations are observed in the Raman spectra. The data obtained in this study is comparable to data obtained in IR spectroscopic studies. The far-IR region of the spectrum of each complex shows two bands attributed to the symmetric and asymmetric vibrations of the *cis*-OsX_2 fragment (Figure 2.4).

The Raman spectrum of *cis,cis,trans*-$[OsBr_2(CO)_2\{P(CH_2C_6H_5)_3\}_2]$, **3b**, is shown in Figure 2.4. Two intense bands assigned to carbonyl stretches are observed in the 1800 – 2200 cm^{-1} region. Two bands due to Os–Br at 216 and 189 cm^{-1} are observed suggesting the bromide ligands are mutually *cis*. Data given in Table 2.2 suggests that this is the case for all of the complexes reported. The Os–X stretching modes are observed for Os–Cl between 305 and 312 cm^{-1}, Os–Br between 210 and 221 and Os–I between 157 and 174 cm^{-1}.

Table 2.2: ν(CO) and far-IR spectra (400 – 100 cm^{-1}) of **1a-c** and **2a-4b** complexes.

Complexes			Carbonyl stretching frequencies (ν_{CO}, cm^{-1})[a] and far-IR for *cis,cis,trans*-$[OsBr_2(CO)_2(PR_3)_2]$ complexes	
	PR_3	X	$\nu_{(CO)}$ Asym, Sym	Os-X Asym, Sym
1a	$P(C_6H_5)_3$	Cl	2042, 1959	308, 284
1b		Br	2041, 1962	229, 210
1c		I	2036, 1973	174, 157
2a	$Ph_2P(CH_2C_6H_5)$	Cl	2045, 1978	312, 285
2b		Br	2041, 1978	210, 190
3a	$P(CH_2C_6H_5)_3$	Cl	2035, 1978	311, 305
3b		Br	2026, 1955	216, 189
4a	$P(C_6H_{11})_3$	Cl	2012, 1919	305, 224
4b		Br	2012, 1941	221, 189

[a]Measured in solid-state.

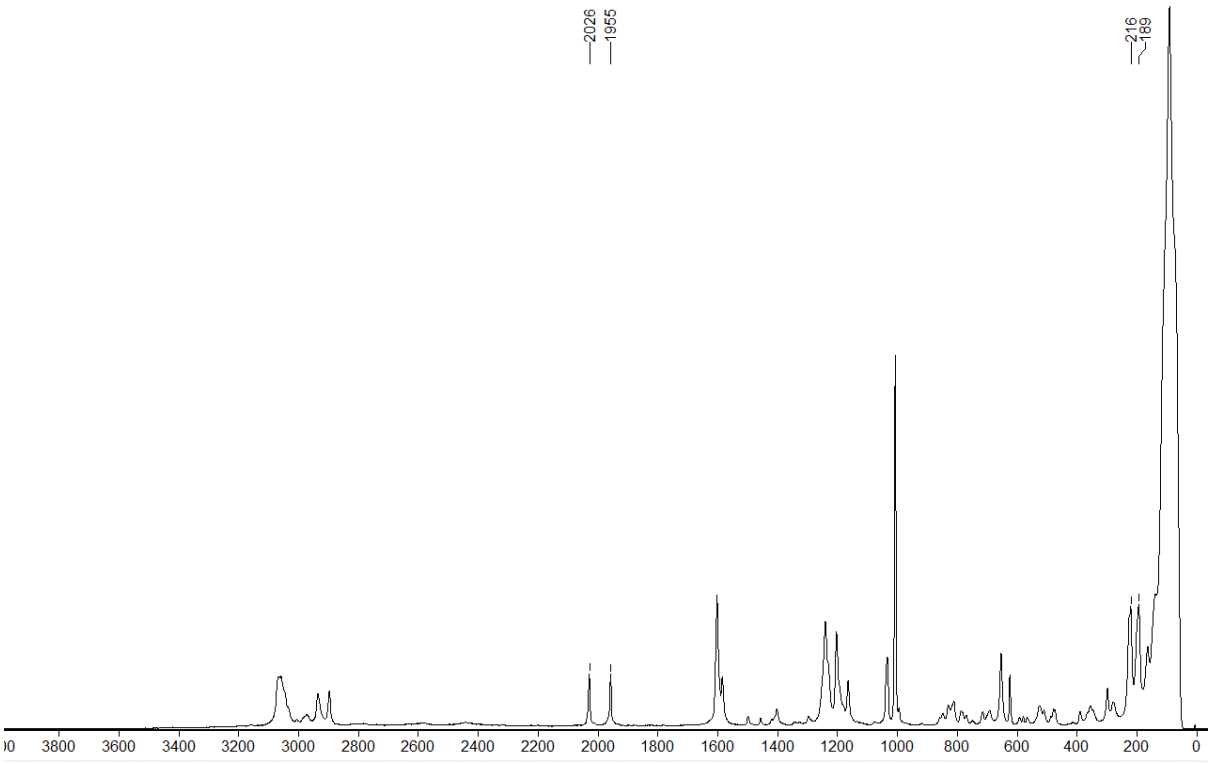

Figure 2.4: Raman spectrum of **3b** illustrating the carbonyl signals and Os–Br stretching modes.

2.3.3 ^{1}H NMR spectroscopy

The NMR data for complexes **1a – c, 2a - 4b** are given in Table 2.3. The NMR spectra show resonances characteristic of a coordinated PR_3 ligand. Coordination of the PR_3 ligand to the metal centre has a marked influence on the PR_3 proton chemical shifts. Comparison of the chemical shifts of the uncoordinated PR_3 ligands and that of the coordinated show a downfield shift (Table 2.3).

Table 2.3: ^{1}H NMR data of complex **1a – c**, **2a - 4b** and free ligands. Spectra recorded in $CDCl_3$.

Complexes	δ (^{1}H NMR) ppm	Coupling constant, *J* (Hz)	Assignment (Proton)
Free $P(C_6H_5)_3$	7.40 – 7.46 (m)		H-aromatic
1a	7.87 (dt)	9.4, 5.3	H-aromatic
	7.40 (dd)	3.7, 2.3	
1b	7.89 (ddd)	9.8, 6.6, 3.4	H-aromatic
	7.48 – 7.30 (m)		
1c	7.90 (dddd)	9.6, 3.7, 2.5, 1.3	H-aromatic
	7.45 – 7.28 (m)		
Free $Ph_2P(CH_2C_6H_5)$	7.80 - 7.65(m)	-	H-aromatic
	7.62 - 7.31(m)	-	H-aromatic
	7.29 - 7.03(m)	-	H-aromatic
	3.45(s)	-	CH_2-benzyl
2a	7.75 – 7.57 (m)	-	H-aromatic
	7.49 – 7.18 (m)	-	H-aromatic
	6.93 (dt)	25.2, 7.2	H-aromatic
	6.60 (d)	7.1	H-aromatic
	4.41 (t)	4.4	CH_2 benzyl
2b	7.69 (ddd)	10.3, 6.1, 1.9	H-aromatic
	7.47 – 7.21 (m)	-	H-aromatic
	6.96 (dt)	25.9, 7.2	H-aromatic
	6.60 (d)	7.2	H-aromatic
	4.56 (t)	4.3	CH_2 benzyl
Free $P(CH_2C_6H_5)_3$	7.94 - 7.84 (m)	-	H-aromatic
	3.26 - 2.87 (m)	-	CH_2 benzyl
3a	7.46 – 7.15 (m)	-	H-aromatic
	7.16 – 6.98 (m)	-	H-aromatic
	3.61 (t)	3.8	CH_2 benzyl
3b	7.23 (t)	3.3	H-aromatic
	7.08 – 6.93 (m)		H-aromatic
	3.72 (t)	3.8	CH_2 benzyl
Free $P(C_6H_{11})_3$	2.04 – 1.03 (m)	-	H- alkyl
	1.24 (d)	7.7	H-alkyl
4a	2.72 – 2.47 (m)	-	H- alkyl
	2.14 (d)	11.7	H-alkyl
	1.77 (d)	35.0	H- alkyl
	1.66 – 1.32 (m)	-	H-alkyl
	1.29 (d)	7.4	H-alkyl
4b	2.82 – 2.51 (m)	-	H- alkyl
	2.19 (d)	11.8	H-alkyl
	1.83 (s)	-	H- alkyl
	1.72 (s)	-	H-alkyl
	1.68 – 1.34 (m)	-	H-alkyl

The shift in resonance is a consequence of the different electronegativity of the substituents on the phosphorus atom. This has also been observed for related complexes.[17]

The multiplets in the aromatic region with relative intensities 2:3 were present in all spectra of complexes $[OsX_2(CO)_2\{P(C_6H_5)_3\}_2]$ (X = Cl (**1a**), Br (**1b**), I (**1c**)) and assigned to the aromatic protons of triphenylphosphine (Table 2.3). The large downfield shift of the aromatic protons is a consequence of coordination to the osmium centre. The chemical shift of the aromatic protons was not found to be influenced by the variation of the halide ligands. This is shown by the minor difference in the chemical shift values of the aromatic protons in complex **1a** (7.87 ppm, 7.40 ppm), **1b** (7.89 ppm, 7.48 – 7.30 ppm) (Figure 2.5) and **1c** (7.90 ppm, 7.45 – 7.28 ppm) for the chlorido, bromido and iodido complexes, respectively.

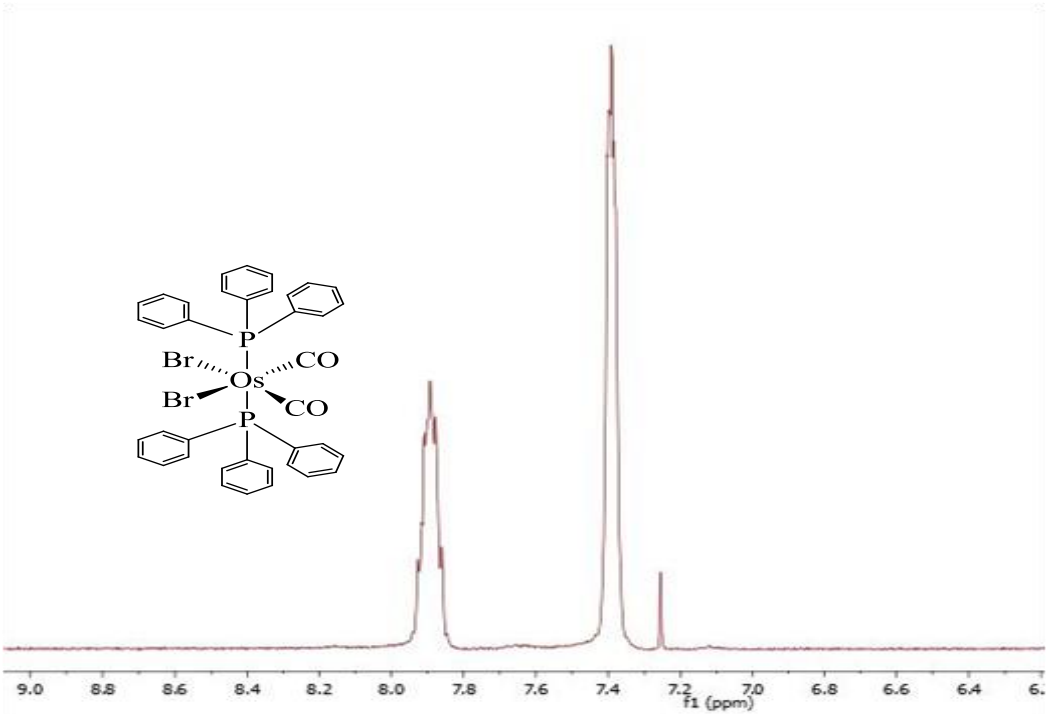

Figure 2.5: ^1H NMR spectrum of complex **1b** in $CDCl_3$.

The ^{1}H NMR spectrum of **2a** showed resonances at δ 7.75 – 7.18, 6.93 – 6.60 and 4.41 ppm for phenyl, benzyl and methylene protons, respectively (Figure 2.6). A triplet assigned to methylene protons is observed in both complexes containing $Ph_2P(CH_2C_6H_5)$ at δ 4.56 ($J_{(PH)}$ = 4.3 Hz) and at δ 4.41 ($J_{(PH)}$ = 4.4 Hz) ppm for the bromido (**2b**) and the chlorido (**2a**) complexes, respectively. The magnitude of these coupling constant suggests that the protons are coupled to phosphorus in a similar manner and that the structures of the two complexes are similar.

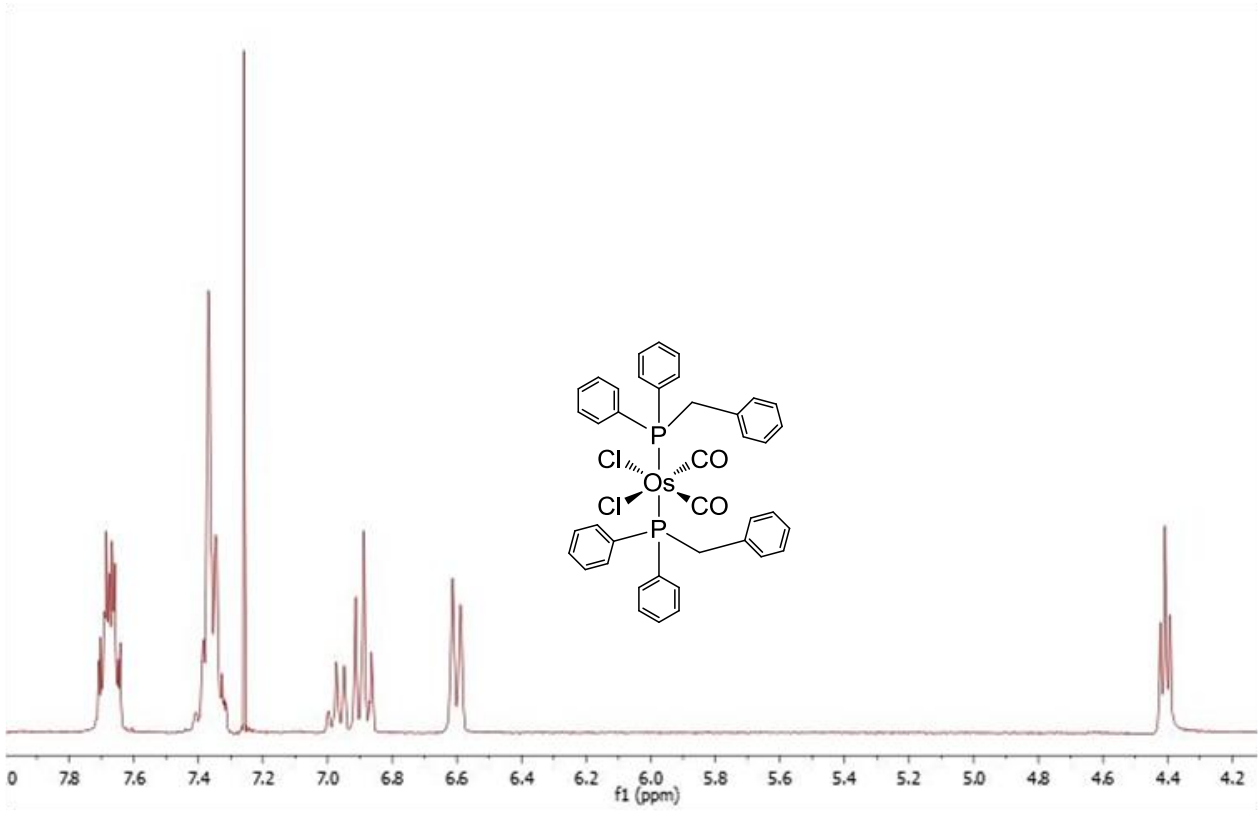

Figure 2.6: ^{1}H NMR spectrum of **2a** in $CDCl_3$

Complex **3a** exhibits the aromatic proton signals between δ 7.46 – 6.98 ppm as multiplets. The methylene protons are seen at δ 3.61 ppm as a triplet (Figure 2.7). The triplet results

from coupling to the the phosphorus atom. Both complexes show triplet resonances at δ 3.72 ($J_{(HP)}$ = 3.8 Hz) and 3.61 ($J_{(HP)}$ = 3.8 Hz) for **3b** and **3a** respectively.

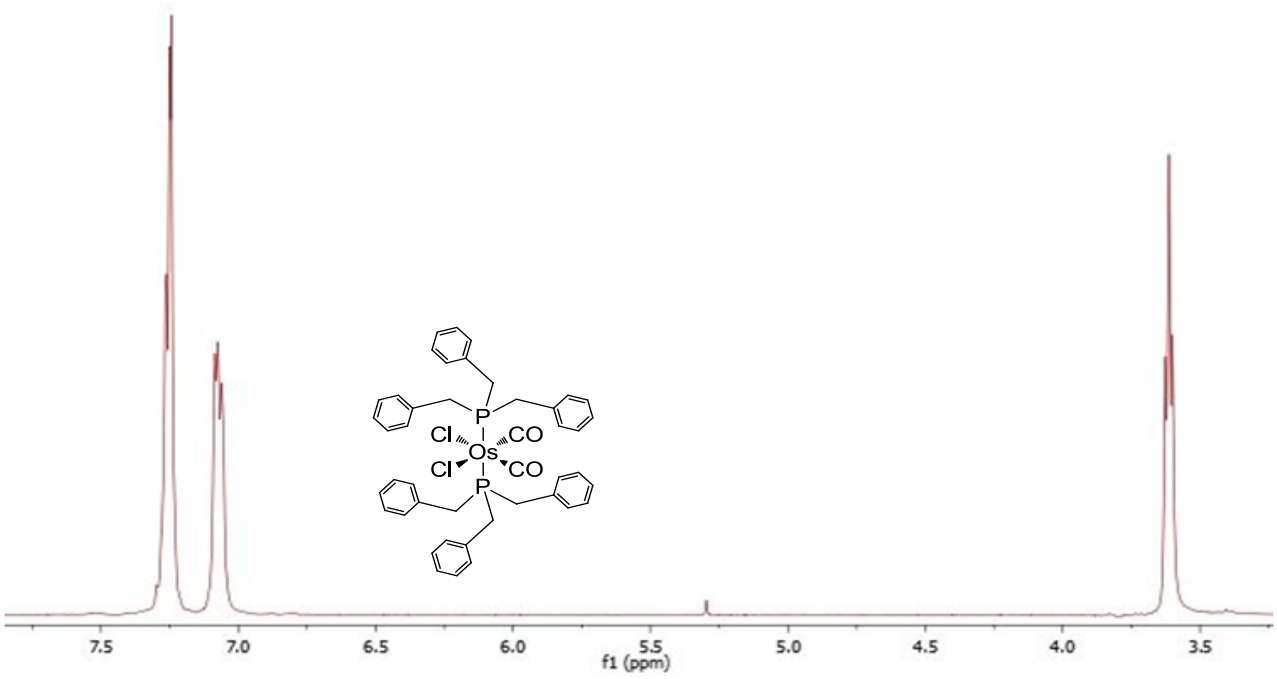

Figure 2.7: ^{1}H NMR spectrum of **3a** in $CDCl_3$.

Five broad multiplets are observed in the ^{1}H NMR spectra of complex **4a** assigned to the aliphatic protons (Figure 2.8). Complex **4b** show similar resonance and data is given in Table 2.3.

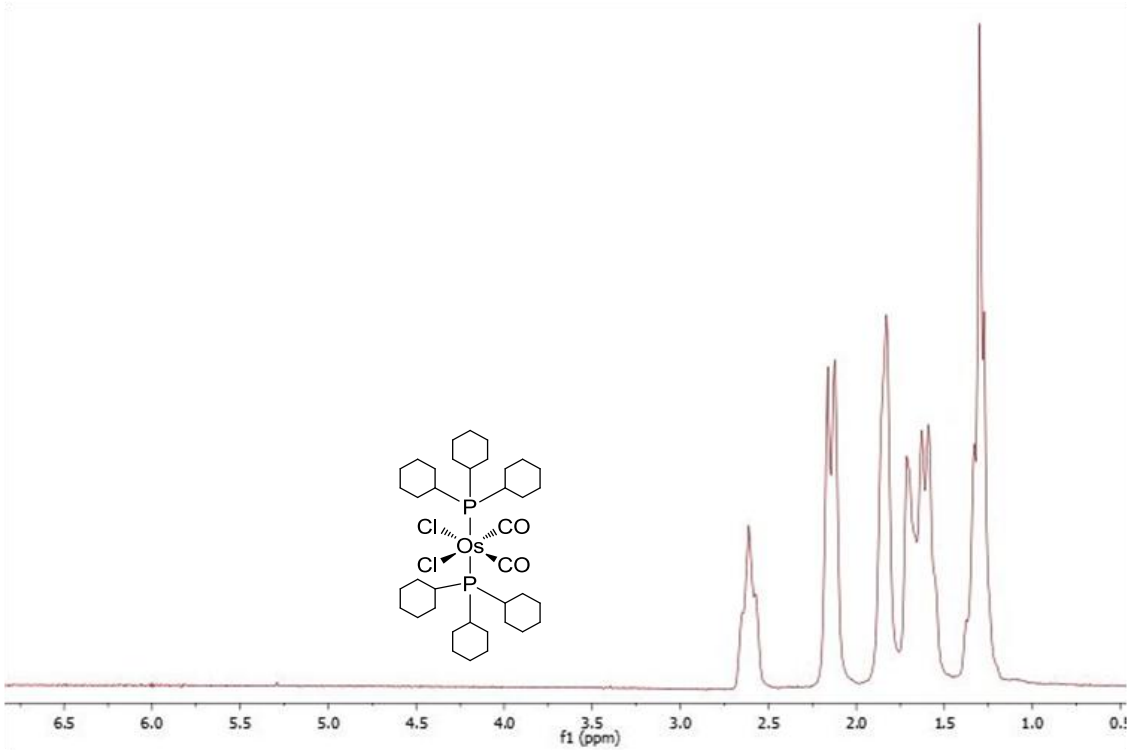

Figure 2.8: ^{1}H NMR spectrum of **4a**.

2.3.4 ^{13}C{H} NMR spectroscopy

The ^{13}C NMR data for complexes **1a – c** and **2a – 4b** are reported in Table 2.4. Figure 2.9 shows the ^{13}C NMR spectrum of complex **3b.** The complex exhibits resonances assigned to the coordinated PR_3 ligands and resonances further downfield assigned to the geometrically equivalent carbonyl ligands with a pattern that is similar to that observed for the corresponding metal(II) carbonyl dihalido complexes containing phosphine ligands.[15,18] The triplet pattern of the resonance downfield is due to coupling of the carbon of CO group to the two phosphorus nuclei.[19] This supports data obtained from IR spectroscopy that these carbonyl groups are *cis* coordinated. Variation of X with PR_3 constant shows an upfield shift, which follows the trend I < Br < Cl. This is in agreement with inductive effect of halide ligands.[15]

Table 2.4: Selected ^{13}C NMR data for **1a-c** and **2a-4b** complexes.

Complex	Chemical shift (δ_{CO}, ppm)[a]	Coupling constant (J, Hz)
1a	172.88 (t)	7.1
1b	171.69 (t)	7.1
1c	169.93 (t)	6.8
2a	172.52 (t)	6.8
2b	171.45 (t)	6.8
3a	172.52 (t)	7.1
3b	171.74 (t)	7.1
4a	176.91 (t)	7.3
4b	175.66 (t)	7.3

[a]Spectra recorded in $CDCl_3$

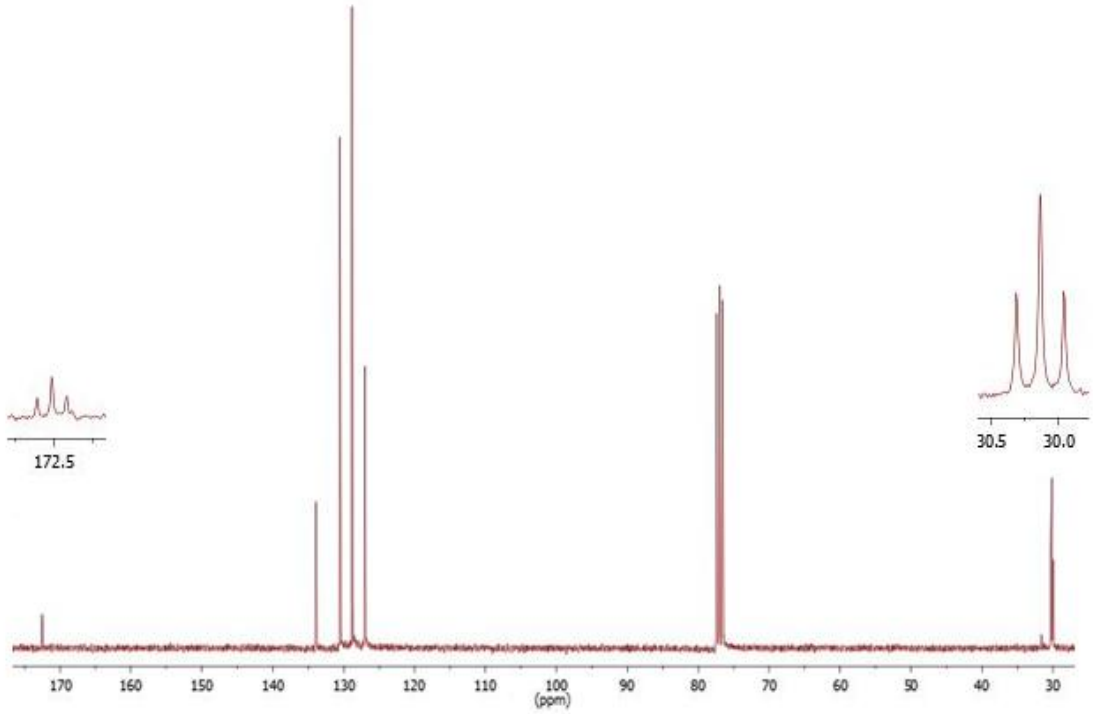

Figure 2.9: $^{13}C\{H\}$ NMR spectrum of **3b** in $CDCl_3$.

2.3.5 $^{31}P\{H\}$ NMR spectroscopy

The ^{31}P NMR data of **1a – c** and **2a – 4b** are given in Table 2.5. These complexes exhibit a single intense peak assigned to two chemically and magnetically equivalent phosphorus nuclei. This further confirms the *trans* coordination of the phosphine groups. On either side of the ^{31}P peak are two pairs of satellite peaks. The phosphorus nuclei, ^{31}P, couples to the spin active nuclei (^{13}C and ^{187}Os), each resulting in a pair of satellites (Figure 2.10).

Table 2.5: ^{31}P NMR chemical shift of free ligands and **1a –c** and **2a – 4b** complexes.

Complexes	Chemical shift (δ, ppm)[a]
Free $P(C_6H_5)_3$	-5.28
1a	-10.21
1b	-17.16
1c	-28.44
Free $Ph_2P(CH_2C_6H_5)$	-9.77
2a	-3.80
2b	-11.06
Free $P(CH_2C_6H_5)_3$	41.08
3a	-12.97
3b	-23.17
Free $P(C_6H_{11})_3$	50.41
4a	-2.63
4b	-10.57

[a]Spectra recorded in $CDCl_3$

Data in the Table 2.5 shows that δ(^{31}P) chemical shift of the uncoordinated phosphine ligand show a downfiled shift with an increase in the phosphine cone angle. Upon coordination to osmium centre the ^{31}P NMR resonance is shifted upfield except for complex **2a**, shown in spectra (Figure 2.11). Electronegativity of the substituents, R, on the phosphorus is also an important contributor to the δ(^{31}P) chemical shift. Upon coordination electron density is

donated from phosphorus to the metal centre and subsequently the increased electron density at the metal promotes π-back donation from the metal to the P–R σ*-orbital result in the upfield shift observed.[20]

The δ (^{31}P) chemical shift is influenced by the change in cone angle of the PR_3 ligand. The δ (^{31}P) for osmium-bromide complexes, $[OsBr_2(CO)_2(PR_3)_2]$ (PR_3 = $P(C_6H_5)_3$, $Ph_2P(CH_2C_6H_5)$, $P(CH_2C_6H_5)_3$, $P(C_6H_{11})_3$) is related to the cone angle of the phosphine ligand, larger cone angles exhibit δ ^{31}P resonance downfield.

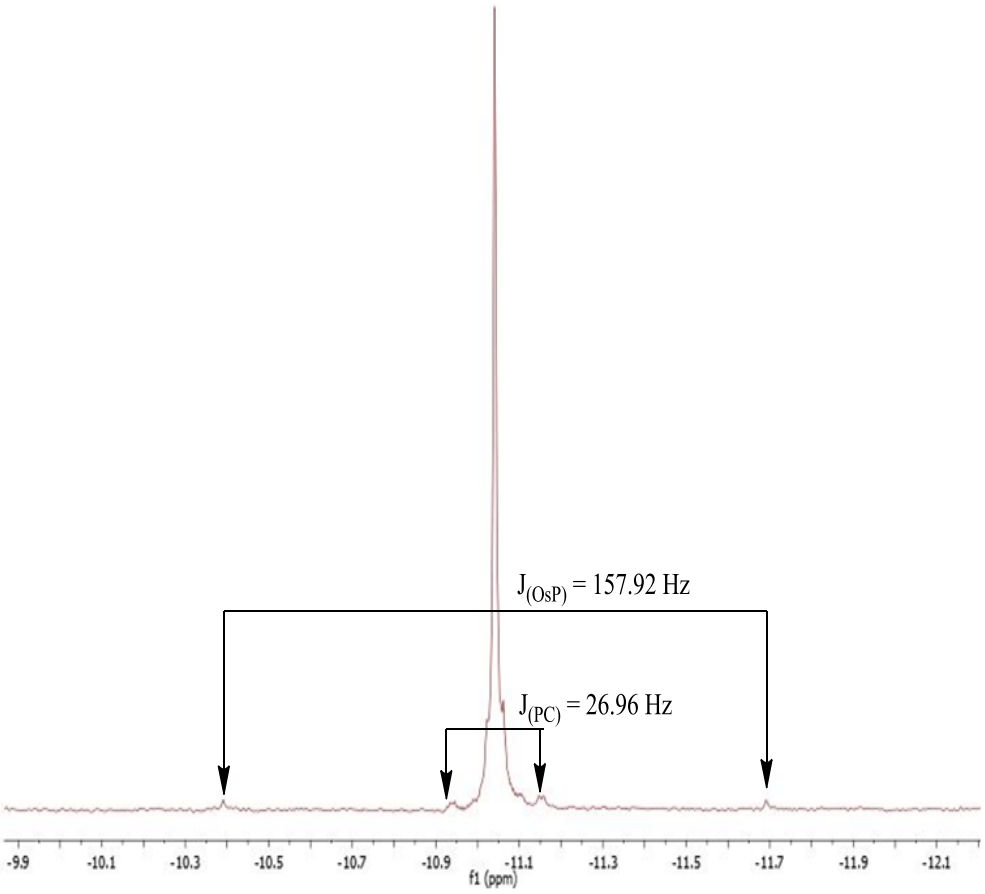

Figure 2.10: ^{31}P{H} NMR spectrum of **2b** showing ^{187}Os and ^{13}C satellites.

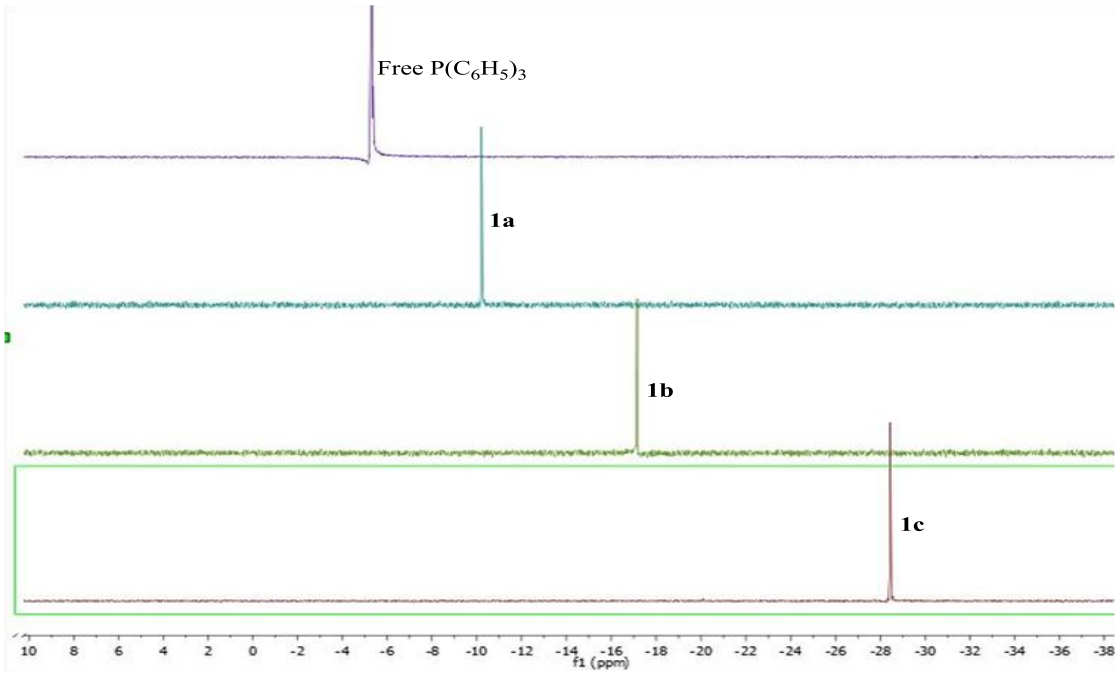

Figure 2.11: $^{31}P\{H\}$ NMR comparing chemical shift of free ligand to the complex **1a**, **1b** and **1c.**

Variation of the halide, with PR_3 unchanged, shows an upfield shift following this trend Cl > Br > I. This trend agrees with the σ-electron withdrawing effect of halides.[12] The chemical shifts have been measured at $\delta(^{31}P)$ = -10.21; -17.16; -28.44 ppm for X = Cl, Br and I, respectively. It is clear that inductive power of the halide ligands is the operating effect in these complexes.

2.3.6 Thermo gravimetrical analysis (TGA)

Thermal decomposition of the complexes was studied and found to be a two-stage process for complex **1a-c** and **2a-3b**, which can be directly related to the loss of ligands. The studies were carried out in the 100 – 1300 °C temperature range under nitrogen gas at a heating rate of 10 °C/min. The first stage is associated with loss of the halide ligands and CO groups. The second stage is characterized by release of phosphine ligands (Figure 2.12). The triphenylphosphine complexes **1a**, **1b** and **1c** are stable to just above 250 °C. Data show that

1a is the most stable with onset of decomposition at 288 °C compared to 251 and 277 °C for **1b** and **1c**, respectively.

The onset of decomposition is 329 and 235 °C for **2a** and **2b**, respectively. Similar to complexes discussed above the initial stage of weight loss is associated with loss of the halides and CO groups. With the loss of benzyldiphenylphosphine ligands occurring in second stage. Similarly for complex **3a** and **3b,** the PR_3 ligands are lost in the second stage. These complexes are stable for up until 336 and 345 °C, respectively.

Interestingly, the tricyclohexylphosphine complexes, **4a** and **4b** totally decompose in a one step (Figure 2.13). Complex **4a** on set of decomposition is at 305 °C, whilst **4b** decomposes at a slightly higher temperature, 363 °C

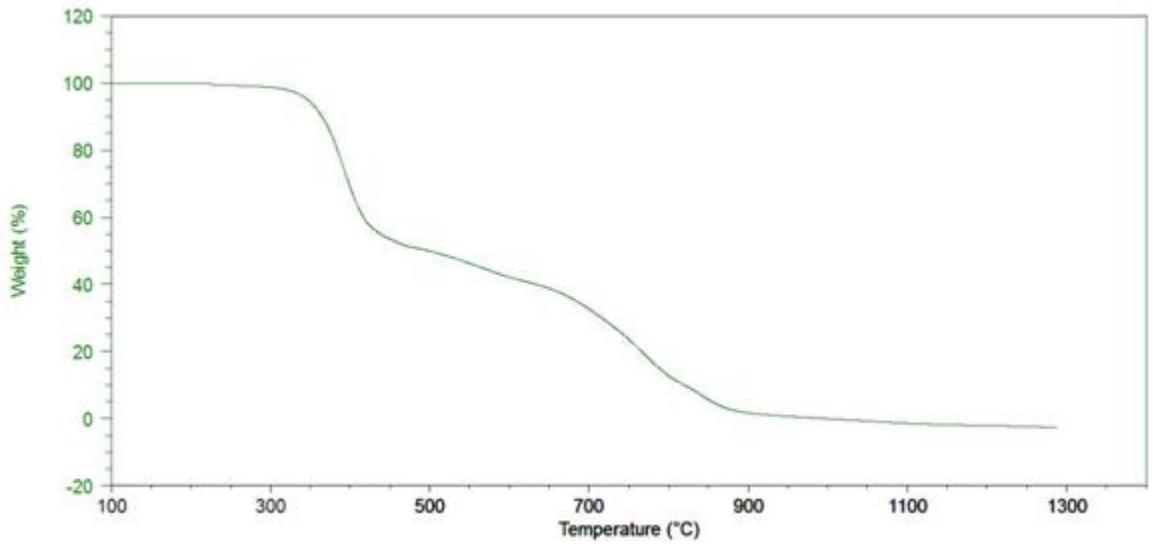

Figure 2.12: Thermogram of **3a** showing two-step decomposition.

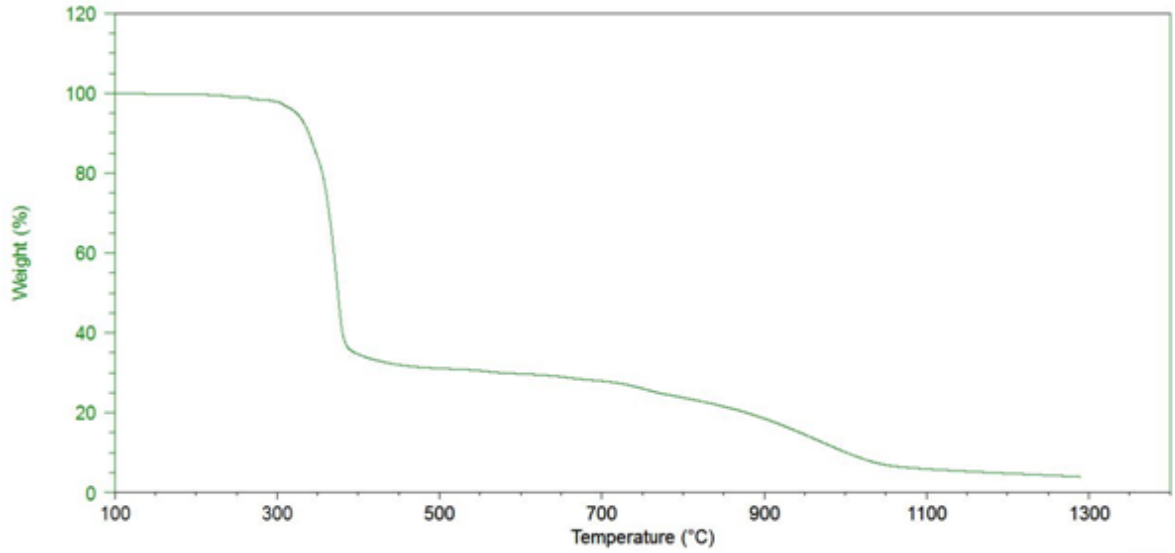

Figure 2.13: Thermogram of **4a** showing single-step decomposition.

2.3.7 Crystallographic studies

To confirm the structure of the complexes X-ray crystallography studies were conducted on selected complexes. The crystal data and experimental parameters are given in Table 2.6. Crystals of **2b**, **3b** and **4b** suitable for X-ray diffraction were grown from dichloromethane (**3b**) and from chloroform solutions (**2b** and **4b**), by slow evaporation of the solvent obtaining colourless/clear crystals of good quality. The geometric structures are represented by ORTEP plots in Figures 2.14 - 2.16. The atom numbering system used for the structural data is also included on the plots. Complexes **2b** and **3b** were found to crystallize in the monoclinic and **4b** in the triclinic crystal system with $P2_1/c$, C2/c and P-1 space groups respectively. The complexes have pseudo-octahedral geometry. The osmium(II) is coordinated by two mutually *trans* phosphines in the axial positions, with the two bromines and two carbonyl groups in equatorial in mutual *cis* positions (Figure 2.14 - 2.16). This confirms data obtained from spectroscopic studies. Selected bond lengths (Å) and angles (°) for **2b** – **4b** are given in Table 2.7.

Table 2.6: X-ray crystal data collection, solution and refinement details for **2b**, **3b** and **4b**.

	2b	**3b**	**4b**
Formula	$C_{40}H_{34}Br_2O_2OsP_2$	$C_{44}H_{24}Br_2O_2OsP_2$	$C_{39}H_{68}Br_2O_2OsP_2$
Molecular weight	958.63	1014.74	1051.79
Crystal size	0.467 × 0.35 × 0.24	0.46 × 0.35 × 0.16	0.67 × 0.42 × 0.21
Temperature(K)	173(2)	173(2)	173(2)
Crystal system	Monoclinic	Monoclinic	Triclinic
Space group	$P2_1/c$	C2/c	P-1
a(Å)	11.4710(7)	23.3375(14)	10.4091 (2)
b(Å)	18.6816(10)	18.3044(10)	10.6868(2)
c(Å)	17.6815(10)	9.4310(10)	21.3533(4)
α(°)	90	90	84.6580(10)
β(°)	104.530(2)	98.962(2)	89.7640(10)
γ(°)	90	90	64.9180(10)
V(Å^3)	3667.9(4)	3979.5(4)	2140.36(7)
Z	4	4	2
D_{calc} (Mg/m^3)	1.736	1.694	1.632
F(000)	1864	1992	1056
μ/mm^{-1}	5.776	5.329	5.077
Reflections collected	99188	42003	88129
Independent reflections	8842	4818	10330
R_{int}	0.0858	0.0707	0.0974
Restrain/ parameters	0/424	0/231	0/433
Final R indices [I > 2 sigma (I)]	R_1 = 0.0226 wR_2 = 0.0524	R_1 = 0.032 wR_2 = 0.0872	R_1 = 0.0289 wR_2 = 0.0716
R indices (all data)	R_1 = 0.0284 wR_2 = 0.0552	R_1 = 0.0351 wR_2 = 0.0872	R_1 = 0.0316 wR_2 = 0.0724
Goodness fit on F^2	1.045	1.028	1.127
Largest diff. peak and hole	0.724 and -2.271 e. Å^{-3}	6.693 and -1774 e. Å^{-3}	2.029 and -2.271 e. Å^{-3}

Table 2.7: Selected bond lengths (Å) and angles (°) with estimated standard deviations in paranthese for **2b**, **3b** and **4b**.

	2b	**3b**	**4b**
Bond lengths			
Os–Br(1)	2.578	2.579(5)	2.596(3)
Os–Br(2)	2.585	2.579(5)	2.582(3)
Os–C	1.873	1.866(5)	1.880(3)
	1.871	1.866(4)	1.867(3)
Os–P(1)	2.407	2.413(9)	2.487(7)
Os–P(2)	2.412	2.413(9)	2.486(8)
C≡O	1.139	1.134(6)	1.140(4)
	1.136		1.125(4)
Bond angles			
Br(1)–Os–Br(2)	89.07	91.43(3)	89.596(11)
P(2)–Os–Br(1)	88.40	83.98(2)	85.985(19)
P(2)–Os–Br(2)	88.54	89.66(2)	90.08(2)
Os–C≡O	177.95	177.3(4)	174.6(3)
	177.91		176.0(3)
P(1)–Os–P(2)	175.42	170.90(4)	173.57(2)

The complexes have approximately C_{2v} symmetry and are isostructural with each other and the related osmium bromide $[OsBr_2(CO)_2\{P(C_6H_5)_3\}_2]$ complex.[2,21] The metal-bromide bond lengths in complex **2b**, **3b** and **4b** (Table 2.7) are similar to other crystallographically

characterized Ru(II)- and Os(II) carbonyl bromide complexes, $[RuBr_2(CO)_2\{P(C_6H_5)_3\}_2]$, Ru–Br(1) = 2.5940(6) Å, Ru–Br(2) = 2.5927(6) Å;[22] $[OsBr_2(CO)_2\{P(C_6H_5)_3\}_2]$, Os–Br(1) = 2.535(19) Å, Os–Br(2) = 2.522(2) Å.[2,21] In these complexes the bromide ligand are similarly *trans* to the CO group. The osmium-phosphorus bond lengths of complex **2b** (2.410 Å (mean)) **and 3b** (2.413(9) Å) are comparable to other d^6 transition metal complexes.[2,12,14,21-23] However, **4b** (2.489(8) Å) has a slightly longer Os–P bond length in contrast to other related d^6 transition metal complexes. The longer Os–P is expected since tricyclohexylphosphine has a larger cone angle and is sterically demanding compared to the other phosphines. Thus, the phosphines with smaller cone angle have shorter M–P bond length.[24]

The Os–C bond lengths for complexes **2b**, **3b** and **4b** are slightly longer than those observed for analogous Ru(II) complexes[14,23] but comparable to other Os(II) complexes.[2,12,21] The Os–CO bond lengths are similar to those complexes containing CO groups that are *trans* to halides.[22,12,14] The C–O bond length in complexes **2b**, **3b** and **4b** are different. Complex **4b** has a longer C–O bond, the tricyclohexyl phosphine ligand in this complex is a better π-donor than the benzyldiphenylphosphine and tribenzylphosphine, which means greater backbonding in **4b** shown by longer C–O bond distance, which correlates to difference in CO stretching frequency in FT-IR spectroscopy [2040 and 1970 cm^{-1} for **2b**; 2023 and 1953 cm^{-1} for **3b**; 2012 and 1939 cm^{-1} for **4b**].

The Os–C≡O bond angles of the complexes under study are distorted slightly from linearity with angles less than 180°. Os–C–O = 177. 95°(**2b)**; 177.3° (**3b**); 175.3° (mean) (**4b**). The bending is a result of conversion of a C≡O to a C=O (Csp to Csp^2 hybridization) caused by backbonding. As it is shown by data the complex with more backbonding is bent more.[25]

The P–Os–P angle changes as the PR_3 ligand is changed. In these complexes the PR_3 ligand are inclined towards the bromine atoms, this is shown by the P–Os–P angle being less than 180° [170.90(4)° (**3b**); 173.67(2) °(**4b**); 175.42° (**2b**). The orientation of the PR_3 ligand also differs. The $P(C_6H_{11})_3$ ligands in complex **4b** (Figure 2.16) are staggered with respect to one another and PR_3 ligands are eclipsed in **2b** and **3b** (Figure 2.14 and Figure 2.15 respectively).

Short intramolecular interactions between hydrogen atoms of the PR_3 ligands and bromides are observed in all complexes. Complex **2b** show non-bonding intramolecular H·····Br distances [between H(4)·····Br(1) at 2.776 Å, H(23)·····Br(1) at 2.867 Å, H(34A)·····Br(1) 2.917 Å and H(15B)·····Br(1) 3.062Å] (Figure 2.13), all except one interactions are shorter than Van der Waals radii of hydrogen and bromine [r_{vdw}(H) = 1.20, r_{vdw}(Br) = 1.85 Å].[26] Similary for complex **3b** two short H·····Br distances are observed between H(10)·····Br(3) at 2.695 Å, and between H(2)·····Br(3) at 2.866 Å (Figure 2.15). In the absence of strong interactions such as C=O·····H–C, this weak Br·····H interactions are significant for crystal packing. In complex **4b** short nonbonding intramolecular interactions are observed between Br(1)·····H(18B) at 2.891 Å, Br(1)·····H(43B) at 2.720 Å, Br(2)·····H(34B) at 2.815 Å, Br(2)·····H(38B) at 2.784 Å and O(2)·····H(8B) at 2.984Å. In addition, stronger C=O·····H–C interactions are also observed between O(1)·····H(9B) 2.423 and O(2)·····H(6B) 2.448 Å. O(2) is involved in both weak and strong interactions which may account for variation in Os–C and C–O bond lengths observed in the complex. Complex **4b** was obtained as a solvate with a molecule of dicloromethane cocrystallized with the metal complex.

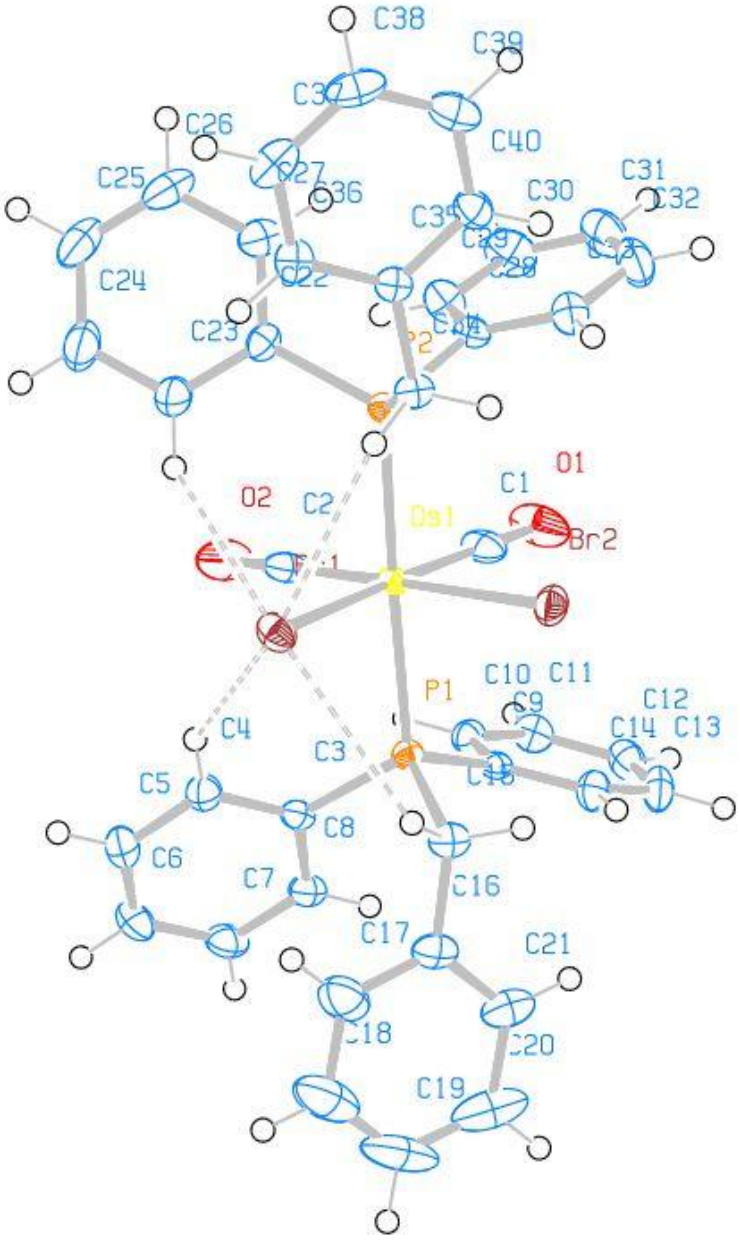

Figure 2.14: Thermal ellipsoid plot (50% probability level) of $[OsBr_2(CO)_2\{Ph_2P(CH_2C_6H_5)\}_2]$ (**2b**).

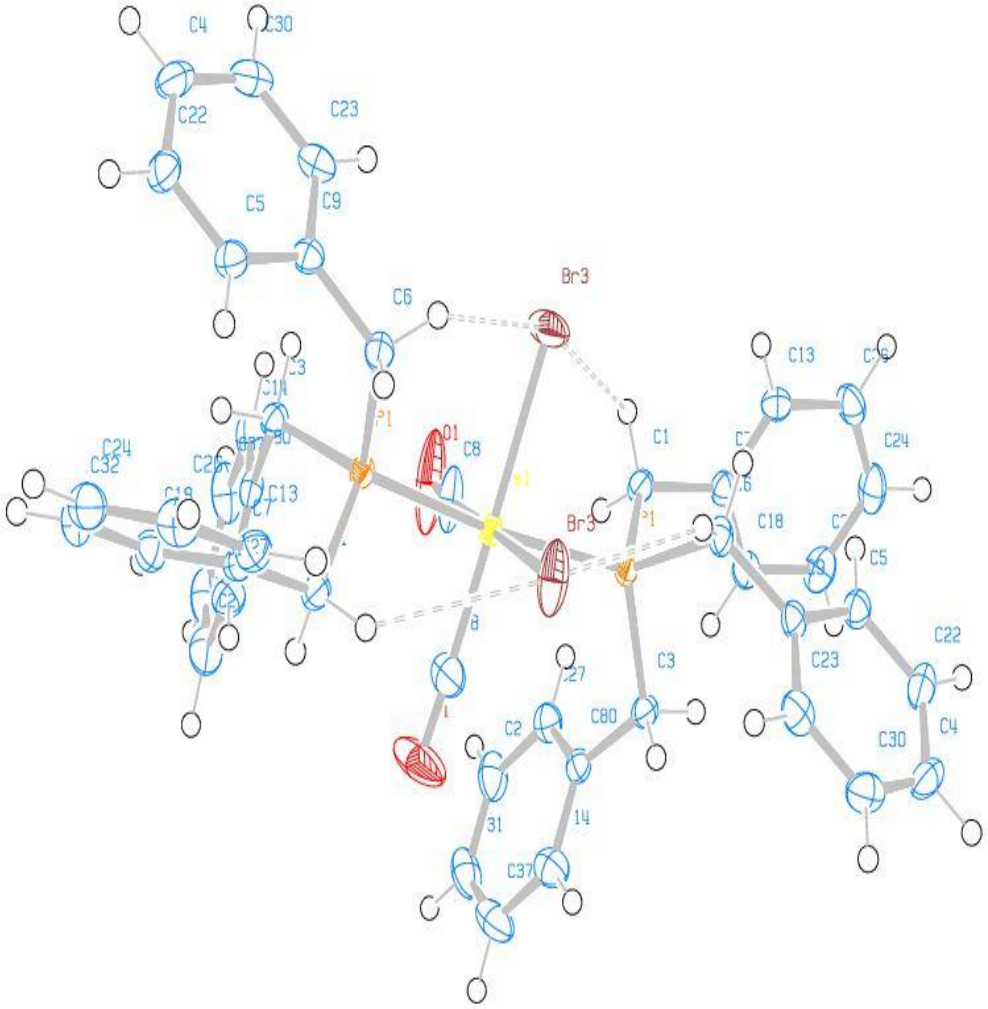

Figure 2.15: Thermal ellipsoid plot (50% probability level) of $[OsBr_2(CO)_2\{P(CH_2C_6H_5)_3\}_2]$ (**3b**).

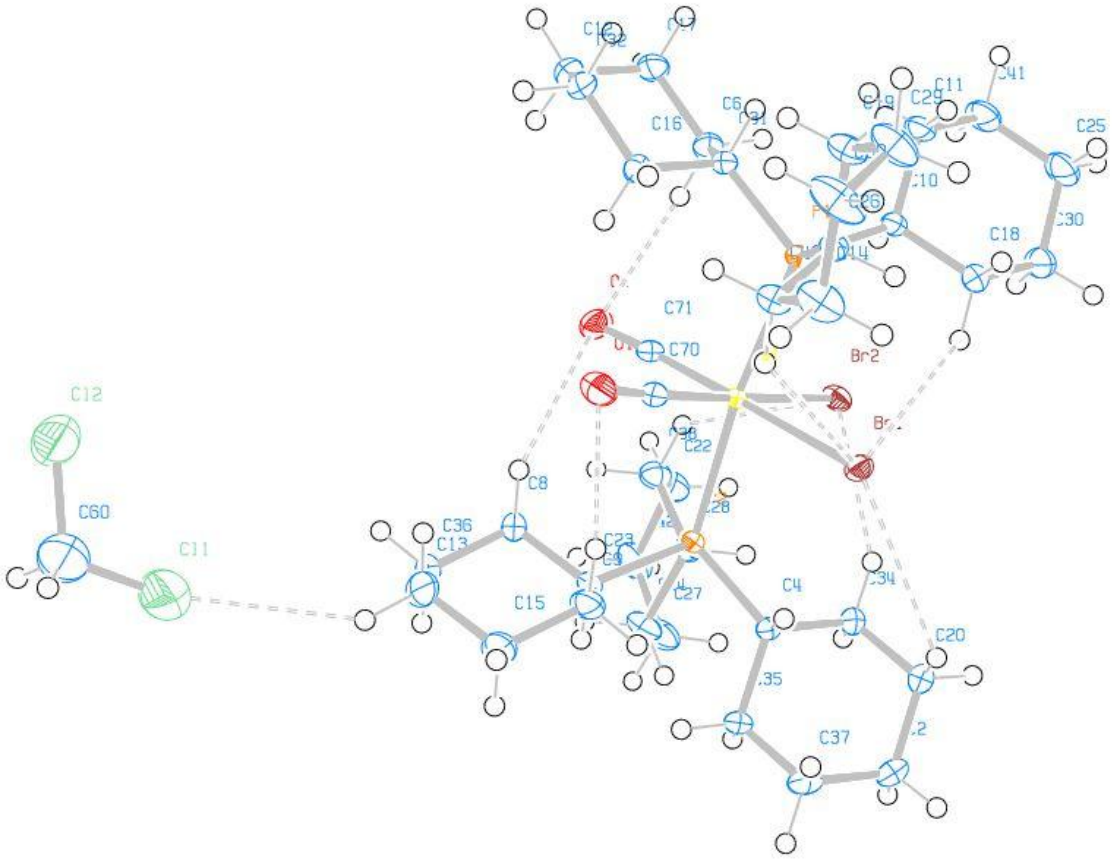

Figure 2.16: Thermal ellipsoid plot (50% probability level) of $[OsBr_2(CO)_2\{P(C_6H_{11})_3\}_2]\cdot CH_2Cl_2$ (**4b**).

2.4 Conclusions

Complexes of the type $[OsX_2(CO)_2(PR_3)_2]$ (where X = Cl, Br, I; PR_3 = $P(C_6H_5)_3$, $Ph_2P(CH_2C_6H_5)$, $P(CH_2C_6H_5)_3$, $P(C_6H_{11})_3$) can easily be prepared using Collman's method of preparation, which involves the reductive carbonylation of $Y_2[OsX_6]^{2-}$ (Y= NH_4 or K; X = Cl, Br, I) with subsequent addition of appropriate phosphine ligand, PR_3, to produce the respective complexes. This is a convenient route for synthesis of *cis*,*cis*,*trans*-configuration of these type of complexes. Vibrational spectroscopic data shows that ν(CO) varies in a systematic way with change in X and PR_3. The carbonyl stretching frequency decreases with increasing π-acceptor ability of PR_3 ligand. Whilst ν(CO) decreases in the order Cl > Br > I, which is constistent with the inductive power of the halide ligands.

Some discrepancies with change in PR_3 were observed in ^{31}P NMR data. Explained by the difference in the π-acceptor capabilities of the phosphine ligands and the size of the cone angle. A downfield chemical shift in the $^{31}P\{H\}$ NMR spectrum correlates with an increase in cone angle.

Thermogravimetrical analysis shows a two-stage decomposition process for complexes **1a-c**, **2a-3b** and one-step for complexes **4a** and **4b**. The first stage is associated with loss of halides and CO groups. The second stage of decomposition correlates with loss of the phosphine ligands. All complexes are stable until temperatures above 190.00 °C.

X-ray crystallographic data further confirmed the stereochemistry of compounds as *cis*,*cis*,*trans*-$[OsBr_2(CO)_2\{Ph_2P(CH_2C_6H_5)\}]$ **2b**, *cis*,*cis*,*trans*-$[OsBr_2(CO)_2\{P(CH_2C_6H_5)_3\}]$ **3b** and *cis*,*cis*,*trans*-$[OsBr_2(CO)_2\{P(C_6H_{11})_3\}]$ **4b** complexes as suggested by other spectroscopic studies.

2.5 References

(1) Das, A.; Peng, S.-M.; Bhattacharya, S. *Polyhedron* **2000**, *19*, 1227.

(2) Gupta, P.; Basuli, F.; Peng, S.-M.; Lee, G.-H.; Bhattacharya, S. *Ind. J. Chem.* **2003**, *42A*, 2406.

(3) Carlson, B.; Phelan, G. D.; Benedict, J.; Kaminsky, W.; Dalton, L. *inorg. Chim. Acta* **2004**, *357*, 3967.

(4) Wozna, A.; Kapturkiewics, A.; Angulo, G. *Inorg. Chem. Commun.* **2013**, *37*, 26.

(5) Kamecka, A.; Kapturkiewicz, A.; Karczmarzyk, Z.; Wysocki, W. *Inorg. Chem. Commun*. **2013**, *27*, 138.

(6) Graux, L. V.; Giorgi, M.; Buono, G.; Clavier, H. *Organometallics* **2015**, *34*, 1864.

(7) Yin, X., -F; Lin, H.; Jia, A., -Q; Chen, Q.; Zhang, Q., -F *J. Coord. Chem.* **2013**, *66*, 3229.

(8) Marhenke, J.; Joseph, C. A.; Corliss, M. Z.; Dunn, T. J.; Ford, P. C. *Polyhedron* **2007**, *26*, 4638.

(9) Dharmaraj, N.; Viswanathamurthi, P.; Natarajan, K. *Transition Met. Chem. (Dordrecht, Neth.)* **2001**, *26*, 105.

(10) Collman, J. P.; Roper, W. R. *J. Am. Chem. Soc.* **1966**, *88*, 3504.

(11) Goeden, G. V.; Haymore, B. L. *Inorg. Chim. Acta.* **1983**, *71*, 239.

(12) Clark, C. S. H.; Coleman, K. S.; Fawcett, J.; Holloway, J. H.; Hope, E. G.; Redding, J.; Russell, D. R. *Polyhedron* **1999**, *18*, 1207.

(13) Hales, L. A. W.; Irving, R. J. *J. Chem. Soc. (A)* **1967**, 1389.

(14) Coleman, K. S.; Fawcett, J.; Holloway, J. H.; Hope, E. G.; Russell, D. R. *J. chem. Soc., Dalton Trans.* **1997**, 3557.

(15) Venturi, C.; Bellachioma, G.; Cardaci, G.; Macchioni, A. *Inorg. Chim. Acta.* **2004**, *357*, 3712.

(16) Irving, R. J.; Magnusson, E. A. *J. Chem. Soc.* **1958**, 2283.

(17) Raj, J. G. J.; Pathak, D. D.; Kapoor, P. N. *J. Mol. Struct.* **2015**, *1087*, 41.

(18) Rath, N. P.; Stouffer, M.; Janssen, M. K.; Bleeke, J. R. *Acta. Crystallograp. Sect E. Struct Rep Online* **2011**, *E67*.

(19) Saunders, D. R.; Stephenson, M.; Mawby, R. J. *J. Chem. Soc.* **1983**, 2473.

(20) Guns, M. F.; Claeys, E. G.; Van der Kelen, G. P. *J. Mol. Struct.* **1979**, *54*, 101.

(21) Robinson, P. D.; Hinckley, C. C.; Ikuo, A. *Acta. Crystallogr. Sect C: Cryst. Struct. Commun.* **1988**, *C44*, 1491.

(22) Diz, E. L.; Therrien, B.; Neels, A.; Suss-Fink, G. *Acta. Crystallograp. Sect E. Struct Rep Online* **2002**, *58*, m404.

(23) Brewer, S. A.; Coleman, K. S.; Fawcett, J.; Holloway, J. H.; Hope, E. G.; Russell, D. R.; Watson, P. G. *J. Chem. Soc., Dalton Trans.* **1995**, 1073.

(24) Kendall, A. J.; Zakharov, L. N.; Tyler, D. R. *Inorg. Chem.* **2016**, *55*, 3079.

(25) Landry, V. K.; Parkin, G. *Polyhedron* **2007**, *26*, 4751.

(26) Batsanov, S. S. *Inorg. Mat.* **2001**, *37*, 871.

Chapter 3

Microwave-assisted synthesis of Os(II) halido diphosphine complexes

3.1 Background

3.1.1 Microwave-promoted synthetic technique

Microwave heating involves applying electromagnetic radiation to chemical reactions. This heating involves conversion of electromagnetic energy to thermal energy, which is dependent on the dielectric constant of the material irradiated. Solvents with a high dielectric constant such as water (H_2O) and dimethylformamide (DMF) are heated rapidly with microwave radiation. However, those with a low dielectric constant, such as hexane (C_6H_{14}) and benzene (C_6H_6), do not couple and therefore do not heat rapidly using microwave radiation. The heating effect utilized in microwave assisted transformations is mainly due to change in dipole moment caused by the interaction of the molecule with the radiation. Microwave-assisted synthesis has many advantages reported by Kappe and other researchers.[1-3] These includes the following:

i. Reduced solvent usage
ii. Accelerated reaction rate
iii. Reduced reaction time
iv. Higher product yield
v. Milder reaction conditions
vi. Different reaction selectivities
vii. Broad applicability – few limitations as to the type of synthesis chemistry

These advantages have attracted a lot of research using microwave reactors in synthesis. Organic synthetic chemists have long enjoyed the benefits that microwave heating affords.[4-7] In contrast, fewer reports on the use of microwave reactors in preparation of organometallic compounds are available.[8-10] Early work on preparation of organometallic compounds was carried out in 1989, a few years after pioneering work in microwave-assisted organic synthesis. This work involved synthesis of rhodium(I) and iridium(I) dimers of the type $[M_2Cl_2(\text{di-olefin})_2]$ from metal halides, MCl_3, in alcoholic solvent.[11] A year later various complexes were prepared using a similar methodology. The reaction rates were demonstrated to have been dramatically increased and product yield improved compared to conventional method of synthesis. Lasri also demonstrated reactions that were accelerated using microwave reactors in the synthesis of palladium tetrazolato complexes.[12]

Not only can microwave heating reduce reaction time of known reactions but it can also result in new chemistry. Pyper and colleagues reported the one-step preparation of compounds of the type $[Os_2(\mu\text{-}O_2CR)_2(CO)_6]$.[3] They obtained higher yields and their reaction did not require an inert environment compared to conventional technique. The reaction rate can also be manipulated by choice of solvent. Subsequent studies have shown that microwave heating is effective in synthesis of a variety of metal-containing compounds using simpler procedures and/or fewer steps than previously reported. The microwave heating technique has proved most fruitful.

Monitoring of reactions in a microwave reactor has been a limitation, however the group of Leadbeater was able to overcome this problem using *in situ* Raman spectroscopy to monitor substitution reaction of $Mo(CO)_6$.[2]

To the best of our knowledge no previous work has been reported on microwave-promoted reactions of $[OsX_6]^{2-}$, including its conversion to $[OsX_2(P{-}P)_2]$.

3.1.2 $OsX_2(P–P)_2$ complexes

Transition metal complexes bearing chelating diphosphine ligands have enjoyed widespread interest for several decades. This is owed to their potential use as catalysts, molecular electronic devices and use in organic synthesis.[13-16] Steric and electronic effects as well as the chelate ring size have been found to influence the reaction rate, stability and selectivity of these complexes.[17]

The chemistry of transition metal-halide complexes containing diphosphine ligands of the type $[MX_2(P–P)_2]$ (M = Ru, Os; P–P = diphosphine ligand) is well established. Considerable research demonstrates the use of these complexes as precursors for preparation of complexes which have found use in various applications.[18-24] These complexes have properties that make the compounds useful molecular electronic components. Some of these properties are achieved by replacement of the halide ligand with aliphatic or benzylic amines or an electron rich ligand which led to preparation of complexes with interesting electrochemical behaviour.[24]

3.1.3 Preparatory methods

Complexes of the type $[MX_2(P–P)_2]$ are commonly prepared by applying methods first reported by Chatt and Hayter.[25] Their work involved the reaction of metal halides, such as $RuCl_3$ and $(NH_4)_2OsCl_6$, as precursors with excess diphosphine ligand in alcohol medium (Scheme 3.1). This method afforded *trans*-$[MCl_2(P–P)_2]$ {P–P = $C_2H_4(PR_3)_2$ (R = Me, Et, Ph), $CH_2(PPh_2)_2$ and *o*-$C_6H_4(PEt_2)_2$ (Scheme 3.1 Eq 1) in 30 – 80% yield. The *cis* isomer is obtained *via* a different method which involves the substitution of a monophosphine ligand with a diphosphine ligand in the absence of a solvent at high temperatures. This method also demonstrated that an increase in the alkyl group spacer in the diphosphine ligands affects the stereochemistry of the product. Reaction with dppm ligand gave the *cis*-isomer while dppe

gave *trans* isomer. The *cis* isomers can also be prepared using a dinuclear complex, $[M_2Cl_3(PR_3)_6]$, as a precursor by reacting with diphosphine ligand in absence of a solvent at high temperatures (Scheme 3.1 Eq 2). Chatt and Hayter also demonstrated preparation of *cis* complex by isomerisation of *trans*-complex in the presence of excess of aluminium trialkyls AlR_3 (R = Me, Et or Pr^n) (Scheme 3.1, Eq 3). Metathetical replacement using the appropriate salt can also produce these complexes (Scheme 3.1, eq. 4).

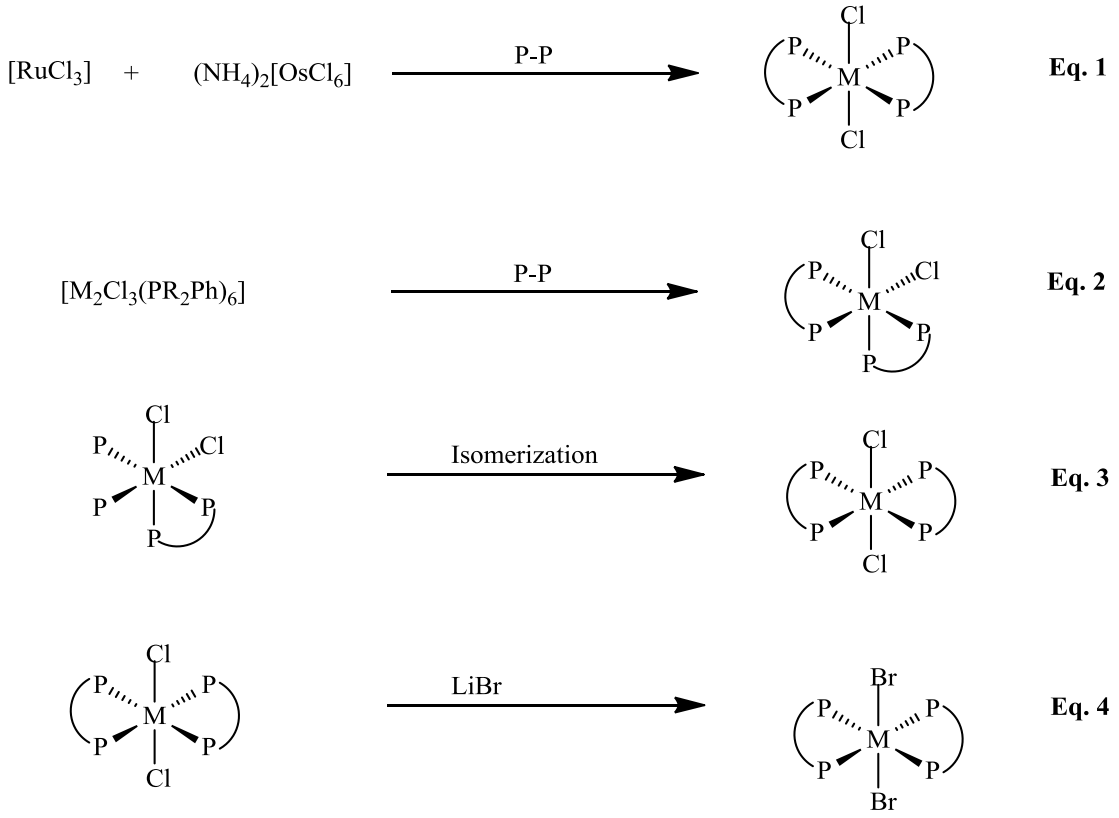

Scheme 3.1: Synthesis of $[MX_2(P–P)_2]$ (where M = Ru, Os; X = Cl, Br; P–P = diphosphine ligand) reported by Chatt and Hayter.[25]

Recently, Al-Noaimi modified one of Chatt procedures. He prepared the *trans*-$[RuX_2(P–P)_2]$ complexes from $[RuCl_2(PPh_3)_3]$ by stirring at room temperature for less than an hour and obtained high yields (Scheme 3.2).[26]

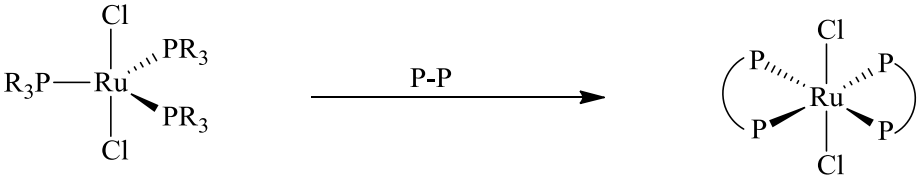

Scheme 3.2: Synthesis of $[OsCl_2(P–P)_2]$ (P–P = diphosphine ligand) reported by Al-Noaimi.[26]

An alternative approach was developed by McDonagh and coworkers (Scheme 3.3). They show selective preparation of either *cis* or *trans*-isomers of the diphosphine complex from DMSO substituted complexes *cis*/*trans*-$[OsCl_2(DMSO)_4]$.[27]

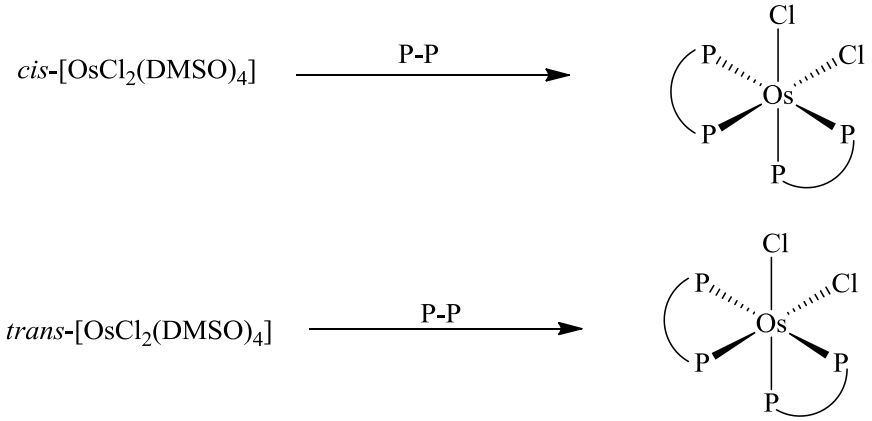

Scheme 3.3: Synthesis of *cis*/*trans*-$[OsX_2(P–P)_2]$ reported by the group of McDonagh.[27]

3.1.4 Focus of this study

In this section we report a synthetic strategy for the convenient preparation of Os(II) halido complexes containing chelating P donor ligands (P–P = dppm, dppe, dppp) using microwave heating techniques (Scheme 3.4). Direct reduction of the osmium salt, $Y_2[OsX_6]$ (Y = NH_4,

K; X = Cl, Br, I) in alcohol solvent is achieved. Chart 3.1 is a representative of complexes synthesised in this chapter.

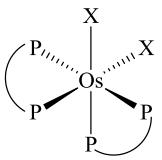

5a X = Cl, P-P = dppm
5b X = Br, P-P = dppm
5c X = I, P-P = dppm

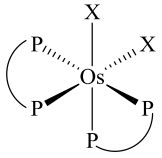

6a X = Cl, P-P = dppe
6b X = Br, P-P = dppe
6c X = I, P-P = dppe
7a X = Cl, P-P = dppp
7b X = Br, P-P = dppp
7c X = I, P-P = dppp

Chart 3.1: List of Os(II) halide diphosphine complexes prepared in this study.

3.2 Synthesis

Direct reduction of $[OsX_6]^{2-}$ is accomplished in the presence of the diphosphine ligands *via* a dissociative substitution pathway (Scheme 3.4). In this mechanism, the metal-halide bond is fully broken before the metal-phosphine bond is formed.

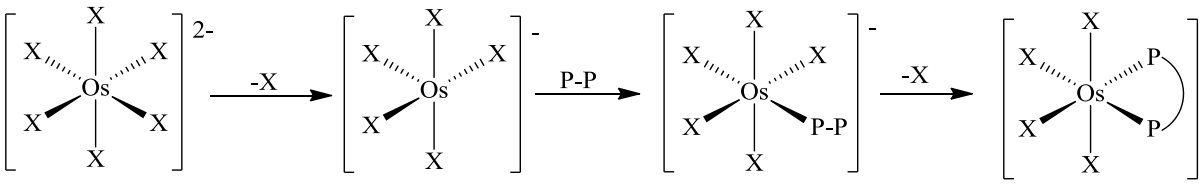

Scheme 3.4: Dissociative ligand substitution pathway.

Excess diphosphine ligand allows subsequent substitution of halide ligand with formation of chelate ring.

Reaction of $[OsX_6]^{2-}$ with 4 equivalents of 1.1-bis(diphenylphosphino)methane, dppm, in 2-methoxyethanol under microwave (MW) irradiation (30 min, 80 °C, 200 W) produced only the *cis* isomer identified by ^{31}P NMR spectroscopy. This reaction selectively gave *cis* isomers

of $[OsX_2(P–P)_2]$. However, using the same reaction conditions where P–P = dppe, dppp, produced *trans* isomers (Scheme 3.5). Increasing the number of methylene groups in the spacer between the two phosphorus atoms exerts significant steric influence. Also increasing the bite angle (Figure 3.1) of diphosphine ligands has an effect on the stereochemistry of the product. Diphosphine ligands with small bite angles occupy equatorial and axial positions. As the bite angle increases the diphosphine ligand preferentially occupies a pair of equatorial positions to avoid steric hindrance. The effect of the bite angle on the regioselectivity is explained by the steric crowding at the metal centre as a consequence of interaction of phenyl groups. Thus, dppe and dppp occupies the equatorial positions.[28]

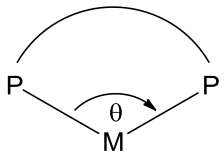

Figure 3.1: Structure illustrating bite angle.

The desired Os(II) halide phosphine complexes are formed in moderate to high yield, 25-92%. The complexes are characterized by ^{1}H and ^{31}P NMR spectrometry as well as FT-IR and Raman vibrational spectroscopy.

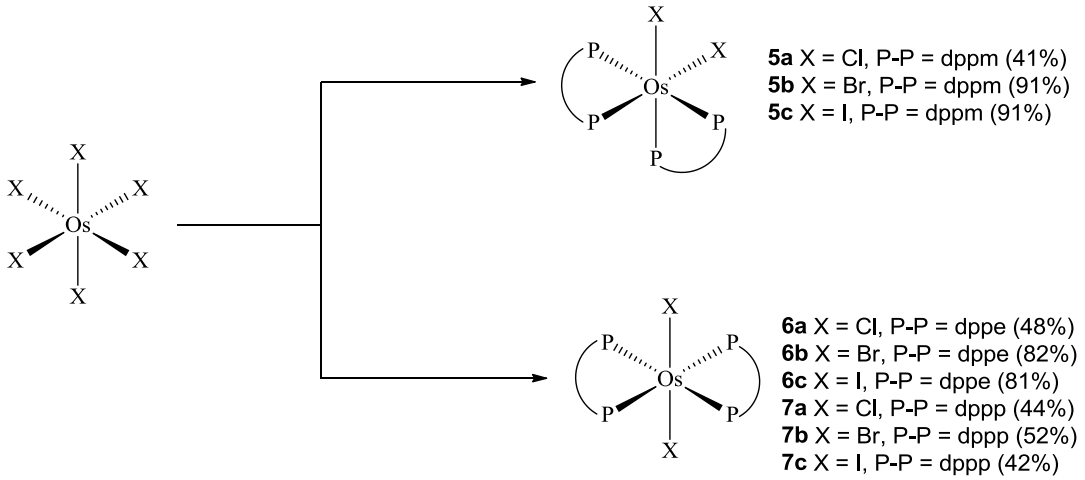

Scheme 3.5: Microwave-promoted synthesis of complex **5a-7c.**

3.3 Results and discussion

The complexes $[OsX_2(P–P)_2]$ **5a-7c** were characterized using NMR spectroscopy, as well as solid state FT-IR and Raman spectroscopy.

3.3.1. ^{1}H NMR spectroscopy

The NMR spectra of complexes **5a-7c** were recorded in $CDCl_3$ and chemical shifts are given in Table 3.1. Slow decomposition of products in solution with time was observed in the spectra with broadening of the signals in most complexes.

The ^{1}H NMR spectra of the prepared complexes featured characteristic resonances arising from diphosphine ligands (dppm, dppe, dppp). Integration of the ^{1}H resonance confirms the P–P ratio is in agreement with the structural composition *cis*-$[OsX_2(P–P)_2]$, **5a-c**, and *trans*-$[OsX_2(P–P)_2]$, **6a-7c**. The complexes *cis*-$[OsX_2(dppm)_2]$, X = Cl, Br, I exhibited similar ^{1}H NMR spectra showing two types of resonances assigned to methylene and aromatic protons. Change in halide ligands influences the resonance as shown by difference in methyl and aromatic chemical shifts for complex **5a** (4.40, 5.90, 6.47 – 8.12 ppm), **5b** (4.79, 5.93, 6.63 – 8.22 ppm) and **5c** (4.92, 6.10, 6.63 – 8.29 ppm). Deshielding is affected by the π-bonding capabilities of the halides.

Table 3.1: NMR spectroscopic data for *cis*-[$OsX_2(P–P)_2$] complexes. Recorded in $CDCl_3$.

Complex	δ($^{31}P\{^1H\}$) ppm	δ(^1H NMR) ppm
free ligand (**dppm**)	-22.2	2.84 (s, 1H, CH_2), 7.32 (s, 12H, Ar), 7.46 (s, 8H, Ar)
5a		4.40(s, 2H, CH_2), 5.90 (s, 2H, CH_2), 6.47 – 8.12 (m, 40H, Ar)
5b	-72.8 (t, $J_{(PP)}$ = 46.0 Hz), -57.9 (t, $J_{(PP)}$ = 46.0 Hz)	4.87 - 4.69 (m, 2H, CH_2), 6.02 - 5.85 (m, 2H, CH_2), 6.63 – 8.22 (m, 40H, Ar)
5c	-83.5 (t, $J_{(PP)}$ = 44.8 Hz), -64.4 (t, $J_{(PP)}$ = 44.8 Hz)	4.99 - 4.84 (m, 2H, CH_2), 6.19 - 6.02 (m, 2H, CH_2), 6.63 – 8.23 (m, 40H, Ar)

The chemical shifts of the methylene as well as the aromatic protons of the coordinated diphosphine ligands occur downfield compared to the free ligands. It is clear that complexation to the metal has a marked influence on the chemical shift of the protons. The downfield shift is caused by withdrawal of the electron density from the diphosphine ligand to the metal centre, deshielding the nucleus and shifting downfield.

The ^1H NMR spectrum of complex **5b** exhibits resonances assigned to methylene and aromatic protons (Figure 3.2). The two CH_2 groups resonate as two sets of broad multiplets at δ 5.93 and 4.79 ppm intergrated to 1:1 ratio. This is an indication that the two protons on CH_2 are diastereotopic (AB spin pattern).[29] This has been reported before for the *cis*-[$Ru(dppm)_2C_2O_4$], *cis*-[$Ru(dppm)_2(N_3)_2$] and *cis*-[$Ru(dppm)_2ClN_3$] complexes.[24] The multiplet nature is due to the ^1H-^1H and ^1H-^{31}P coupling.

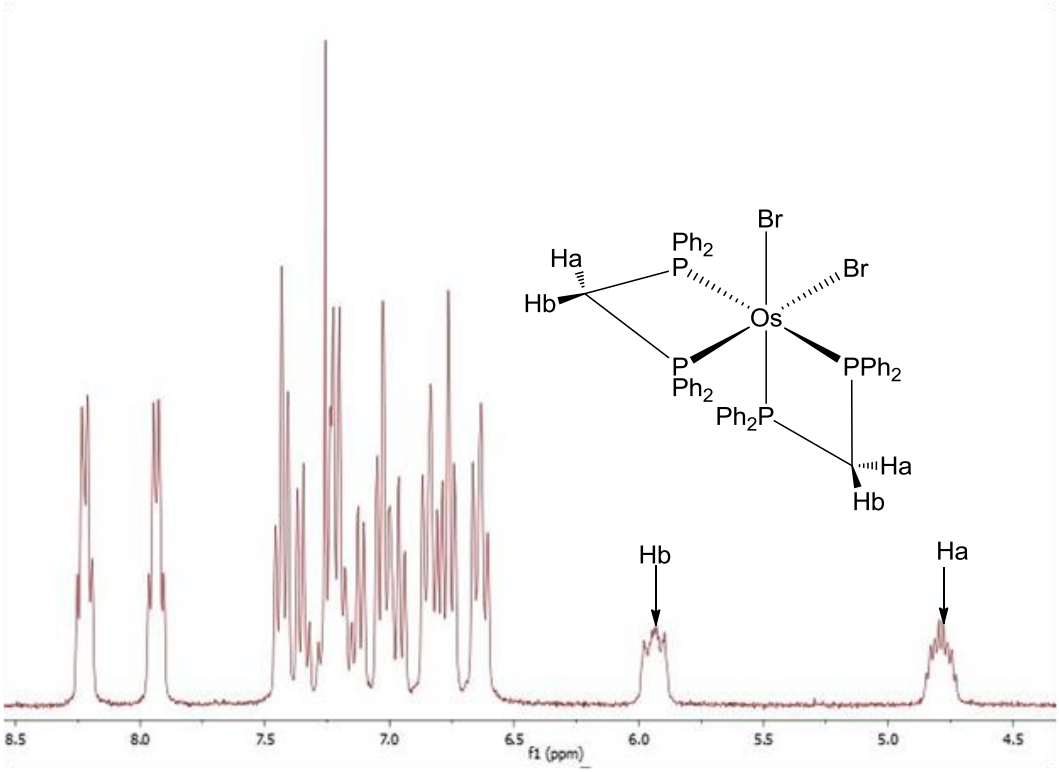

Figure 3.2: ^{1}H NMR spectrum of *cis*-[$OsBr_2(dppm)_2$], **5b.**

The aromatic region in the spectrum consists of several coupled multiplets due to the aromatic protons of the phenyl rings of the diphosphines. The distinct proton signals for the phenyl rings indicate the different environment, phenyl protons in *cis* position with the halide exhibits resonances further downfield and those that are in *trans* arrangement with the halide are upfield.

The NMR spectra of the complexes **6a-c** exhibit resonances assigned to the aromatic and methylene protons (Table 3.2). The ^{1}H NMR spectrum of complex **6b** is shown in Figure 3.3. The 4 methylene protons resonate as two broad singlets at δ 2.60 and 2.13 ppm intergrated to a 1:1 ratio. This is an indication that the two protons on CH_2 are diastereotopic (AB spin pattern). A downfield shift is also observed with change in X for complex *trans*-[$OsX_2(dppe)_2$] with the iodido complex showing chemical shifts at higher resonance and the

chlorido complex at lower resonance (Table 3.2). A consequence of π-bonding capabilities of halide ligands.

Table 3.2: NMR spectroscopic data for *trans*-[$OsX_2(P–P)_2$] complexes. Recorded in $CDCl_3$.

Complex	$\delta(^{31}P\{^1H\})$	δ (^1H NMR)
Free ligand (**dppe**)	-12.6	2.13 (s, 2H, CH_2), 7.34 (d, *J* = 12.0 Hz, 20H)
6a		2.29 (s, 4H, CH_2), 6.92 - 7.45 (m, 20H, Ar)
6b	29.6 (s)	2.13 (s, 2H, CH_2), 2.67 (s, 2H, CH_2), 6.96 - 7.27 (m, 20H, Ar)
6c	26.5 (s)	2.12 (s, 2H,CH_2), 2.67 (s, 2H, CH_2), 6.70 – 7.91 (m, 20H, Ar)
Free ligand (**dppp**)	-17.5	1.66 (m, 2H, CH_2), 2.24 (m, 4H, CH_2), 7.30 (m, 12H, Ar), 7.37 (d, *J* = 38.6 Hz, 8H, Ar)
7a		2.38 (m, 3H, CH_2), 3.07 (m, 3H, CH_2), 6.85 – 7.35 (m, 20H, Ar
7b	-25,2 (s)	1.58 (d, *J* = 12.2 Hz, 4H), 2.39 (m, 2H, CH_2), 3.07 (m, 2H, CH_2), 7.11 (m, 40H, H-aromatic)
7c	31.9 (s)	2.48 (m, CH_2), 3.10 (m, CH_2), 6.86 – 7.68 (m, 20H, Ar)

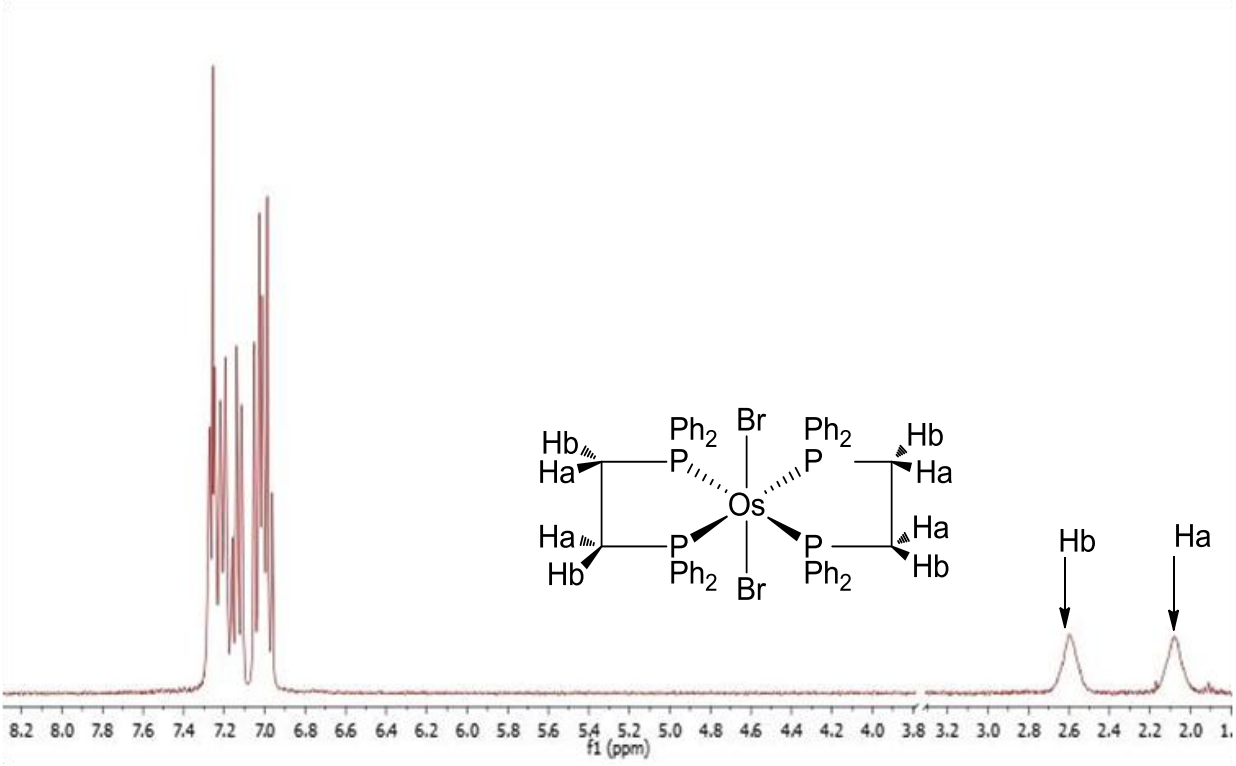

Figure 3.3: ^{1}H NMR spectrum of *trans*-[$OsBr_2(dppe)_2$], **6b**.

The ^{1}H NMR spectrum of **7b** exhibits proton signals of phenyl groups as multiplets in the range δ 6.85 – 7.35 ppm, and signals of methylene protons at δ 3.07, 2.38 and 1.58 ppm, their peak intergration ratio is about 10:1:1:1 (Figure 3.4). The methylene protons give rise to three resonances because the protons are diastereotopic. The strong P-*trans*-P coupling gives rise to the multiplet pattern seen in the alkyl region.[23] A downfield shift is observed with change in X with the iodido complex **3c** showing resonances at higher frequencies compared to the bromido and chlorido complex.

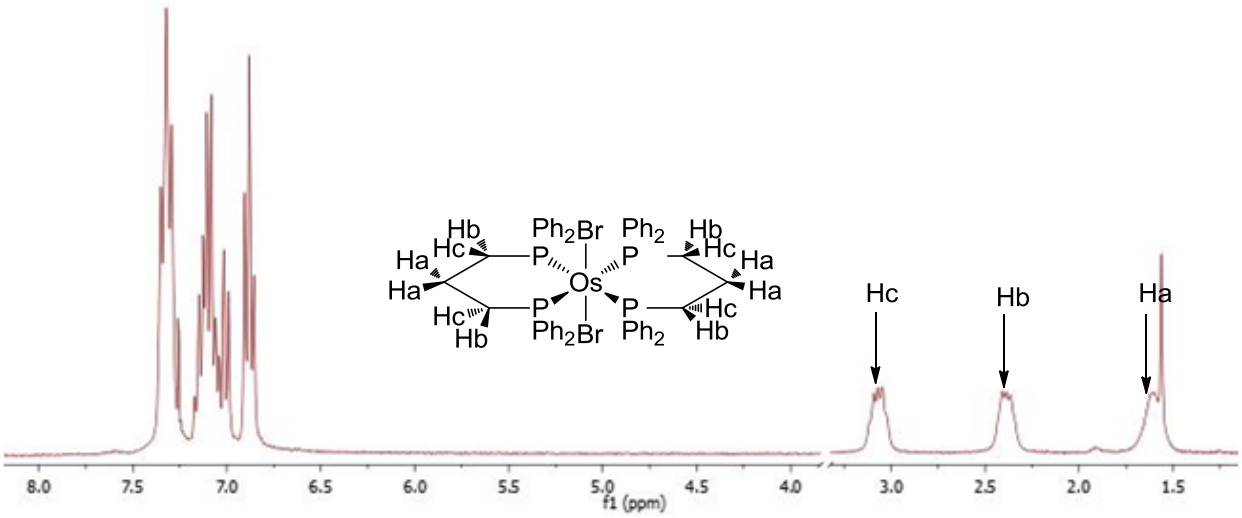

Figure 3.4: ^{1}H NMR spectrum of *trans*-[$OsBr_2(dppp)_2$], **7b**.

3.3.2 ^{31}P{H} NMR spectroscopy

The ^{31}P NMR data for complexes **6a-7c** are given in Table 3.2. The *cis* and *trans* isomers are easily distinguished by their ^{31}P NMR spectra. The ^{31}P NMR spectra of *cis* complexes show a pair of triplets which suggests that two pairs of P atoms that are magnetically inequivalent.[26] The ^{31}P{H} NMR spectra of the *trans* isomer exhibits a singlet which suggets the presence of four equivalent nuclei.

The ^{31}P{H} NMR spectrum in $CDCl_3$ solution show a pair of triplets at δ -72.8 and -57.9 (t, $J_{(PP)}$ = 46.0 Hz) ppm for **5b** (Figure 3.5) , δ -83.5 and -64.4 (t, $J_{(PP)}$ = 44.8 Hz) ppm for **5c**. The shielded signal is assigned to the pair of phosphorus atoms *cis* to the halides and the deshielded signal is due to the phosphorus atoms trans to the halides, which is consistent with

the proposed structure in which halides are mutually *cis*.[30,31] Unfortunately, attempts to observe $^{31}P\{H\}$ NMR spectrum for complex **1a** were unsuccessful.

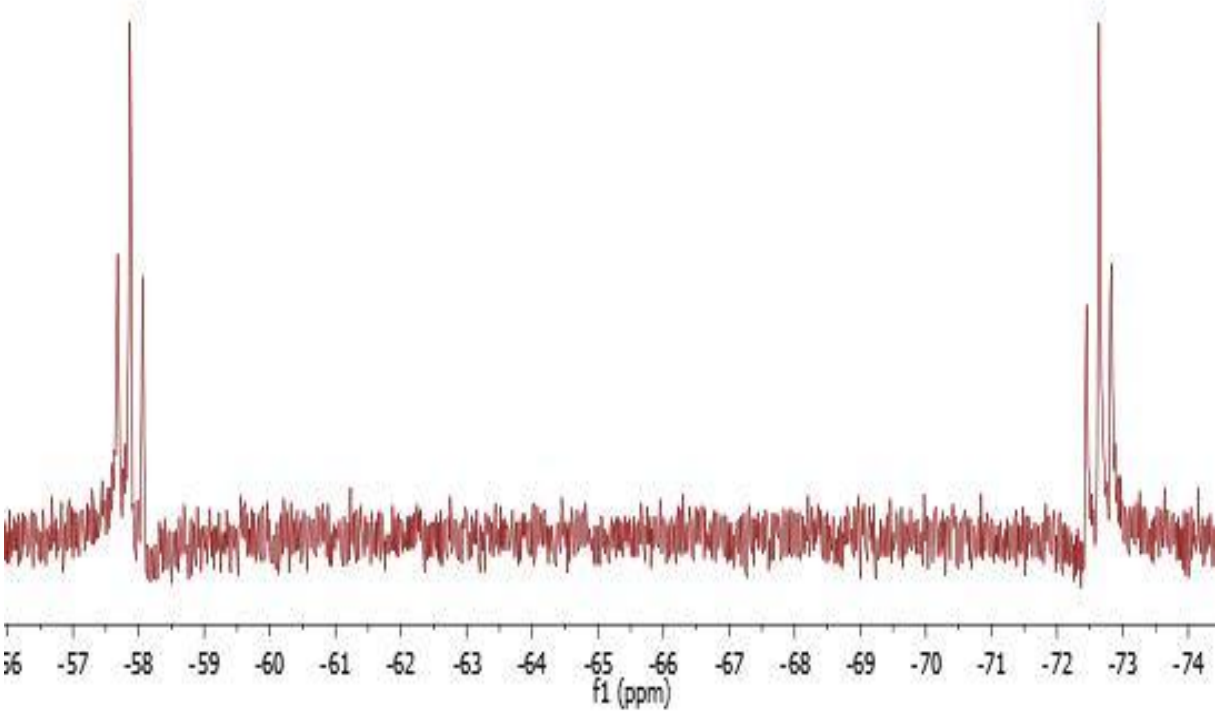

Figure 3.5: $^{31}P\{H\}$ NMR spectrum of *cis*-[$OsBr_2(dppm)_2$], **5b**.

A decrease in chemical shift and *J* coupling constant is observed as X is varied from Br to I in the *cis*-[$OsX_2(P–P)_2$] complex. The decrease in coupling constant is in agreement with the order of *trans* influence of I > Br > Cl.[32]

The ^{31}P NMR spectra exhibit a sharp singlet at δ 23.0 ppm for **6b** (Figure 3.6), at δ 26.4 ppm for **6c,** at δ -25.2 for **7b** and at δ 32.4 ppm for **7c**. The singlet suggests that the P atoms in these complexes are chemically and magnetically equivalent, which suggests that the phosphine ligands occupy the equatorial positions with halide ligands *trans* to each other.

The difference in ^{31}P NMR chemical shift can be explained by the size of the cone angle. As this angle increases, the phosphorus chemical shift moves upfield. Analyses of the ^{31}P NMR data obtained reveal that the ring size of the chelating phosphine ligand also contributes to the chemical shift. As explained by Slack and Baird, the 5-membered ring has positive (deshielding) ring contributions while the 4 and 6-membered rings have negative (shielding) contributions to the chemical shift as observed in ^{31}P NMR spectra of **6b-7c**.[26,33,34] It has been suggested that the shift is a consequence of a large ring strain introduced by the 5-membered chelate ring. An extremely large downfield shift of the P nuclei occurs upon complexation of the dppe ligand. This is also observed in complexes containing phosphorus in 5-membered ring.[26,30]

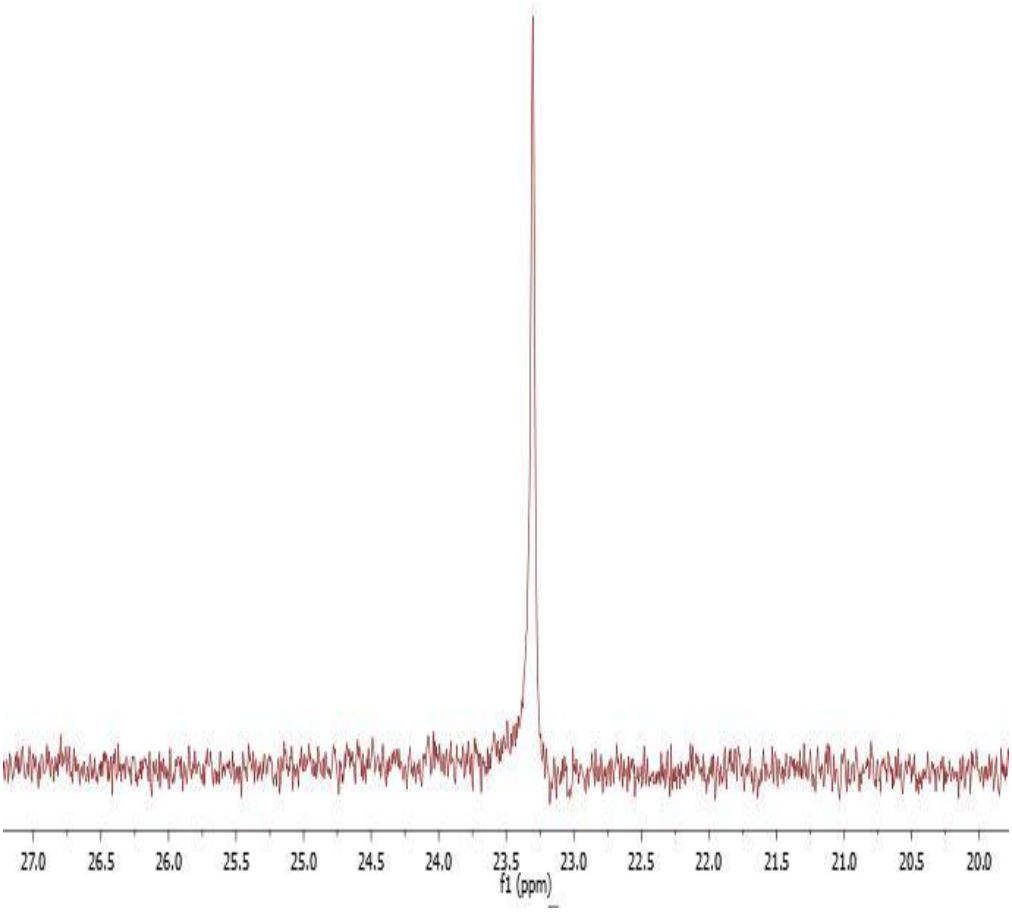

Figure 3.6: ^{31}P NMR spectrum of *trans*-[$OsBr_2(dppe)_2$], **6b.**

3.3.3 FT-IR spectroscopy

The IR data of complexes **5a-7c** are given in Table 3.3. These complexes show four sets of characteristic absorptions in the ranges 3000 - 3100, 2984 – 2912, 1588 - 1572 and 1090-1087 cm^{-1}, which can be assigned to aromatic C-H stretches, alkane C-H bending, and P-Ar stretches respectively (Figure 3.7).

Table 3.3: Selected IR spectroscopic data.

Complex	IR stretches (cm^{-1})[a]			
	Aromatic C–H	Alkane C–H	Aromatic C=C	P-Ar
5a	3055	2913	1572	1090
5b	3070	2984	1572	1093
5c	3045	2913	1584	1090
6a	3052	2917	1585	1090
6b	3071	2922	1585	1088
6c	3050	2950	1583	1087
7a	3046	2925	1588	1090
7b	3047	2912	1585	1091
7c	3071	2940	1585	1089

[a]Recorded in solid state

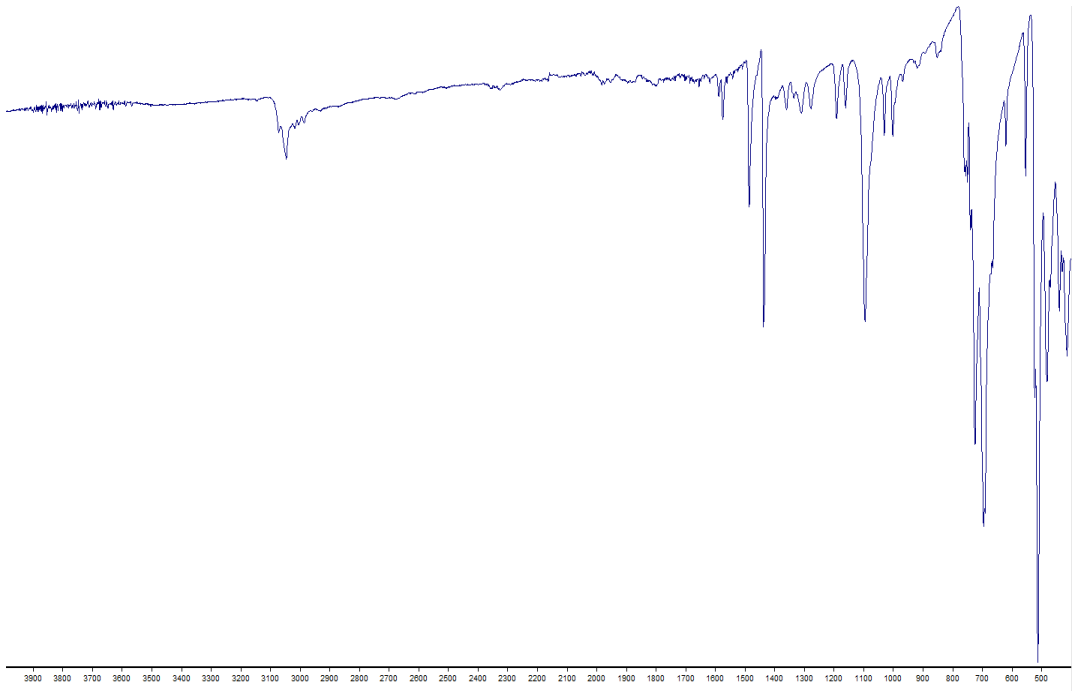

Figure 3.7: Solid FT-IR spectrum of complex *cis*-[$OsI_2(dppm)_2$].

3.3.4 Thermogravimetric analysis

Thermal decomposition of the complexes was studied and found to be a two-stage process that can be directly related to the ligands loss. The studies were carried out in the 100 – 1300 °C temperature range under nitrogen gas at a heating rate of 10 °C/min. The first stage is associated with loss of halides and second stage associated with loss of diphosphine ligand (Figure 3.8 – 3.10). Onset of decomposition is at 370, 374 and 343 °C for complex **5a**, **5b** and **5c**, respectively (Figure 3.8). The *trans* complexes **6a**, **6b** and **6c** are stable to temperatures just above 300 °C (Figure 3.9). Complexes **7a**, **7b** and **7c** start to decompose in the range 195 – 251 °C (Figure 3.10).

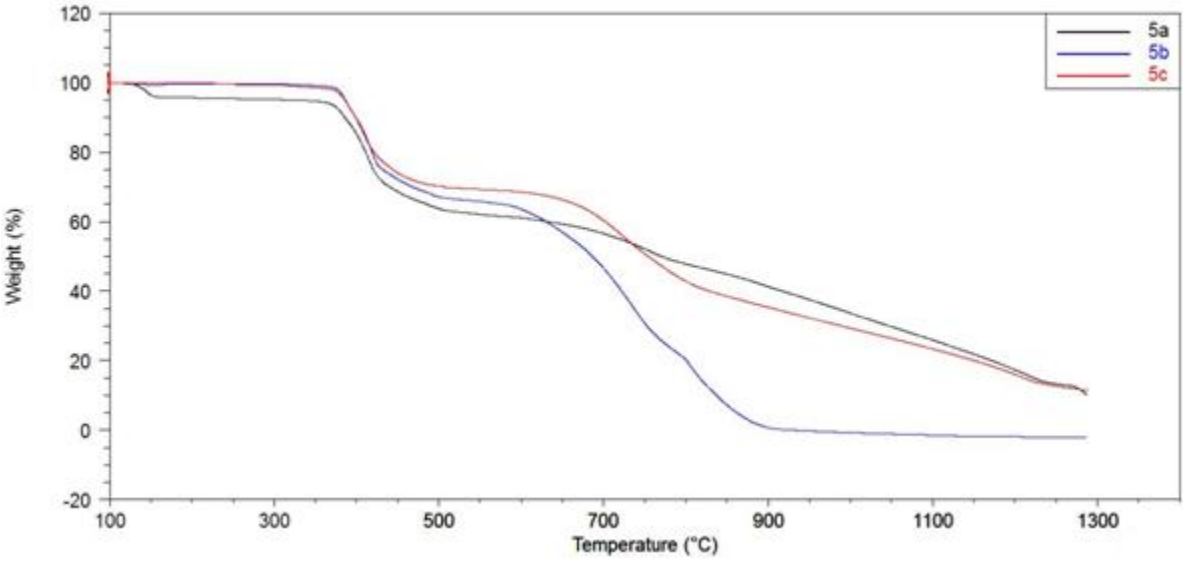

Figure 3.8: Thermogram showing decomposition of complexes **5a-c**.

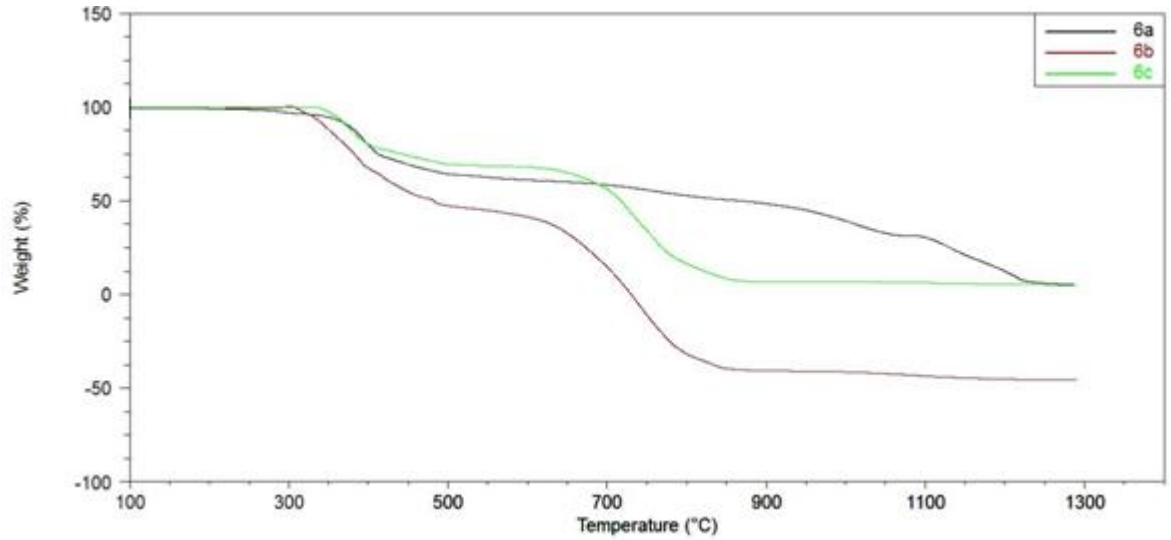

Figure 3.9: Thermogram showing decomposition of complexes **6a-c**.

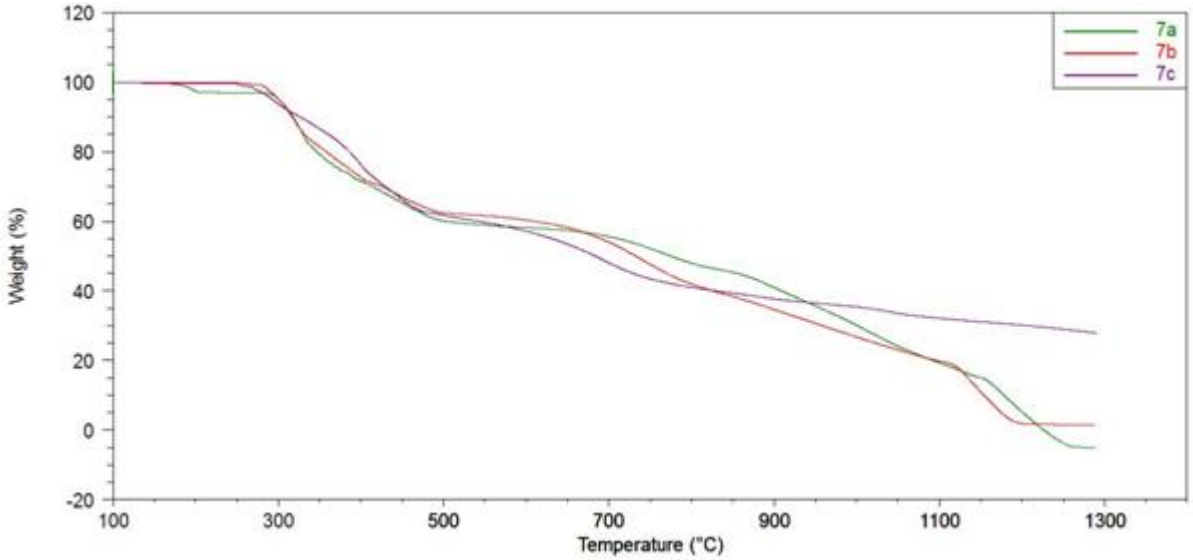

Figure 3.10: Thermogram showing decomposition of complexes **7a-c**.

3.4 Conclusions

Complexes *cis*-$[OsX_2(dppm)_2]$ (where X = Cl, Br, I) and *trans*-$[OsX_2(P–P)_2]$ (X = Cl, Br.I; P–P = dppe, dppp) are conveniently prepared directly from $[OsX_6]^{2-}$ in high yield with the use of microwave heating. The use of a microwave reactor greatly reduces the reaction time compared to conventional methods with the complexes prepared in minutes instead of hours. The reactions are less complex and require fewer reagents. The solvent usage is significantly reduced. We have also demonstrated that it is not necessary to carry out this synthesis under inert conditions. With isolated yields up to 92%, the yields are better than those obtained by conventional methods. Product purity was established by ^{31}P NMR spectroscopy.

Increasing the alkyl spacer group between to the P atoms of diphosphine ligand has a pronounced effect on the outcome of the reaction. Reaction of $[OsX_6]^{2-}$ with dppm selectively yields *cis*-$[OsX_2(dppm)_2]$ (X = Cl, Br, I). Under the same reaction condition dppe and dppp each reacts with $[OsX_6]^{2-}$ to give *trans* geometric complexes. It is hypothesised that the *cis*-isomer is formed and subsequently isomerises to the *trans*-form because of the sterically demanding phenyl rings.

The aromatic signals in the ^1H NMR spectra of complexes consists of several coupled multiplets due to aromatic protons of the phenyl rings of the diphosphine ligands and resonance is observed in the alkyl region for methylene protons. The $^{31}P\{H\}$ NMR spectra of *trans*-$[OsX_2(P–P)_2]$ (where P–P = dppe, dppp; X = Cl, Br, I) shows a singlet suggesting that the four phosphorus atoms of the chelating ligands are magnetically equivalent. From ^{31}P NMR data it can be seen that the preferred ring size for formation of *cis*-$[OsX_2(P–P)_2]$ are 4-membered chelating rings and *trans*-$[OsX_2(P–P)_2]$ is preferred for 5- and 6-membered chelating rings. There are a number of published methods for preparation of these complexes of the type $[OsX_2(P–P)_2]$ but microwave-assisted synthesis was found simple, convenient

and a selective synthesis method which improved reaction rates and improved product yields.

3.5 References

(1) Kappe, C. O.; Dallinger, D. *Nat Rev Drug Discovery* **2006**, *5*, 51.

(2) Leadbeater, N. E.; Shoemaker, K. M. *Organometallics* **2008**, *27*, 1254.

(3) Pyper, K. J.; Yung, J. Y.; Newton, B. S.; Nesterov, V. N.; Powell, G. L. *J. Organomet. Chem.* **2013**, *723*, 103.

(4) Perreux, L.; Loupy, A. *Tetrahedron: Asymmetry* **2001**, *57*, 9199.

(5) Kappe, C. K.; Dallinger, D. *Mol. Diversity* **2009**, *13*, 71.

(6) Kappe, C. O. *Chem. Soc. Rev.* **2008**, *37*, 1127.

(7) Caddick, S.; Fitzmaurice, R. *Tetrahedron: Asymmetry* **2009**, *65*, 3325.

(8) Powell, G. L. *Microwave Heating as a Tool for Inorganic and Organometallic Synthesis in Microwave Heating as a Tool for Sustainable Chemistry*; CRC Press, 2011.

(9) Kothe, T.; Martschke, R.; Fischer, H. *J. Chem. Soc., Perkin Trans.* **1998**, *2*, 503.

(10) Winkelmann, O. H.; Navarro, O. *Adv. Synth. Catal.* **2010**, *352*, 212.

(11) Baghurst, D. R.; Mingos, D. M. P.; Watson, M. J. *J. Organomet. Chem.* **1989**, *368*, C43.

(12) Lasri, J.; Rodriguez, M. J. F.; Guedes da Silva, F. C.; Smolenski, P.; Kopylovich, M. N.; Frausto da Silva, J. J. R.; Pombeiro, A. J. L. *J. Organomet. Chem.* **2011**, *696*, 3513.

(13) Mayer, H. A. *Chem. Rev.* **1994**, *94*, 1239.

(14) van Rijn, J. A.; Siegler, M. A.; Spek, A. L.; Bouwman, E.; Drent, E. *Organometallics* **2009**, *28*, 7006.

(15) Lindner, E.; Warad, I.; Eichele, K.; Mayor, H. A. *Inorg. Chim. Acta* **2003**, *350*, 49.

(16) Warad, I.; Lindner, E.; Eichele, K.; Mayor, H. A. *Inorg. Chim. Acta* **2004**, *357*, 1847.

(17) Polam, J. R.; Porter, L. C. *J. Coord. Chem.* **1993**, *29*, 109.

(18) Kayaki, Y.; Shimokawatoko, Y.; Ikariya, T. *Inorg. Chem.* **2007**, *46*, 5791.

(19) Lynam, J. M.; Nixon, T. D.; Whitwood, A. C. *J. Organomet. Chem.* **2008**, *693*, 3103.

(20) Winter, R. F.; Klinkhammer, K.-W. *Organometallics* **2001**, *20*, 1317.

(21) Fox, M.; Harris, J. E.; Heider, S.; Perez-Gregorio, V.; Zakrzewska, M. E.; Farmer, J. D.; Yufit, D. S.; Howard, J. A. K.; Low, P. J. *J. Organomet. Chem* **2009**, *694*, 2350.

(22) Raj, J. G. J.; Pathak, D. D.; Kapoor, P. N. *J. Mol. Struct.* **2015**, *1087*, 41.

(23) Barkley, J. V.; Grimshaw, J. C.; Higgins, S. J.; Hoare, P. B.; McCart, M. K.; Smith, A. K. *J. Chem. Soc. Dalton Trans.* **1995**, 2901.

(24) Yu, Y.-L.; Huang, L.-H.; Zhou, Y.-F.; Lou, J.-D.; Lu, X. L. *J. Coord. Chem.* **2014**, *67*, 1208.

(25) Chatt, J.; Hayter, R. G. *J. Chem. Soc.* **1961**, 896.

(26) Al-Noaimi, M.; Warad, I.; Abdel-Rahman, O. S.; Awwadi, F. F.; Haddad, S. F.; Haddad, T. B. *Polyhedron* **2013**, *62*, 110.

(27) McDonagh, A. M.; Humphrey, M. G.; Hockless, D. C. R. *Tetrahedron: Asymmetry* **1997**, *8*, 3579.

(28) Kamer, P. C. J.; Van Leeuwen, P. W. N. M.; Reek, J. N. H. *Acc. Chem. Res.* **2001**, *34*, 895.

(29) Nguyen, D. H.; Daran, J.-C.; Mallet-Ladeira, S.; Davin, T.; Maron, L.; Urrutigoity, M.; Kalck, P.; Gouygou, M. *Dalton Trans.* **2013**, *42*, 75.

(30) Al-Noaimi, M.; Sunjuk, M.; El-khateeb, M.; Haddad, S. F.; Haniyeh, A.; AlDamen, M. *Polyhedron* **2012**, *42*, 66.

(31) Lopes, L.; Castellano, E. E.; Ferreira, A. G.; Davanzo, C. U.; Clarke, M. J. *Inorg. Chim. Acta.* **2005**, *358*, 2883.

(32) Momeni, B. Z.; Kazmi, H.; Najafi, A. *Helvetica Chim. Acta.* **2011**, *94*, 1618.

(33) Al-Noaimi, M.; Sunjuk, M.; El-khateeb, M.; Haddad, S. F.; Haniyeh, A.; AlDamen, M. *Polyhedron* **2012**, *42*, 66.

(34) Slack, D. A.; Baird, M. C. *Inorg Chim Acta* **1977**, *24*, 277.

Chapter 4

Microwave-promoted synthesis of phosphine-substituted osmium carbonyl cluster complexes.

4.1 Introduction

4.1.1 Triosmium carbonyl cluster complexes

Clusters are defined as compounds containing two or more metal-metal bonds.[1] Transition metal clusters have several important properties relative to their mononuclear counterparts. The polynuclear framework is unique because ligands are able to coordinate to more than one metal centre.

The organometallic cluster compound triosmium dodecacarbonyl, $[Os_3(CO)_{12}]$, can undergo a wide range of chemical reactions to produce a variety of products, often with no change in nuclearity. Many different ligands have been used in these reactions for development of triosmium clusters that can be used in various applications. The wealth of chemistry of triosmium clusters has led to the rapid growth of research and preparation of cluster compounds that has found application in catalytic systems[2-5] and more recently in chemotherapy.[6,7]

The chemistry of phosphine-substituted derivatives of $[Os_3(CO)_{12}]$ has been extensively studied.[8-15] Phosphines, PR_3, find widespread use as ligands in coordination chemistry because they constitute one of the few ligands in which the steric and electronic properties of the ligand can be easily tunable by varying the R group. Diphosphine ligands give extra stability in complexes as a result of their ability to chelate metal centres.[16]

4.1.2 Preparatory methods

4.1.2.1 $[Os_3(CO)_{12}]$

The cluster $[Os_3(CO)_{12}]$ was first prepared by Hieber and Stallman in 1943.[17] The initial method of preparation involves direct reaction of osmium tetroxide, OsO_4, with CO gas. They obtained two products which they formulated as $[Os(CO)_5]$ and $[Os_2(CO)_9]$.[17] However, the latter was later shown to be $[Os_3(CO)_{12}]$ *via* X-ray crystallographic studies and trimeric formulation.[18,19] The little yield of $[Os_3(CO)_{12}]$ obtained using method by Hieber hindered its use. Several routes that involve preparation of the cluster have since been reported. Bradford and co-workers reported a method with improved yields of approximately 70%. The method involves reaction of OsO_4 with CO gas in xylene.[20] A popular method for preparation of $[Os_3(CO)_{12}]$ involves carbonylation of osmium tetroxide in a methanol solution at moderate pressure (75 atm) and temperature (125 °C) for 12 h.[21]

Osmium tetroxide, OsO_4, is a toxic material and makes the preparation of osmium carbonyls difficult. Roveda and colleagues demonstrated the synthesis of $[Os_3(CO)_{12}]$ in 65% yield under mild conditions by silica-mediated reductive carbonylation of the non-toxic $[Os(CO)_3Cl_2]_2$ or $[Os(CO)_3Cl_2(HOSi)]$. $[Os(CO)_3Cl_2]_2$ in presence of the base Na_2CO_3 at 1 atm of carbon monoxide at 160 - 165 °C.[22] Bruce and co-workers reported the preparation of $[Os_3(CO)_{12}]$ from a stable osmium-halide precursor such as ammonium hexabromoosmate in the presence of zinc using methanol as a solvent. In this method $[Os_3(CO)_{12}]$ is prepared in carbon monoxide gas under pressure between 4 to 25 atm.

4.1.2.2 $[Os_3(CO)_{12-n}(PR_3)_n]$

The common method of preparing phosphine-substituted triosmium clusters involve the use of the labile cluster complexes $[Os_3(CO)_{11}CNMe]$ and $[Os_3(CO)_{10}(CNMe)_2]$ as precursors (Scheme 4.1, Eq 4.1).[8,10-12,14,23-27] Direct reaction of the $[Os_3(CO)_{12}]$ cluster complex with

phosphines has also been reported in literature (Scheme 4.1, Eq 4.2). This method yields a mixture of phosphine-substituted products. Thermal reaction of $[Os_3(CO)_{12}]$ with phosphine ligands was found to give a mixture of products.[9,28-30] Leadbeater[29] and Poe[30] have demonstrated the photochemical synthesis of $[Os_3(CO)_{12-n}(PR_3)_n]$ (where n = 1-3) from $[Os_3(CO)_{12}]$ solution in the presence of phosphine ligands (Scheme 4.1, Eq 4.3).

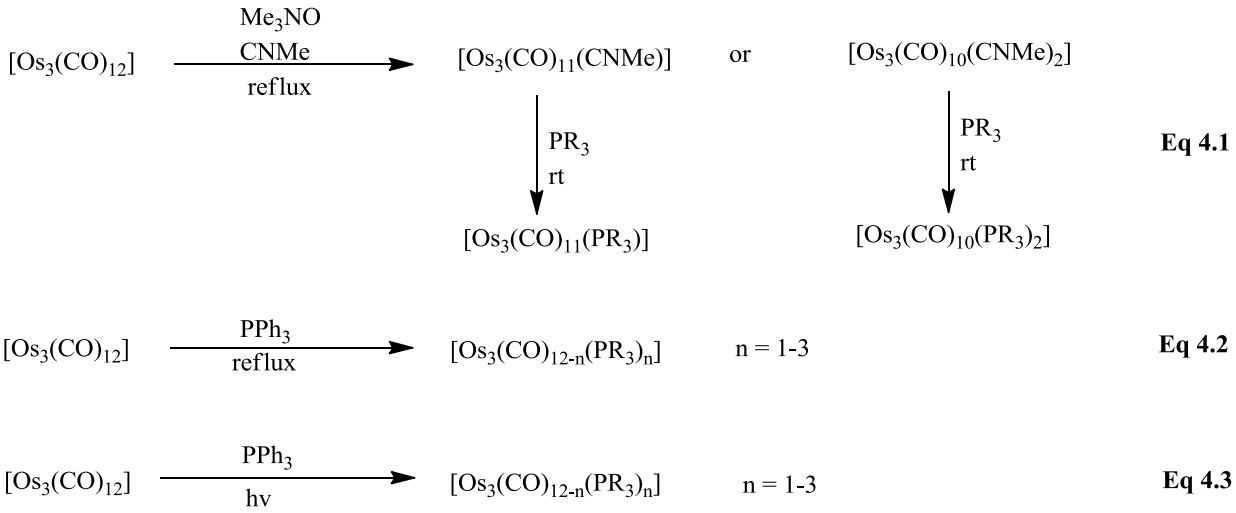

Scheme 4.1: Preparatory methods of $[Os_3(CO)_{12-n}(PR_3)_n]$ (n = 1-3).

4.1.2.3 $[Os_3(CO)_{11}\{\eta\text{-}(P–P)\}]$, $[Os_3(CO)_{10}\{\mu_2\text{-}(P–P)\}]$ and $[Os_3(CO)_{10}\{\kappa^2\text{-}(P–P)\}]$

The reactivity of cluster compound with bidentate phosphine ligands, $Ph_2P(CH_2)nPPh_2$, have also been investigated. The ability of the ligands to chelate thus increasing the stability of the metal framework is an interesting property. These complexes are commonly prepared from labile cluster complexes $[Os_3(CO)_{11}CNMe]$ and $[Os_3(CO)_{10}(CNMe)_2]$. Reactivity of the activated cluster with diphosphine ligands yields $[Os_3(CO)_{11}(P–P)]$ and $[Os_3(CO)_{10}(P–P)]$, respectively.[25] In the latter cluster, the diphosphine ligand can chelate to a single metal atom or bridge two adjacent metal atoms. Example of chelating and bridging $[Os_3(CO)_{10}(P–P)]$ are shown in Figure 4.1

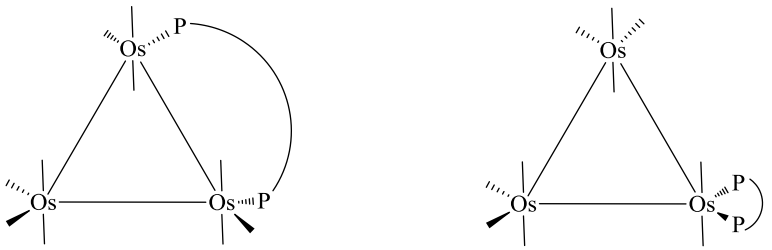

Bridging isomer
$[Os_3(CO)_{10}\{\mu_2\text{-}(P\text{-}P)\}]$

Chelating isomer
$[Os_3(CO)_{10}\{k^2\text{-}(P\text{-}P)\}]$

Figure 4.1: Examples of bridging and chelating isomers of $[Os_3(CO)_{10}(P–P)]$.

The use of microwave irradiation in synthesis is rapidly increasing and has found widespread use.[31-35] A number of recent studies have investigated the microwave-promoted transformation of $[Os_3(CO)_{12}]$ into other trinuclear clusters.[6,13,36] Microwave heating usually produce higher product yield, increase reaction rates, reduced reaction time and milder reaction conditions. This method yields substituted triosmium clusters directly without the use of the labile cluster $[Os_3(CO)_{12-n}(CNMe)_n]$ (where n = 1-2).

4.1.3 Focus of this study

We have studied the reactivity of $[Os_3(CO)_{12}]$ with PPh_3 and dppm in a microwave reactor. Also the effect of different solvents in the reaction of PPh_3 with $[Os_3(CO)_{12}]$ was evaluated. Our studies have shown that by microwave irradiation of $[Os_3(CO)_{12}]$ in varying solutions in the presence PPh_3 produce different substituted products. Similar work has been done with UV irradiation of $[Os_3(CO)_{12}]$ in the presence of PPh_3, which led to formation photosubstituted product $[Os_3(CO)_{12-n}(PPh_3)_n]$ (n = 1-3). The use of hexane as a photolysis media led to photofragmentation of the cluster and yield mononuclear $Os(CO)_3(PPh_3)_2$.[29]

4.2 Synthesis

Bruce's approach with slight modification was used in the preparation of $[Os_3(CO)_{12}]$. Higher pressures and temperatures are used in this study. Reaction of the osmium halide precursor, ammonium hexachloroosmate(IV), $(NH_4)_2[OsCl_6]$ in methanol at 140 °C under pressurized carbon monoxide in the presence of zinc leads to formation of $[Os_3(CO)_{12}]$ in 64% yield (Scheme 4.2).

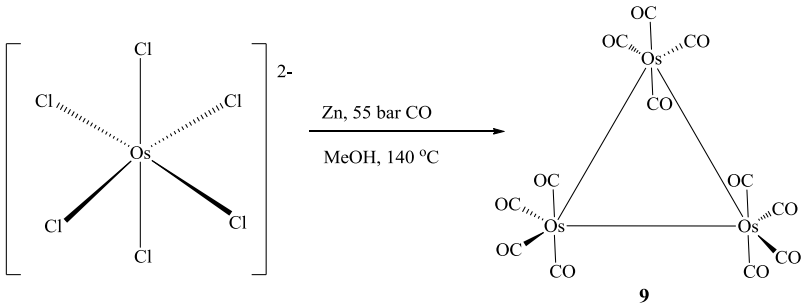

9

Scheme 4.2: Preparation of $[Os_3(CO)_{12}]$.

Microwave irradiation of $[Os_3(CO)_{12}]$ in acetonitrile solution in the presence of triphenylphosphine resulted in substitution of CO ligands to give a mixture of two products, the trisubstituted $[Os_3(CO)_9(PR_3)_3]$ complex (**10**) and disubstituted $[Os_3(CO)_{11}(PR_3)_2]$ complex (**11**) (Scheme 4.3). This method represent a fast and efficient route of synthesizing phosphine-substituted clusters directly from $[Os_3(CO)_{12}]$ without initial preparation of the activated cluster.[11]

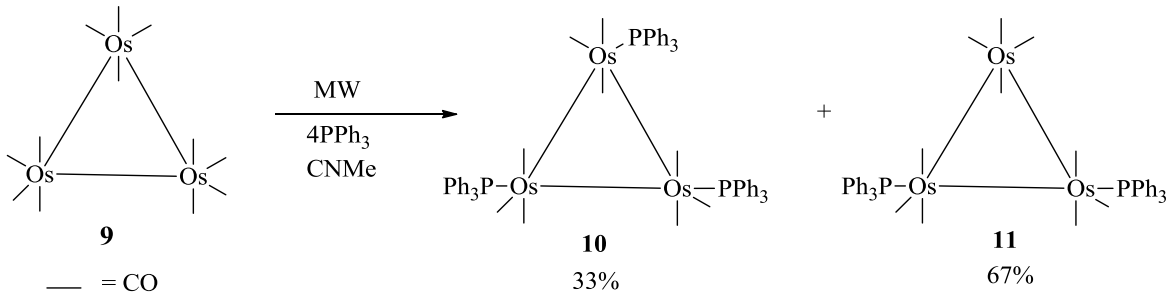

Scheme 4.3: Preparation of triphenylphosphine-substituted triosmium cluster complexes *via* microwave irradiation.

Microwave heating of $[Os_3(CO)_{12}]$ in the presence of PPh_3 in other solvents (DCM, DCE, $CHCl_3$) gives a mixture of substituted products. Unfortunately, the products were not separated chromatographically and could be identified using ^{31}P NMR. The mixture contains $[Os_3(CO)_{11}(PPh_3)]$, $[Os_3(CO)_{10}(PPh_3)_2]$ and triphenylphosphine oxide.

Reaction of $[Os_3(CO)_{12}]$ and dppm via microwave heating gives a single product identified as $[Os_3(CO)_{11}(\eta^1\text{-dppm})]$ (Scheme 4.4). However, this reaction gives $[Os_3(CO)_{10}(\mu\text{-dppm})]$ when carried out by conventional methods.

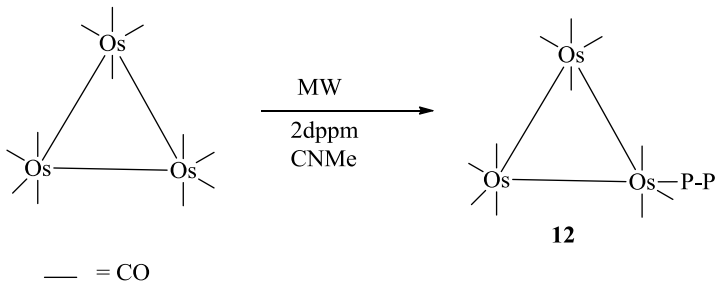

Scheme 4.4: Microwave preparation of $[Os_3(CO)_{11}(\eta^1\text{-dppm})]$.

Based on the intensities of the signals in ^{31}P NMR spectra the major product in the mixture is complex **11** in all the solvents used. Dichloroethane as a solvent yields a single product based on ^{31}P NMR spectrum. No further characterization was done.

4.3 Results and discussions

The Os(0) carbonyl clusters complexes were characterized in solution using NMR spectroscopy and IR as well as solid state Raman spectroscopy.

4.3.1 IR and Raman spectroscopy

The IR data of complex **9-12** are given in Table 4.1. The data indicate that increasing substitution from the parent carbonyl cluster **9** leads to progressive lowering of the remaining CO stretching frequencies.

The FT-IR spectrum of cluster complex **9** in CH_2Cl_2 shows four principal carbonyl stretching vibration bands in the region 1900 - 2100 cm^{-1} (Figure 4.2), as expected for a D_{3h} symmetry. The spectrum is similar to that reported in literature.[29,37] The carbonyl absorptions are grouped into two groups, the axial and equatorial, which have a different bond order due to π-bonding effects. Axial CO ligands compete for the same π-electrons and have slightly higher bond order than each of the carbonyls in equatorial position. It is therefore expected for the equatorial modes to be centered at a lower energy than the axial modes.

The Raman spectrum of complex **9** shows presence of bands in the region 1900 – 2100 cm^{-1} (Figure 4.2). These bands can be satisfactorily attributed to C–O stretching vibrations.[38] The centrosymmetric complexes show an infrared-Raman exclusion although near-coincidences occur. There is no significant distinction between the IR and Raman spectra. A similar general peak pattern is observed. However, the intensities of the bands are different. The raman spectrum shows medium to low intensities whilst the corresponding IR spectrum shows very intense bands as expected. This can be explained by the different principles. Raman bands depend solely on the relative orientations of the CO groups and not the bonding within the molecule. Vibrations involving polar bonds are weak Raman scatterers. The intensity of the bands in IR is dependent on the polarity of the bond.

Table 4.1: IR data in the carbonyl region of complex **9 - 12**.

Complexes	IR (ν_{CO}, CH_2Cl_2) cm^{-1}
9	2060(s), 2037(vs), 2015(s), 1995(s)
10	2049(w), 2023(m), 1996(m), 1964(vs), 1940(w)
11	2984(w), 2055(m), 2029(m), 1996(s), 1967(mw)
12	2109(w), 2061(m), 2047(mw), 2020(mw), 1999(s), 1965(m)

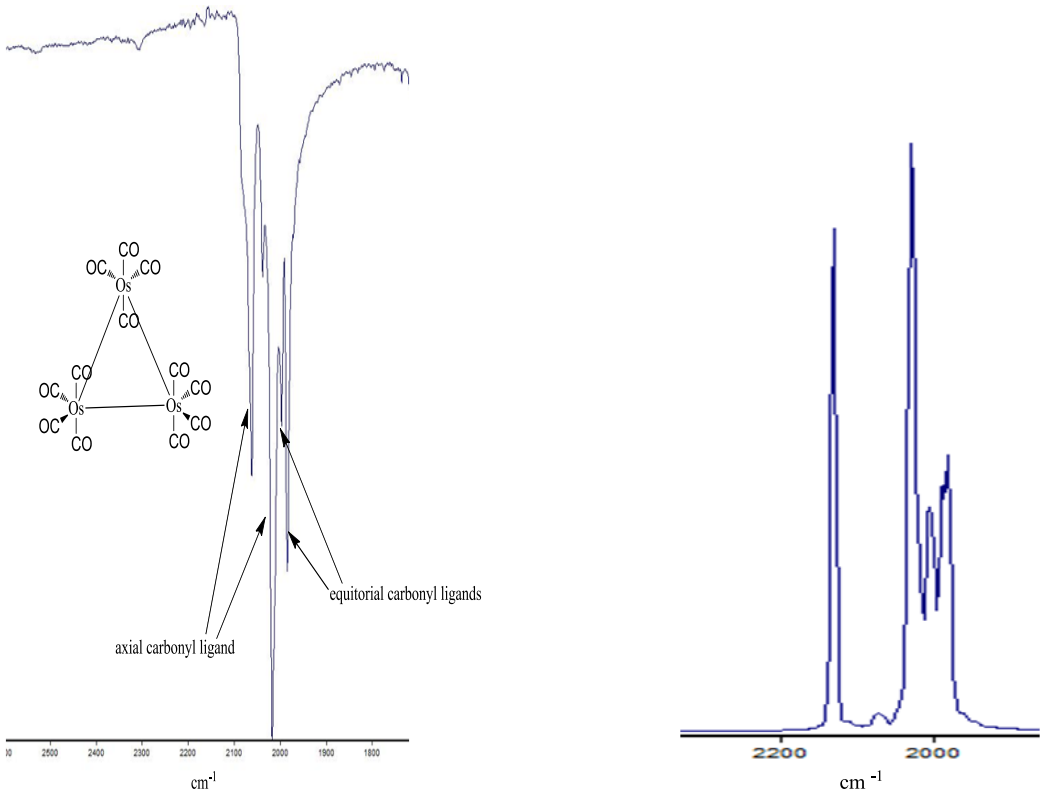

Figure 4.2: FT-IR and Raman spectra of cluster complex **9**.[19-20]

The IR data of complex **10**-**12** is similar to data previously reported,[29,39] with cluster complex $[Os_3(CO)_9(PPh_3)_3]$ (**10**) and $[Os_3(CO)_{10}(PPh_3)_2]$ (**11**) exhibiting a carbonyl stretching patterns

that are similar to a typical trisubstituted and disubstituted-phosphine cluster $[Os_3(CO)_{12-n}(PR_3)_n]$, respectively. The carbonyl stretching pattern of complex **12** corresponds to triosmium clusters with diphosphine ligand coordinated in a monodentate mode. IR spectra of the products obtained from reaction of $[Os_3(CO)_{12}]$ with PPh_3 shows a pattern that is typical of a monosubstituted phosphine cluster complex. Raman spectra of complex **11** and **10** are given in Figure 4.4 and 4.3, respectively. These spectra provide further evidence for CO substitution.

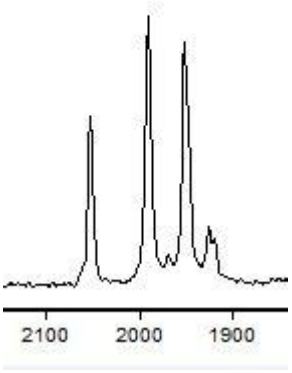

Figure 4.3: Raman spectrum of complex **10**.

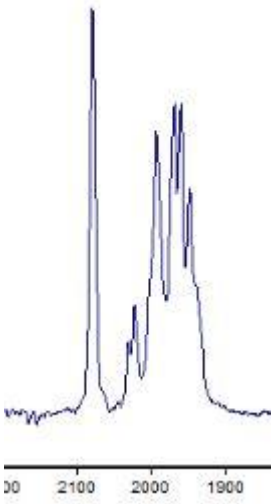

Figure 4.4: Raman spectrum of complex **11**.

4.3.2 NMR spectroscopy

^{1}H and ^{31}P NMR data for complexes **10** – **12** are given in Table 4.2. The chemical shifts of aromatic protons of the triphenylphosphine in ^{1}H NMR spectra of complexes **10** and **11** is observed. A multiplet centred at δ 7.47 ppm is observed for complexes **10** and a multiplet centred at δ 7.45 ppm. The methylene protons of the η^{1}-dppm ligand give rise to a triplet at δ 4.77 ppm in the ^{1}H NMR spectrum in addition to the aromatic protons (Figure 4.5).

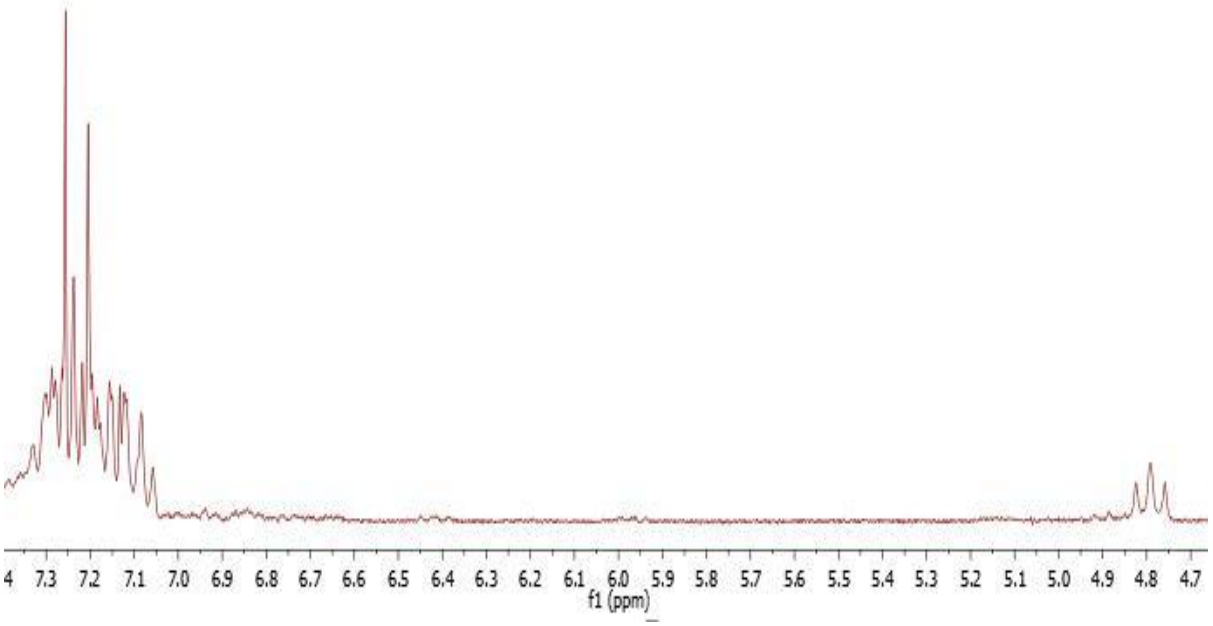

Figure 4.5: ^{1}H NMR spectrum of $[Os_3(CO)_{11}(\eta^1\text{-dppm})]$, **12**.

Table 4.2: ^{1}H and ^{31}P NMR for cluster complexes prepared.[a]

Complexes	δ (^{1}H NMR) ppm	δ (^{31}P{H} NMR) ppm
10	7.45 (m, 45H, H-aromatic)	-2.29
11	7.44 (m, 30H, H-aromatic)	-1.76
12	7.16 (m, 20H, H-aromatic), 4.77 (t, $J_{(PH)}$ = 7.8 Hz, 2H, CH_2)	-20.0 (d, *J* = 49.1Hz), -23.4 (d, *J* = 49.1 Hz)

[a] In chloroform solution

Both complexes **10** and **11** exhibit a singlet in the ^{31}P{H} NMR spectrum. A singlet at δ = -2.29 ppm for complex **10** and a singlet at δ = -1.76 ppm for complex **11** are observed. This indicates that the phosphorus atoms occupy a similar environment. The phosphine ligands have been found to occupied the equatorial positions with respect to the triosmium plane. Two doublets at δ = -20.0 and -23.4 ppm are observed in the ^{31}P{H} NMR spectrum of complex **12** (Figure 4.6)**.** This data suggests that the phosphorus atoms are magnetically non-

equivalent. The doublet in low-field is assigned to the coordinated phosphorus, whereas the uncoordinated phosphorus atom gives a signal in high field region.

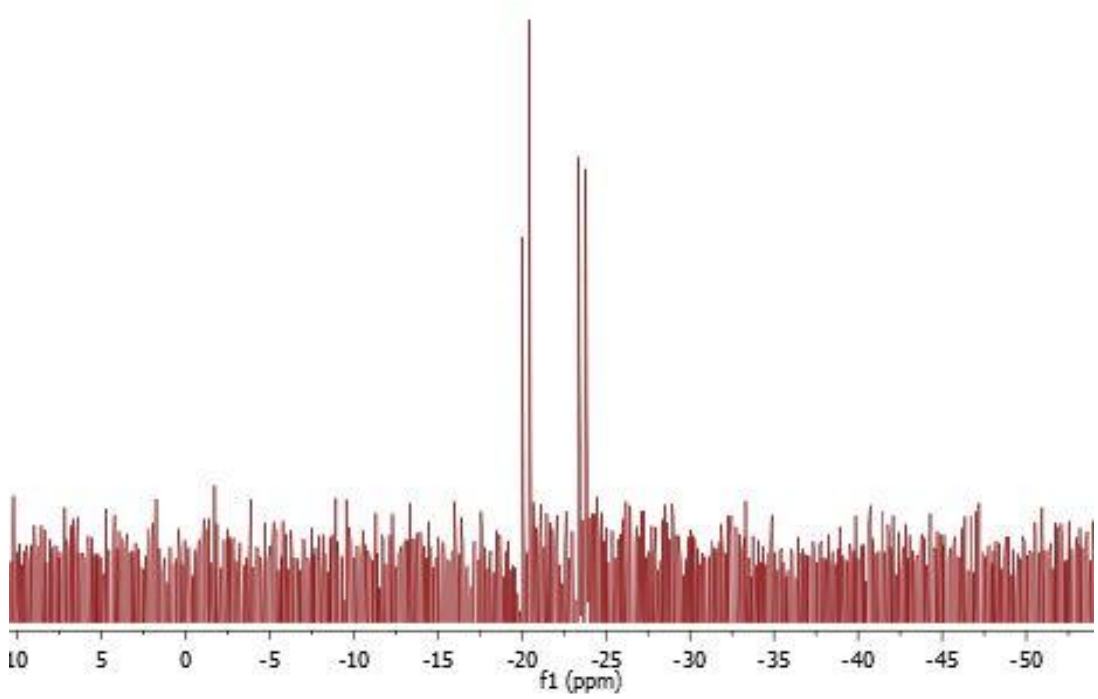

Figure 4.6: ^{31}P NMR of complex **12.**

This data suggest that the diphosphine ligand has coordinated in a monodentate mode. The dppm ligand has the ability to either bridge two trinuclear metal complexes or chelate forming a 1,1-isomer. In this case either of the coordination mode is less likely the bulky phenyl rings limit the ability of dppm to bridge two $Os_3(CO)_{11}$ fragments. Also chelation is not favourable presumable because of the strain in a 4-membered ring, in addition chelation will cause distortion from an octahedral geometry which is not favourable.[39]

The ^{31}P NMR spectra of product where DCE, DCM and $CHCl_3$ are used as solvents in the microwave irradiation of $[Os_3(CO)_{12}]$ and PPh_3 exhibit 3 signals indicating the presence of 3 isomers. The resonance at d -1.74 ppm is identified as $[Os_3(CO)_{10}(PPh_3)_2]$. Resonance at δ -

10.3 ppm is not identified but it is hypothesized to be the monosubstituted phosphine cluster based on the combination of ^{31}P NMR and the IR spectroscopic data. As discussed above a pattern in the CO region of a typical monosubstituted triosmium cluster. Unfortunately, the product was not chromatographically separated and thus no further characterization was done. A small third signal at δ 28.5 ppm is likely the triphenylphosphine oxide.

^{13}C NMR could not be obtained. This is caused by carbonyl undergoing axial-equatorial fluxional mechanism. At temperatures above -50 °C selective carbonyl exchange occurs in these complexes which cause the resonance to broaden and collapse to the baseline at different rates.[10,15,40,41]

4.3.3 Thermogravimetric analysis (TGA)

Thermal decomposition studies of complexes **9**-**11** were carried out. The data show that the phosphine-substituted cluster complexes, **10** and **11**, are thermally more stable compared to the parent triosmium carbonyl cluster, complex **9**. Complex **9** when heated was found to be a single stage process. The onset of decomposition occurs between 180 – 246 °C. At this temperature to about 246 °C a total decomposition of the cluster is observed.

Onset of decomposition for complex **10** is ca. 213 °C. The initial stage of decomposition is accompanied by 10.5% mass loss associated with the loss of five CO ligands. The second stage (265 – 455 °C) is associated with loss of the remaining CO ligands and two PPh_3. The third PPh_3 is lost at temperatures above 1000 °C.

Complex **11** was found to undergo a multistage process of decomposition. The stages can be directly related to the loss of ligands. The first stage between 209 – 238 °C was accompanied by an 8.2% mass loss associated with the release of four carbonyl ligands. We hypothesize that these four are the axial carbonyls on the metal center where the phosphine is coordinated. The M–CO axial bonds of the $Os(CO)_4$ center are much stronger than the other axial bonds

and hence the CO ligands are lost in second stage of decomposition along with the equatorial CO ligands and one triphenylphosphine. The second stage (238 – 468 °C) and the third stage (468 – 968 °C) involved loss of remaining PPh_3 ligand.

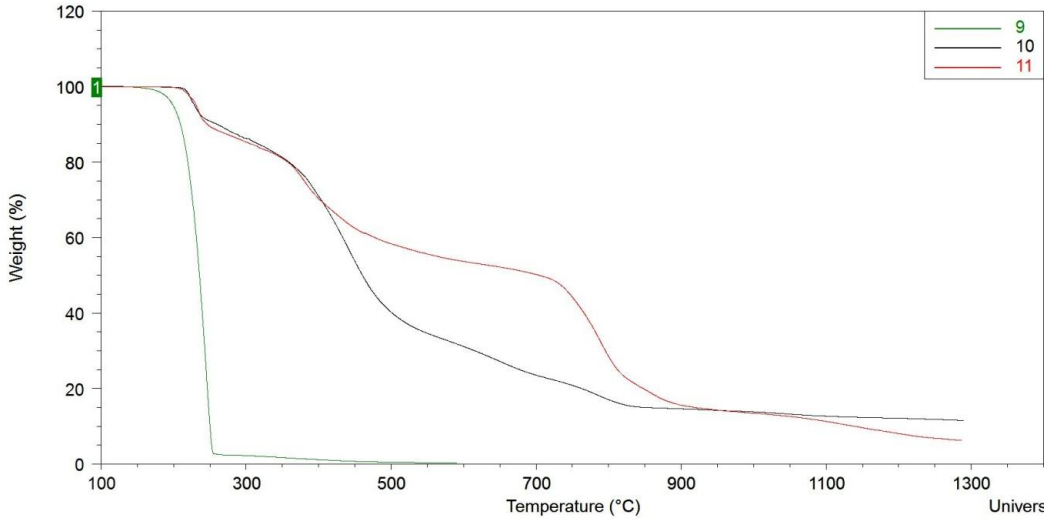

Figure 4.7: Thermogram of cluster complexes **9**, **10** and **11**.

4.4 Conclusions

Microwave-promoted conversion of $[Os_3(CO)_{12}]$ allows for fast and efficient synthesis of substituted trinuclear cluster derivative. Microwave irradiation of a mixture of $[Os_3(CO)_{12}]$ and PPh_3 gave a mixture of phosphine substituted cluster complexes. It is worth noting that these substituted clusters are obtained directly from the parent carbonyl $[Os_3(CO)_{12}]$. This eliminates the multi-step method described in literature for synthesis of similar cluster complexes which involves activation of the parent cluster $Os_3(CO)_{12}$ to labile cluster complexes, $[Os_3(CO)_{11}(CNMe)]$ and $[Os_3(CO)_{10}(CNMe)_2]$, with subsequent reaction with relevant ligand. Microwave reaction of $[Os_3(CO)_{12}]$ and dppm leads to formation of $[Os_3(CO)_{11}(dppm)]$, complex **12,** as the only isolable product.

We have also studied the ligand substitution reaction of $[Os_3(CO)_{12}]$ with triphenylphosphine in different solvent such as CH_2Cl_2, $C_2H_4Cl_2$ and $CHCl_3$. In this case the disubstituted phosphine complex $[Os_3(CO)_{10}(PPh_3)_2]$ is a minor product in addition to the monosubstituted complex $[Os_3(CO)_{11}(PPh_3)]$ which appears as an intense peak in the ^{31}P NMR spectrum. No trisubstituted $[Os_3(CO)_{11}(PPh_3)]$ complex was formed.

Compared to conventional preparatory methods microwave heating produced desired complexes with fewer reaction steps and less solvent required. Complex **9** was found to be the least stable compared to the other complexes. On set of decomposition is at temperatures below 200 °C. Complex **10** and **11** showed thermal stability and started decomposition in temperatures just above 200 °C.

4.5 References

(1) Cotton, F. A. *Q. Rev. Chem. Soc.* **1966**, *20*, 389.

(2) Deeming, A. J. *Adv. Organomet. Chem.* **1986**, *26*, 1.

(3) Kondo, T.; Tsuji, Y.; Watanabe, Y. *Tetrahedron letters* **1988**, *29*, 3833.

(4) Caulton, K. G.; Thomas, M. G.; Sosinsky, B. A.; Muetterties, E. L. *Proc. Natl. Acad. Sci U.S.A.* **1976**, *73*, 4274.

(5) Thomas, M. G.; Beier, B. F.; Muetterties, E. L. *J. Am. Chem. Soc.* **1976**, *98*, 1296.

(6) Jung, J. Y.; Kempe, D. K.; Loh, L.-H.; Schoultz, S. E.; Powell, G. L. *J.Organomet. Chem* **2012**, *700*, 219.

(7) Colangelo, D.; Ghiglia, A.-L.; Ghezzi, A.-R.; Ravera, M.; Rosenberg, E.; Spada, F.; Osella, D. *J. Inorg. Biochem.* **2005**, *99*, 505.

(8) Johnson, B. F. G.; Lewis, J.; Pippard, D. A. *J. Chem. Soc, Dalton Trans.* **1981**, *2*, 407.

(9) Bruce, M. I.; Liddell, M. J.; Hughes, C. A.; Skelton, B. W.; White, A. H. *J. Org. Chem.* **1988**, *347*, 157.

(10) Hansen, V. M.; Ma, A. K.; Biradha, K.; Pomeroy, R. K.; Zaworotko, M. J. *Organometallics* **1998**, *1998*, 5267.

(11) Leong, W. K.; Liu, Y. *J. Org. Chem.* **1999**, *584*, 174.

(12) Persson, R.; Monari, M.; Gobetto, R.; Russo, A.; Aime, S.; Calhorda, M. J.; Nordlander, E. *Organometallics* **2001**, *20*, 4150.

(13) Jung, J. Y.; Newton, B. S.; Tonkin, M. L.; Powell, C. B.; Powell, G. L. *J. Organomet. Chem.* **2009**, *694*, 3526.

(14) Malosh, T. J.; Shapley, J. R. *Organometallics* **2010**, *695*, 1776.

(15) Persson, R.; Stchedroff, M. J.; Gobetto, R.; Carrano, C. J.; Richmond, M. G.; Monari, M.; Nordlander, E. *J. Inorg. Chem.* **2013**, *2013*, 2447.

(16) Kabir, S. E.; Hogarth, G. *Coord. Chem. Rev.* **2009**, *253*, 1285.

(17) Hieber, W.; Stallman, H. *Z. Elektrochem.* **1943**, *49*, 288.

(18) Corey, E. R.; Dahl, L. F. *J. Am. Chem. Soc.* **1961**, *83*, 2203.

(19) Corey, E. R.; Dahl, L. F. *Inorg. Chem.* **1962**, *1*, 521.

(20) Bradford, C. W.; Nyholm, R. S. *Chem. Commun.* **1967**, *8*, 384.

(21) Johnson, B. F. G.; Lewis, J. *Inorg. Synth.* **1972**, *13*, 92.

(22) Roveda, C.; Cariata, E.; Lucenti, E.; Roberto, D. *J. Organomet. Chem.* **1999**, *580*, 117.

(23) Tichikawa, M.; Shapley, J. R. *J. Organomet. Chem.* **1977**, *124*, C19.

(24) Johnson, B. F. G.; Lewis, J.; Odiaka, T. I.; Raithby, P. R. *J. Organomet. Chem.* **1981**, *216*, C56.

(25) Deeming, A. J.; Donovan-Mtunzi, S.; Kabir, S. E. *J. Organomet. Chem.* **1984**, *276*, C65.

(26) Johnson, B. F. G.; Lewis, J.; Pippard, D. A. *J. Organomet. Chem.* **1978**, *160*, 263.

(27) Deeming, A. J.; Johnson, B. F. G.; Lewis, J. *J. Organomet. Chem.* **1969**, *17*, p40.

(28) Abdul, M. M.; Kabir, S. E.; Tocher, D. A.; Deeming, A. J.; Nordlander, E. *J. Org. Chem.* **2007**, *692*, 5007.

(29) Leadbeater, N. E. *J. Org. Chem.* **1999**, *573*, 211.

(30) Poe, J. A.; Sekhar, V. C. *J. Am. Chem. Soc.* **1986**, *108*, 3673.

(31) Baghurst, D. R.; Mingos, D. M. P.; Watson, M. J. *J. Organomet. Chem.* **1989**, *368*, C43.

(32) Mingos, D. M. P. *Res. Chem. Intermed.* **1994**, *20*, 85.

(33) Larhed, M.; Moberg, C.; Hallberg, A. *Acc. Chem. Res.* **2002**, *35*, 717.

(34) Collins, J. M.; Leadbeater, N. E. *Org. Biomol. Chem.* **2007**, *5*, 1141.

(35) Gedye, R.; Smith, F.; Westaway, K.; Ali, H.; Baldisera, L.; Laberge, L.; Rousell, J. *Tetrahedron lett.* **1986**, *27*, 279.

(36) Leadbeater, N. E.; Shoemaker, K. M. *Organometallics* **2008**, *27*, 1254.

(37) Huggins, D. K.; Flitcroft, N.; Kaesz, H. D. *Inorg. Chem.* **1964**, *4*, 166.

(38) Kettle, S. F. A.; Boccaleri, E.; Diana, E.; Rossetti, R.; Stanghellini, P. L.; Lapalucci, M. C.; Longoni, G. *Inorg. Chem.* **2003**, *42*, 6314.

(39) Deeming, A. J.; Donovan-Mtunzi, S.; Kabir, S. E. *J. Organomet. Chem.* **1987**, *333*, 253.

(40) Johnson, B. F. G.; Lewis, J.; Reichert, B. E.; Schorpp, K. T. *J. chem. Soc., Dalton Trans.* **1976**, *14*, 1403.

(41) Alex, R. F.; Pomeroy, R. K. *Organometallics* **1987**, *6*, 2437.

Chapter 5

In vitro antimicrobial and anticancer activities

This chapter has two parts. The first part includes a brief background on the success of transition-metal antimicrobial agents. A brief section on the principle of laboratory methods used for screening antimicrobial agents is included. Selected complexes prepared in this thesis were evaluated for antimicrobial activity and the results obtained are discussed. The second part gives a brief background on platinum containing complexes in the fight against cancer and the potential of non-platinum complexes as new anticancer agents is also discussed. In addition, some of the compounds prepared in this thesis were screened against 4 human cancer cell lines. A conclusion on the overall results is given at the end of the chapter.

5.1 *In vitro* antimicrobial screening

5.1.1 Introduction

Microbes are micro-organisms that can be divided into two groups depending on the type of cells they have. Those that have membrane-bound nuclei and other defined organelles are called eukaryotes which include fungi and protists. The other group of micro-organisms are called prokaryotes, these are identified by their lack of nuclei. They are unicellular organisms that lack organelles or other membrane-bound structures, an example is bacteria.[1]

Bacterial and microbial infections are associated with the cause of high mortality and morbidity worldwide.[2,3] Over centuries leading laboratories have made progress in the development of antimicrobials. It started with the accidental discovery of penicillin and later

its clinical use.[4,5] Penicillin was found to have a wide spectrum of activity, including the ability to inhibit strains of *Streptococcus* and *Staphylococcis*. This was followed by development and subsequent clinical use of a number of related organic compounds.[6-8] Unfortunately, the success of these compounds has been hampered by resistance and decrease in efficacy. The micro-organisms developed resistance to multiple antimicrobial agents which consequently lead to treatment failures.[9] Multidrug-resistant bacteria have become a global concern to public health. Hence, there is a great need for new compounds with antimicrobial activity with novel mechanisms of action.

Metal-based antimicrobial agents tend to offer advantages over organic-based antimicrobial agents. The complexes offer a range of coordination geometries, different oxidation states and more stereochemical variability than is possible in organic molecules as well as the ability to influence the kinetic properties by rational design of the ligands which may be important for interaction with biomolecules. The metal complexes can also be charged and since many biological structures are also charged, possible electrostatic interaction could aid the binding with intracellular targets.

A number of transition metal complexes have shown antimicrobial activities. These include Paul Erlich's organoarsenic compound for treatment of syphilis.[10] Copper-sulfonamide complexes have showed an increased activity compared to the free ligand.[11] These copper complexes have been found to be active against *Staphylococcus aureus* and *Escherichia coli*. A range of metal complexes (Fe, Co, Ni, Cu, Cd, Zn and Mn) containing Schiff base ligands have demonstrated moderate antibacterial activity.[12] Metal complexes offer novel mechanism of action not available to organic compounds. Phenanthroline and 2,2-bipyridine chelates of Ni, Fe, Zn and Rb have been reported to show activity against Gram-positive (*Staphylococcus aereus*, *Streptococcus pneumonia* and *Clostridium perfringes*) and Gram-negative bacteria (*Escherichia coli* and *Proteus vulgaris*).[13] It was hypothesized that

inhibition of growth of some microbes was a result of production of reactive oxygen species (ROS). Ruthenium(II) bis-(2,2'-bipyridine) complexes containing a N-phenyl-substituted diazafluorene ligand increased production of ROS in methillin-resistant *Staphylococcus aureus*.[14] Labile ligands were reported to have an effect on the activity of complexes prepared by Ramos. The water-soluble ruthenium complexes containing PTA (1,3,5-triaza-7-phosphaadamantane) and labile ligands (Cl, Br, I and SCN) were screened. Complexes containing Cl and SCN exhibited antifungal activity in contrast with Br and I containing complexes.[15,16]

In this study, a series of complexes of osmium-phosphine complexes prepared were evaluated against well known multi-resistant bacteria and some strains of fungi.

5.1.2 *In vitro* antimicrobial assays

A variety of laboratory methods such as the disk-diffusion and broth and agar dilution methods can be used to evaluate the *in vitro* antimicrobial activity of compounds. To determine the minimum inhibitory concentration (MIC) values dilution methods are the most appropriate to employ. The objective of both agar and broth dilution methods is to determine the MIC of assayed antimicrobial agent that under tested conditions inhibits growth of the microbes being investigated either in agar (agar dilution) or broth medium (macrodilution or microdilution). These dilution methods can be used to quantitatively measure the *in vitro* antimicrobial activity against bacteria and fungi.

5.1.2.1 Agar dilution method

This method involves incorporation of the antimicrobial agent into an agar, which is then placed in dilution plates and diluted to various concentrations with water. Followed by the inoculation of standard number of pathogens onto each plate. After incubation the lowest concentration of antimicrobial agent that completely inhibits growth is considered the MIC of that micro-organism.

5.1.2.2 Broth dilution method

Broth dilution method is often determined in a 96-well microtiter plate format. Two-fold dilutions of antimicrobial agent is prepared in liquid growth medium and added to the plate. Then each well is inoculated with the microbial inoculums prepared in the same medium. Growth is assessed after incubation for a defined period of time under suitable conditions depended upon the test micro-organism. The MIC is the lowest concentration of antimicrobial agent that completely stops the growth of micro-organisms in tubes or microdilution wells as detected visually. Tetrazolium salts such as 2-(4-iodophenyl)-3-(4-nitrophenyl)-5-phenyl-2*H*-tetrazolium salt (INT) (Figure 5.1) is often used in the MIC endpoint determination for both antifungal and antibacterial microdilution assays. Broth micro or macro-dilution employs the same principle except the volume of the broth differs. Macro dilution uses a volume of about 1 mL in standard test tubes while microdilution uses about 0.05 – 0.1 mL total broth volume in a microtitre plate. However, unlike microdilution, the macrodilution method is tedious, and comparatively large amounts are required.

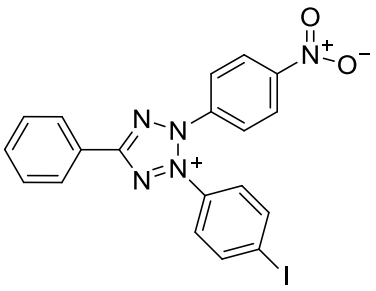

Figure 5.1: Structure of 2-(4-iodophenyl)-3-(4-nitrophenyl)-5-phenyl-2*H*-tetrazolium (INT) salt.

5.1.3 Antimicrobial activity

In this study 15 test compounds were evaluated *in vitro* for antimicrobial activity against 2 Gram-negative strains (*Escherichia coli* ATCC 35218, *Pseudomonas aeruginosa* ATCC 7700), 2 Gram-positive strains (*Enterococcus faecalis* ATCC 19433, *Staphylococcus aureus* ATCC 25925) and 2 fungal strains (*Candida albicans* ATCC 24433, *Cryptococcus neoformans* ATCC 14116).

The antimicrobial activity of the compounds was evaluated using the microplate serial dilution assay.[17,18] Bacterial cultures were maintained on Muller-Hilton (MH) agar and in MH broth at 37 °C for 14 h before being used in screening assays. The fungal strains were maintained on Sabouraud dextrose agar and Sabouraud dextrose broth prior to antifungal testing. Following incubation of the plates, the MIC values were determined in mg/mL. The results obtained were compared with those of the reference antimicrobial drugs Gentamicin and Amphotericin-B (Figure 5.2).

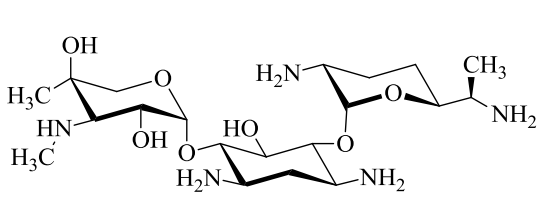

Gentamicin

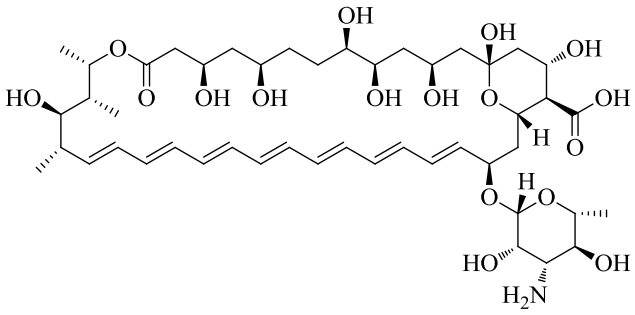

Amphotericin B

Figure 5.2: Chemical structure of reference antimicrobial agents

Gentamicin is a type of aminoglycoside used to treat several bacterial infections. It has a broad spectrum of activity against bacterial infections mostly against Gram-negative bacteria such as *Pseudomonas*, *Escherichia coli* and *Enterobacter aerogenes* and Gram-positive *Staphylococcus*. It operates by inhibiting protein synthesis which leads to death of the pathogen.

Amphotericin-B is a polyene used to treat a range of systematic fungal infections such as aspergillosis, blastomycosis, candida and cryptococcosis. At relevant clinical concentration Amphotericin-B is fungicidal. Amphotericin-B is associated with toxicities and is most commonly prescribed for patients who suffer from severe life-threatening invasive antifungal infection. This polyene antifungal agent exerts its activity by disruption of fungal cell wall synthesis. Due to its amphiphilic structure, these molecules bind to lipid bilayer and form a complex with the ergosterol pores causing disruption of the cell membrane. Disruption of the cell wall structure have an effect on the growth and morphology of the fungal cell, often rendering it susceptible to lysis and death.[19,20]

5.1.4 Results and discussions

The results of the *in vitro* antimicrobial testing against selected Gram-positive bacteria, Gram-negative bacteria and fungi are reported in Table 5.1. The antimicrobial effect of DMSO against the test micro-organisms was investigated and no significant inhibitory effect was reported. To avoid any inhibitory effect DMSO was used at 1% (v/v).

Data presented in Table 5.1 demonstrate that all the tested carbonyl complexes of the type $[OsX_2(CO)_2(PR_3)_2]$ (**1a**, **2a-4b**), with the exception of **1b**, **1c** and **3b**, had little effect on growth inhibition of bacteria. Complex **1b**, **1c** and **3b** show moderate activity against Gram-negative *Pseudomonas aeruginosa*. In addition **3b** showed bactericidal activity against *Escherichia coli*. The fungus *Candida albicans* was relatively resistant against the osmium(II) carbonyl complexes. Interestingly, the chlorido analogues showed moderate activity against *Cryptococcus neoformans* while the bromido and iodido showed little activity. This is consistent with the findings for Ru(II)-arene complexes $[Ru(\eta^6\text{-p-cymene})X_2(pta)]$, the Cl containing complexes inhibited growth of microorganisms and the Br and I bearing complexes were shown to exhibit little activity.[16] The bromido and the iodido complexes were found to exhibit more DNA damage than other compounds in the series. If DNA damage is the contributing factor to toxicity then these compounds would be predicted to be the most active. Variation of phosphine ligands in the series $[OsX_2(CO)_2(PR_3)_2]$ under study was found to exert no influence on the activity. It appears substitution of halide ligands influences the microbial activity of the test compounds.

Complexes of the type *cis*/*trans*-$[OsBr_2(P–P)_2]$ exhibit moderate to good antibacterial activity. Data show that the *trans* complexes **6b** and **7b** are more active than the *cis* complex **5b**. Compound **5b** shows MIC values that is comparable to *cis*-$[RuCl_2(P–P)_2]$ (P–P = dppm, dppe) against *Mycobacterium tuberculosis*.[21] Furthermore, **6b** appeared to be more active

than **7b** against fungal strain *Cryptococcus neoformans* and Gram negative *Escherichia coli* and *Pseudomonas aeruginosa*.

Table 5.1: Minimum Inhibitory Concentration (MIC)[1] of two Gram-negative, two Gram-positive and two fungal strains.

Microorganisms	*C. neoformans*		*C. albicans*		*E.coli*		*P. aeroginosa*		*E. faecalis*		*S. aureus*	
Time (h)	24	48	24	48	24	48	24	48	24	48	24	48
Complexes	MIC values (mg/mL)											
1a	0.063	0.031	0.250	0.250	0.250	0.250	0.250	0.250	0.250	0.250	0.250	0.250
1b	0.063	0.250	0.250	0.250	0.250	0.250	0.250	0.063	0.250	0.250	0.250	0.250
1c	0.250	0.250	0.250	0.250	0.250	0.250	0.063	0.250	0.250	0.250	0.250	0.250
2a	0.031	0.063	0.250	0.250	0.250	0.250	0.250	0.250	0.250	0.250	0.250	0.250
2b	0.125	0.250	0.250	0.250	0.250	0.250	0.250	0.250	0.250	0.250	0.250	0.250
3a	0.063	0.031	0.250	0.250	0.250	0.250	0.250	0.250	0.250	0.250	0.250	0.250
3b	0.031	0.250	0.250	0.250	0.031	0.031	0.016	0.031	0.031	0.063	0.031	0.250
4a	0.125	0.250	0.250	0.250	0.250	0.250	0.250	0.250	0.250	0.250	0.250	0.250
4b	0.250	0.250	0.250	0.250	0.250	0.250	0.250	0.250	0.250	0.250	0.250	0.250
5b	0.016	0.250	0.250	0.250	0.031	0.031	0.016	0.016	0.016	0.250	0.125	0.250
6b	0.004	0.031	0.250	0.250	0.004	0.004	0.002	0.002	0.002	0.250	0.002	0.250
7b	0.008	0.016	0.063	0.031	0.016	0.016	0.004	0.004	0.004	0.031	0.004	0.031
9	0.031	0.031	0.250	0.250	0.250	0.063	0.250	0.031	0.063	0.250	0.250	0.250
10	0.016	0.031	0.031	0.063	0.250	0.125	0.031	0.063	0.031	0.250	0.031	0.250
11	0.063	0.063	0.016	0.031	0.250	0.250	0.250	0.250	0.125	0.250	0.016	0.031
Gentamycin	-	-	-	-	0.0008	0.0008	0.0002	0.0002	0.0008	0.0063	0.0004	0.0016
Amphotericin	0.031	0.0125	0.0016	0.0031	-	-	-	-	-	-	-	-

[1] MIC determined after 24 and 48 h incubation at 30 °C for fungi and 37 °C for bacteria.

The varying degree of antimicrobial activity of these derivatives depends either on the impermeability of the cells of the microbes or difference in ribosomes of microbial cells.[22] The effectiveness of **6b** can be explained by overtone's concept and chelation theory.[23] According to overtone's concept of cell permeability, the lipid membrane surrounding the cell favours lipophilic compounds, due to which liposolubility is an important antimicrobial property. On chelation, the π-electrons in P–P ligands are delocalized over the whole chelate ring and lipophilicity is enhanced which in turn increases membrane penetration of the complexes. In the ligand series evaluated in this study the tendency for chelation is greatest for dppe.[21] Thus, **6b** is expected to be more lipophilic and penetration enhanced hence it has a higher antimicrobial activity. The MIC values of **6b** on Gram-negative *Escherichia coli* and *Pseudomonas aeruginosa* was very similar (though slighthly smaller) than those of the reference drug Gentamycin.

Results show that Gram-positive bacteria and the fungal strain *Candida albicans* are resistant toward cluster complex **9**. Moderate activity is observed against Gram-negative *Escherichia coli* and *Pseudomonas aeruginosa* and the fungal strain *Candida albicans* for complexes **10** and **11**. Though the complexes exhibit some activity, it does not reach the effectiveness of the reference agents used in this study at conditions under study. Fungicidal activity against the fungal strain *Cryptococcus neoformans* is observed. It appears in this series of the complexes evaluated, introduction of aromatic functionality had a particular influence on the overall inhibitory action of the complex against tested *Candida albicans* and *Staphylococcus aureus* strains.

5.2 *In vitro* anticancer screening

5.2.1 Introduction

Cancer is the uncontrolled proliferation of genetically altered cells. Chemotherapy, surgery and radiotherapy are some of the methods used for treatment of cancer. Chemotherapy includes the use of cytotoxic agents to attack and destroy cancer cells. Platinum compounds have been the leading agents in cancer chemotherapy.

The success of platinum compounds as anticancer agents has formed the basis for the study of metal based compounds as potential anticancer agents. As alternatives to the platinum compounds other transition metals have been explored and a number of metal complexes with potential application as anticancer agents have been developed.[24] Ruthenium complexes appear to be the most promising alternative of platinum complexes.[25,26]

The search for innovative metal-based drugs has focused on evaluation of the role of the central metal and coordinated ligands. The ligand exchange kinetics of Ru(III) complexes are very similar to the platinum(II) complexes. Ru complexes are less toxic compared to the platinum compounds. In contrast to platinum complexes, the ruthenium complexes have shown a selectivity for cancerous cells;[27,28] this is thought to be due to the ability of ruthenium to mimic iron in binding to biomolecules. As cancer cells over-express transferrin because of demand for Fe, ruthenium-based compounds may be delivered more efficiently to cancer cells.[24,29]

Ruthenium compounds are represented by three complexes which have successfully completed phase I clinical trail.[26,30,31] NAMI-A a leading compound that demonstrated antimetastatic activity,[31] KP1019 and the Na analogue KP1339 exhibited activity against a wide range of primary tumours including the *Cisplatin*-resistant colorectal carcinoma.[26,30]

These Ru(III) complexes are thought to be pro-drugs activated in tumour to give the active species, postulated to be Ru(II) compounds.[26] This theory has stimulated interest in the preparation of Ru(II) complexes as potential anticancer agents. Ru(II) arene complexes have been synthesized and anticancer activity evaluated. They have been found to be active both *in vitro* and *in vivo*. These complexes have been shown to undergo hydrolysis in a similar fashion to cisplatin, subsequently binding to nuclear DNA. Furthermore, extended arene ligands such as biphenyl are capable of intercalating between DNA bases.[32-34]

Ruthenium complexes have shown potential which encouraged the continued search for other transition metals as alternatives to platinum complexes. Osmium belongs to the same group in the periodic table as ruthenium and is expected to possess similar biological activity. However, in comparison to ruthenium complexes, osmium complexes are more inert and have very slow hydrolysis rate. Nevertheless, osmium complexes have potential as anticancer agents. Hence, in this study a series of osmium complexes are screened for their potential activity as new anticancer agents.

5.2.2 *In vitro* cytotoxicity studies

The evaluation of preliminary anticancer activity of both synthetic and natural products on human cancer cell lines uses methods such as [3-(4,5-dimethylthiazol-2-yl)-2,5-diphenyltetrazolium bromide] (MTT) and Sulforhodamine B (SRB) assay methodologies. These assays give an indication of whole cell cytotoxicity, and thus to determine the exact biomolecular target would require further experiments to be performed.

5.1.2.1 MTT assay

MTT assay is a colorimetric assay used to assess cell metabolic activity. Its principle is based on the ability of living cells to reduce MTT, a yellow tetrazole, into purple formazan by

mitochondrial enzyme succinate dehydrogenase (Schme 5.1). The formazan formed is solubilised by addition of dimethylsulfoxide (DMSO) and determined spectrophotometrically. Thus, after treatment with anticancer agents it is possible to determine the number of cells that are living with respect to those cells that are untreated i.e control cells. The number of living cells can be plotted against different concentrations of the anticancer agents on x-axis.[35]

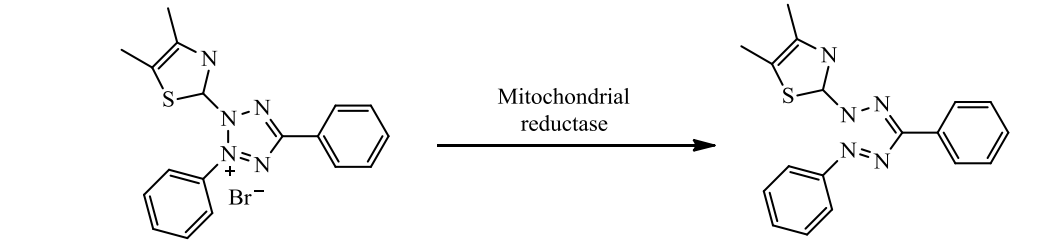

3-(4,5-dimethylthiazol-2-yl)-2,5-diphenyltetrazolium bromide (MTT) (Yellow)

(E,Z)-5-(4,5-dimethylthiazol-2-yl)-1,3-diphenylformazan (Formazan) (Purple)

Scheme 5.1: Reduction of MTT to formazan by cellular reductase enzyme.

5.1.2.2 SRB assay

The Sulforhodamine B (SRB) assay is used to measure drug-induced cytotoxicity and cell proliferation for drug screening applications. SRB is a bright pink aminoxanthene dye with two sulfonic groups (Figure 5.3). It has the ability to electrostatically bind to protein basic amino acid in a pH dependent environment. Under mild acidic conditions the dye binds and under mild basic conditions it is extracted from cells and solubilised for measurement. This assay is simple, accurate, reliable and reproducible. The method not only allows a large number of samples to be tested within a few days, but also requires only simple inexpensive reagents. The SRB assay is therefore an efficient and highly cost effective method for screening.

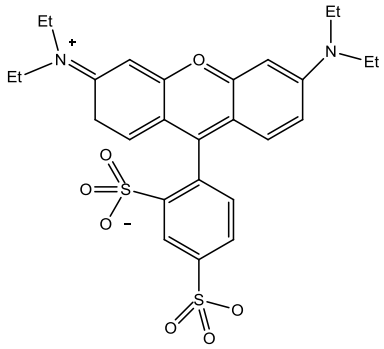

Figure 5.3: Structure of Sulforhodamine B (SRB) dye.

In vitro anticancer activity of a total of 15 compounds have been investigated. This include 12 organometallic complexes of the type $[OsX_2(CO)_2(PR_3)_2]$ and $[Os_3(CO)_{12-n}(PPh_3)_n]$ (n = 2 – 3), and 3 coordination complexes of the type $[OsX_2(P–P)_2]$ using SRB assay method.

5.2.2.1 Materials and Methods

Drugs and reagents

The $[OsX_2(CO)_2(PR_3)_2]$ complexes (X = Cl, Br, I; PR_3 = tertiary phosphine) were prepared as described by Collman and Roper[36] by carbonylation of $[OsX_6]^{2-}$ under pressurised CO gas in 2-methoxyethanol with subsequent addition of the tertiary phosphine under reflux.

The $[OsX_2(P–P)_2]$ complexes were prepared via microwave-promoted synthesis from hexahalo osmate salts $Y_2[OsX_6]$ (Y = K, NH_4; X = Cl, Br, I) in the presence of the corresponding bidentate phosphine ligand.

Cluster complexes of the type $[Os_3(CO)_{12-n}(PPh_3)_n]$ (n = 2-3) were prepared from $Os_3(CO)_{12}$ using microwave promoted synthesis.

5.2.3 *In vitro* anticancer activity

The *in vitro* anticancer activity of the synthesized complexes was determined using an SRB assay against 4 human cancer cell lines: renal (TK-10), melanoma (UACC-62), mammary adenocarcinoma (MCF-7) and HeLa cell lines. Parthenolide and Emetine were used as standards. Structures of the drugs used as standards are shown in Figure 5.5.

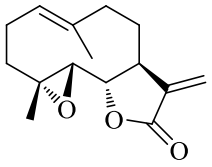

Parthenolide

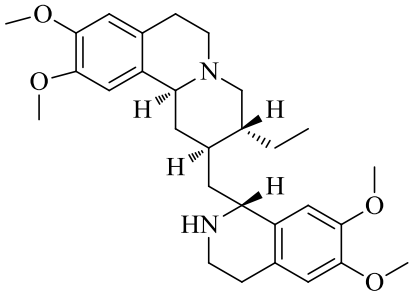

Emetine

Figure 5.4: Chemical structure of compounds used as standards.

Parthenolide, a naturally occurring lactone, has recently attracted considerable attention because of its anticancer effects. The mechanism of action exerted by parthenolide has not been entirely elucidated. However, Yang and colleagues have attempted to define the mode of action in osteosarcoma cancer cells.[37] They reported that parthenolide induces reactive oxygen species (ROS) as a consequence of increased autophagy and mitophagy.[37] Cell death is a consequence of increased ROS.

Emetine is a naturally occurring alkaloid. This compound has been shown to possess important biological activities that make it an important tool for pharmacologists and molecular biologists. Emetine has potential to inhibit DNA, RNA and protein synthesis. It is usually used to block protein synthesis in eukaryotic cells. It acts by blocking the early S phase of DNA replication.[38] It irreversibly inhibits protein synthesis in HeLa cells by

depleting free ribosomes and subsequently increasing the polyribosomes.[39] It binds to 40S ribosomal subunit.[40] Further studies showed that the compound also inhibits DNA synthesis in HeLa cells irreversibly. The compound is also known to inhibit viral RNA synthesis in poliovirus infected HeLa cells.[39]

5.2.4 Results and discussions

The IC_{50} values, defined as the concentration corresponding to 50% growth inhibition, are represented in Table 5.2. The plot of log concentration versus percentage cell viability of complexes **1a-c**, **2a-4b**, **5b-7b**, **9**, **10** and **11** are depicted in Charts 5.1 – 5.5.

A total of 15 compounds were screened against 4 different human cancer cell lines: TK-10 (renal cell adenocarcinoma), UACC-62 (melanoma), MCF-7 (mammary adenocarcinoma) and HeLa cell line and a broad range of IC_{50} values were obtained. The IC_{50} values were in the range 3.46 to >100 μM. In general, the carbonyl containing complexes (**1a - c**, **2a - 4b** and **9 – 11**) tested gave IC_{50} > 100μM against the cancer cell lines under study and were defined as essentially inactive. Inactivity is likely because there is no ligand exchange with biomolecules or the hydrolysis rate is too slow. Hydrolysis is an essential prerequisite for biological activity for some compounds.[41-43]

The active compounds were **5b**, **6b** and **7b** with IC_{50} values in the range 4.25 – 40.97 μM. In TK-10 cells complex **6b** showed potency with IC_{50} value of < 10 μM and **5b** and **7b** showed a moderate effect (IC_{50} at range 10 - 50 μM). Complex **5b** also showed a moderate effect against UACC-62 (IC_{50} = 26.38 μM) and MCF-7 (IC_{50} = 25.01 μM) cell line, respectively. Complex **6b** and **7b** showed comparable effect against the breast cancer cell line (MCF-7) and potency against UACC-62 was also observed. The activity of these complexes is comparable to that of the standard used. *In vitro* antitumour studies indicate greater

sensitivity of **6b** towards UACC-62 than other cancer cell lines displaying IC_{50} values in lower concentrations. A higher activity was observed (IC_{50} = 4.25 μM) compared to the standard, Parthenolide, with IC_{50} value of 5.76 μM indicating the excellent cytotoxicity of this compound. A comparable cytotoxicity of **6b** with parthenolide is observed against the TK-10 and MCF-7 cell line.

Table 5.2: IC_{50} values of **1a-c**, **2a-4b**, **5b-7b** and **9-11** towards TK-10, UACC-62, MCF-7 and HeLa cell.

Tissue		Renal	Melanoma	Breast	Cervix
Cell line		TK-10	UACC-62	MCF-7	HeLa
Entry no.	Complex	IC_{50} (μM)			
1	**1a**	>100	>100	>100	>100
2	**1b**	>100	>100	>100	>100
3	**1c**	>100	>100	>100	>100
4	**2a**	>100	>100	>100	>100
5	**2b**	>100	>100	>100	>100
6	**3a**	>100	>100	>100	>100
7	**3b**	>100	>100	>100	>100
8	**4a**	>100	>100	>100	>100
9	**4b**	>100	>100	>100	>100
10	**5b**	41.0	26.4	25.0	69.9
11	**6b**	9.96	4.25	6.63	3.46
12	**7b**	11.9	9.36	7.01	3.56
13	**9**	>100	>100	>100	>100
14	**10**	>100	>100	>100	>100
15	**11**	>100	>100	>100	>100
	Parthenolide	5.94	5.76	5.66	-
	Emetine	-	-	-	0.08

Results show that complex **6b** demonstrated the highest activity with an IC_{50} value of 4.25 μM against UACC-62, 9.96 μM against TK-10 and 6.63 μM against MCF-7 cell lines. The *trans*-$[OsBr_2(P–P)_2]$ (where P–P = dppe, dppp) complexes exhibit higher anticancer activity against the three cell lines compared with the *cis*-$[OsBr_2(P–P)_2]$ isomer, with IC_{50} = 25.0 μM against MCF-7, 26.4 μM against UACC-62 and 41.0 μM against TK-10.

Under the experimental conditions used in this study the cytotoxicity on TK-10 cells followed the order **6b** > **7b** > **5b**. The same order was followed for both UACC-62 and MCF-7 cancer cell lines. These compounds contain potentially labile Br ligands that can be cleaved to create a vacant coordination site at the metal centre. Cellular components such as DNA, proteins and enzymes have potential to then bind to this vacant site. The Os(II) metal ion is a soft acid and will interact with soft bases such as the sulfur containing amino acids. In addition to halide ligands the chelating phosphine ligands (dppm, dppe and dppp) which contain phenyl groups that have the potential to intercalate DNA bases.

Structural modifications of the complexes could have significant effects on the antitumour activity of the complexes. *In vitro* potency of the *trans*-$[OsBr_2(P–P)_2]$ complex (where P–P = dppe, dppp) increases with a decrease in alkyl chain between the donor P atoms. This can be explained by chelation theory and overtone's concept of cell permeability.[44] Liposolubility is greatest in dppe complex. Hence, it exhibits the highest activity in comparison to the dppp complex. Interestingly, the complex *cis*-$[OsBr_2(dppm)_2]$ exhibited moderate cytotoxicity with IC_{50} higher than the *trans* isomers. This low activity suggests that the *cis* complex has a different mechanism of action compared to the *trans* complexes.

The different anticancer activity observed of a single complex, as shown by the IC_{50} values, against the different human cancer cell lines might be related to the structural composition of the cell wall, since this is the first structural difference between the TK-10, UACC-62 and MCF-7 cell lines. Hence, we hypothesize that the different anticancer activity of the compounds against the different cancer cell lines could be explained by the ability to cross the membrane into the cell and interact, producing changes that eventually cause death of cancerous cells. Also the proliferation of any two different cell lines is expected to differ hence variation in the IC_{50} values is observed.

The compounds were further evaluated for general cytotoxicity on the HeLa cell line using SRB assay. Some of the complexes showed comparable cytotoxicity for tumour cells and HeLa cells. Compound **5b** presented lower cytotoxicity on HeLa cell line (IC_{50} = 69.9 μM) than TK-10, UACC-62 and MCF-7 (IC_{50} = 41.0, 26.4, 25.0 μM). Compound **6b** and **7b** exhibited higher sensitivity towards HeLa cell (IC_{50} = 3.46, 3.56 μM) than TK-10 (9.96, 11.9 μM), UACC-62 (4.25, 9.36 μM) and MCF-7 cell line (IC_{50} = 6.63, 7.01 μM), respectively. Complex **5b**, **6b** and **7b** were all found to be significantly less cytotoxic relative to the Emetine standard.

The cytotoxicity profiles of all the compounds clearly identified compound **6b** as a potential candidate for further investigation, displaying IC_{50} values in lower concentrations against both UACC-62 and MCF-7 cells. Compound **6b** is evidently more potent in inducing cytotoxicity compared to other derivatives. From the cell viability (%) vs complex concentration graph, a dose dependent activity was observed towards the cell lines. The results demonstrated that the complexes suppressed the growth rate in a dose-dependent manner.

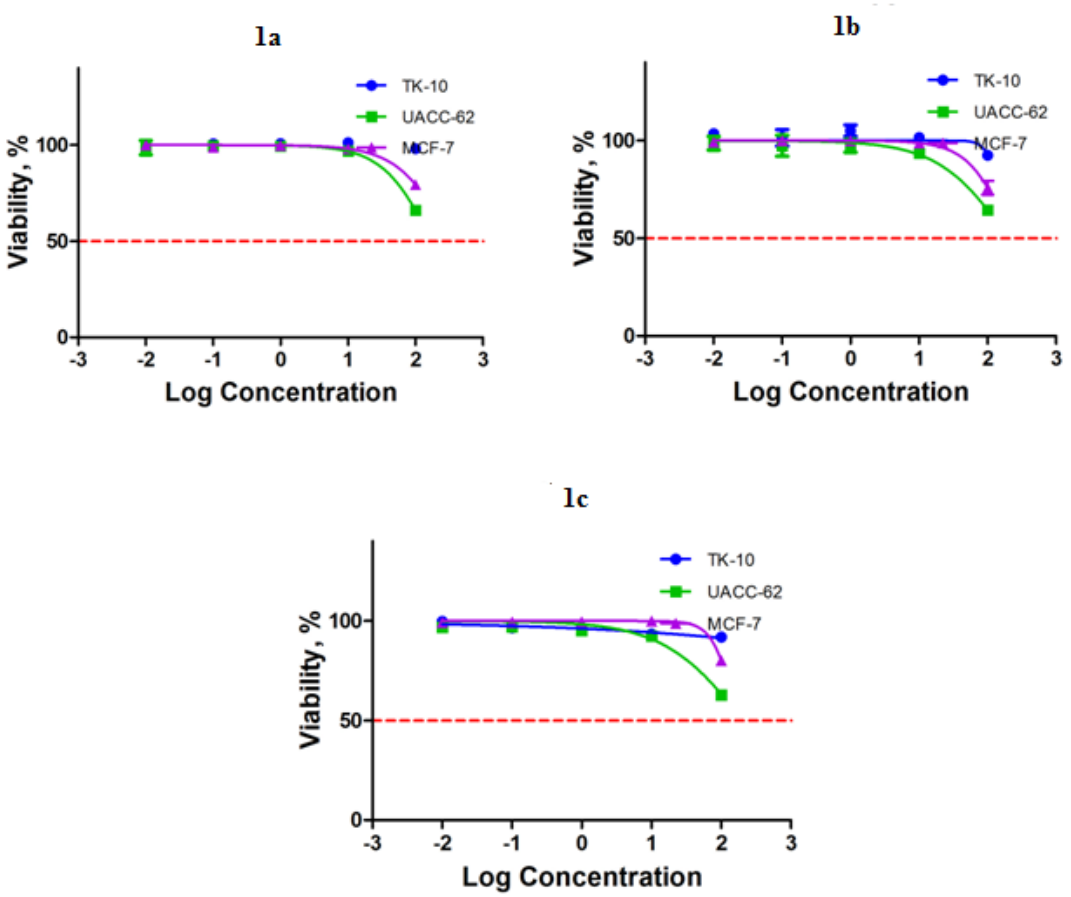

Chart 5.1: The plot of log concentration versus percentage cell viability of **1a**, **1b** and **1c** against TK-10, UACC-62 and MCF-7.

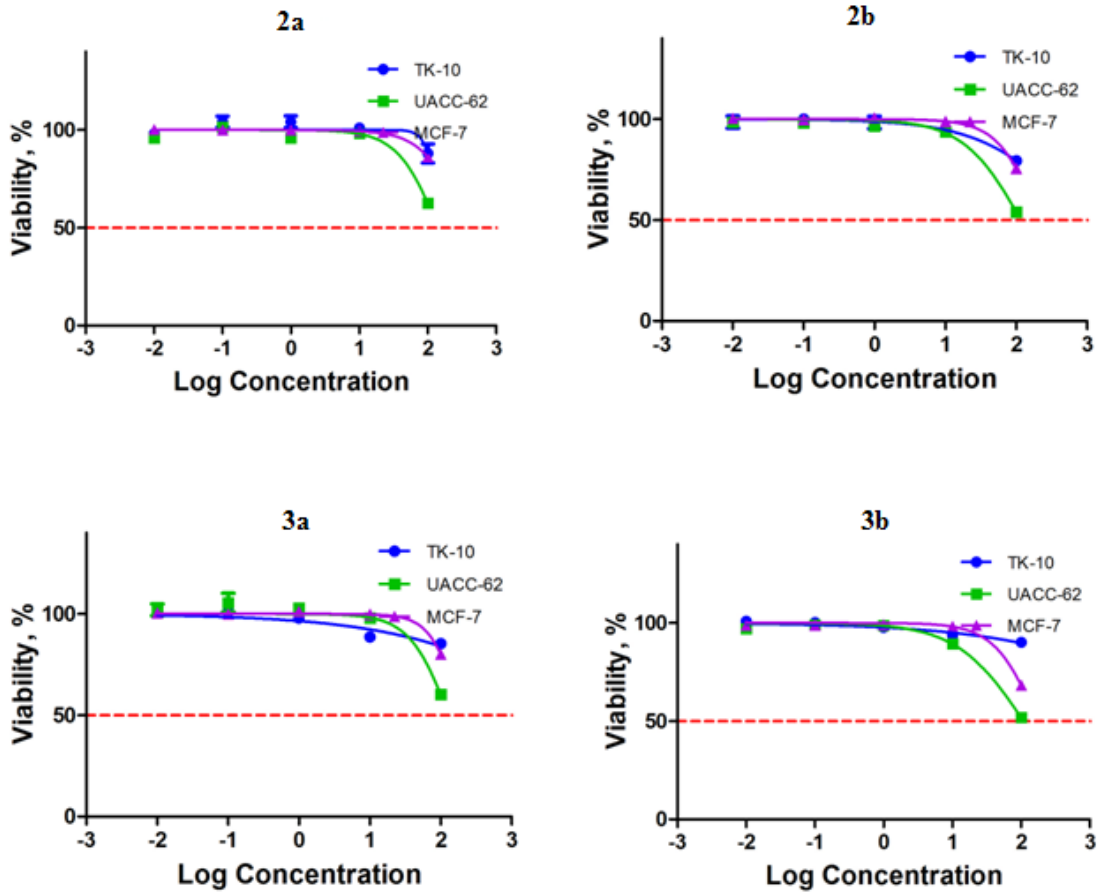

Chart 5.2: The plot of log concentration versus percentage cell viability of **2a**, **2b, 3a** and **3b** against TK-10, UACC-62 and MCF-7.

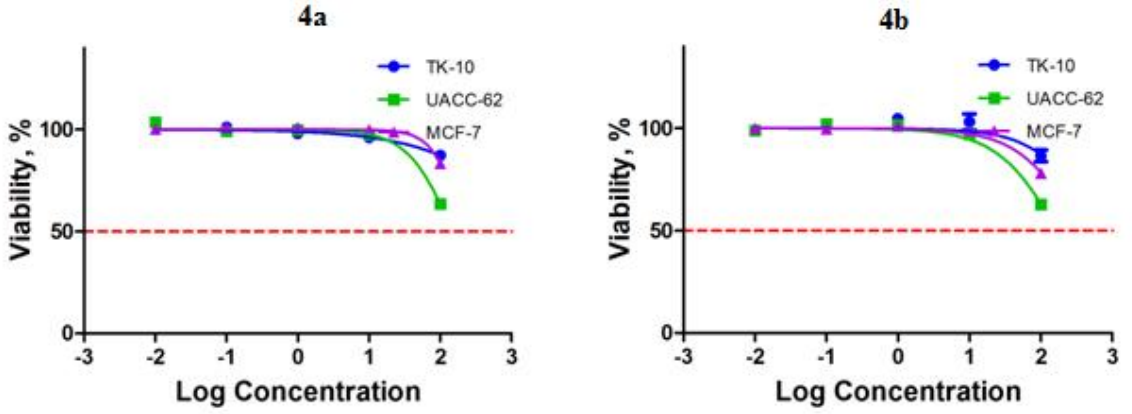

Chart 5.3: The plot of log concentration versus percentage cell viability of **4a** and **4b** against TK-10, UACC-62 and MCF-7.

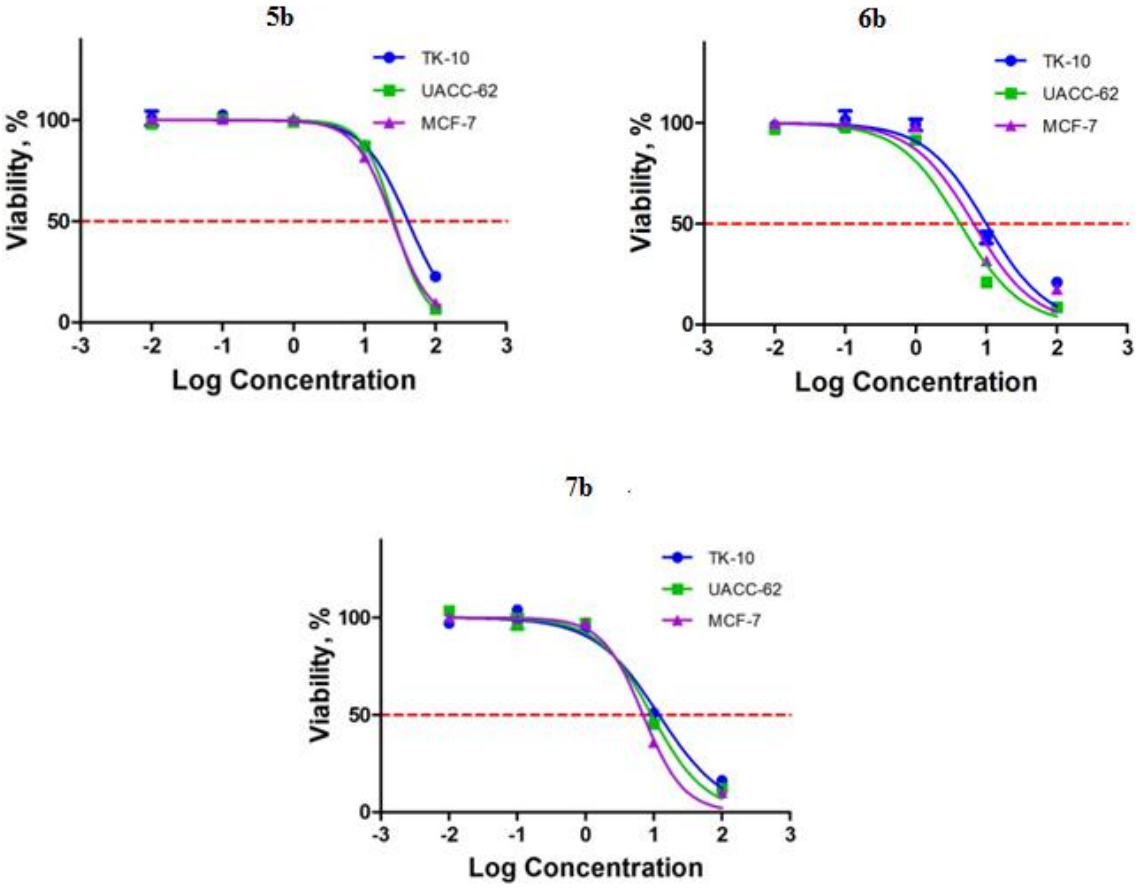

Chart 5.4: The plot of log concentration versus percentage cell vialbility of **5b**, **6b** and **7b** against TK-10, UACC-62 and MCF-7.

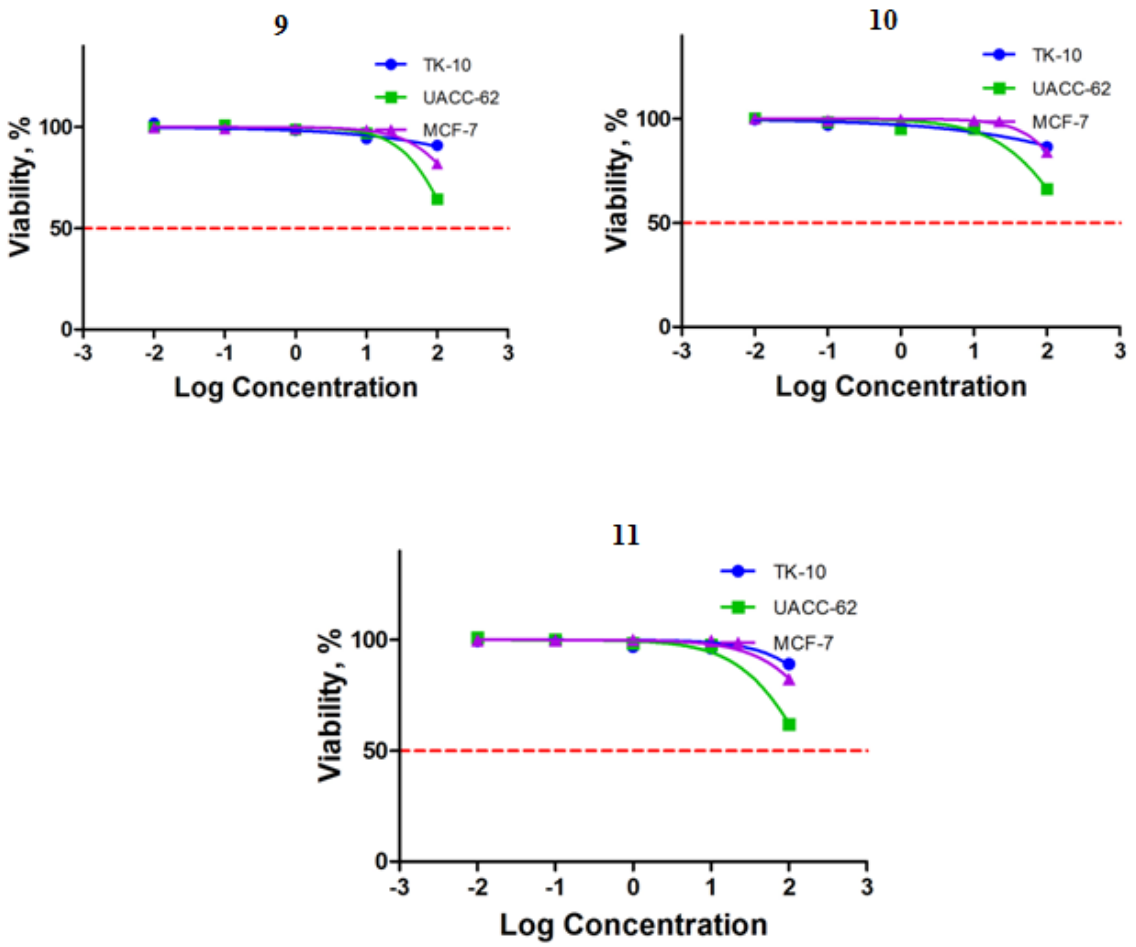

Chart 5.5: The plot of log concentration versus percentage cell vialbility of **9**, **10** and **11** against TK-10, UACC-62 and MCF-7.

5.3 Conclusions

The microdilution assay revealed the effectiveness of the tested compounds on Gram-positive, Gram-negative and fungal strains. These micro-organisms showed resistance against mononuclear Os(II) carbonyl complexes. A moderate antimicrobial activity was observed for Os(0) carbonyl cluster complexes with a coordinated PPh_3 ligand. The non-substituted phosphine cluster complex $[Os_3(CO)_{12}]$ exhibited little to moderate activity against fungal strains. Os(II) coordinate complexes of the type $[OsX_2(P–P)_2]$ generally exhibited good antimicrobial activity which is comparable with the reference antibiotics in some instances. The difference in degree of activity may be related to the ability of the compounds in penetrating the microbe cell wall. The proposed mechanism of action for the active $[OsX_2(P–P)_2]$ complex is protein synthesis inhibition because of selectivity of Gram-negative versus Gram-positive bacteria.

Results from the SRB assay on TK-10, UACC-62 and MCF-7 cell lines show that compounds **5b**, **6b** and **7b** exhibit antitumuor activity. Among these complexes compound **6b** showed the highest potency with IC_{50} value < 10 μM against all cancer cell lines. This compound also showed a higher activity relative to the standard compound Parthenolide. Compound **7b** was potent against the UACC-62 and MCF-7 cell lines and showed moderate activity against the renal cell line. The active compounds could be considered to be useful templates for further development to obtain more potent anticancer agents.

Interestingly, compound **6b** shows the highest antimicrobial and anticancer activity. Having both this activity is ideal because more often for some cancer patients, treatment weakens the immune system and the patient is more susceptible to other infections. Having the potential to inhibit the growth of microbes and cytotoxicity against cancerous cell could be beneficial.

5.4 References

(1) Li, F.; Collins, J. G.; Keene, F. R. *Chem. Soc. Rev.* **2015**, *44*, 2529.

(2) Boucher, H. W.; Talbot, G. H.; Bradley, J. S.; Edwards, J. E.; Gilbert, D.; Rice, L. B.; Scheld, M.; Spellberg, B.; Bartlett, J. *Clin. Infect. Dis.* **2009**, *48*, 1.

(3) Salem, S. S.; Ali, M., A, M *Biol. Pharm. Bul.* **2016**, *39*, 473.

(4) Fleming, A. *Br. J. Exp. Pathol.* **1929**, *10*, 226.

(5) Chain, E.; Florey, H. W.; Gardner, A. D.; Heatley, N. G.; Jennings, M. A.; Orr-Ewing, J.; Sanders, A. G. *Lancet* **1940**, *2*, 226.

(6) Schatz, A.; Waksman, S. A. *Exp. Boil. Med.* **1944**, *57*, 244.

(7) Abraham, E. P.; Newton, G. G. F. *Biochem. J.* **1961**, *79*, 377.

(8) Hamilton-Miller, J. M. T. *Int. J. Antimicrob. Agents* **2000**, *15*, 179.

(9) Ventola, C. L. *P.T.* **2015**, *40*, 277.

(10) Aminov, R. J. *Front. Microbiol* **2010**, *1*, 1.

(11) Tommasino, J.-B.; Pilet, G.; Renaud, F. N. R.; Novitchi, G.; Robert, V.; D, L. *Polyhedron* **2012**, *27*, 27.

(12) Neelakantan, M. A.; Esakkiammal, M.; Mariappan, S. S.; Dharmaraja, J.; Jeyakumar, T. *Ind. J. Pharmaceut. Sci.* **2010**, *72*, 216.

(13) Dwyer, F. P.; Reid, G.; Shulman, L. N.; Laycock, G. M.; Dixson, S. *Aust. J. Exp. Biol. Med. Sci.* **1969**, *47*, 203.

(14) Lam, P.-L.; Lu, G.-L.; Hon, K.-M.; Lee, K.-W.; Ho, C.-L.; Wang, X.; Tang, J. C.-O.; Lam, K.-H.; Wong, R. S.-M.; Kok, S. H.-L.; Bian, Z.-X.; Li, H.; Lee, K. K.-H.; Gambari, R.; Chui, C.-H.; Wong, W.-Y. *Dalton Trans.* **2014**, *43*, 3949.

(15) Ramos, A. I.; Braga, T. M.; Braga, S. S. *Mini-Rev. Med. Chem.* **2012**, *12*, 227.

(16) Allardyce, C. S.; Dyson, P. J.; Ellis, D. J.; Salter, P. A.; Scopelliti, R. *J. Organomet. Chem.* **2003**, *668*, 35.

(17) Eloff, J. N. *Planta. Medica.* **1998**, *64*, 711.

(18) Masoko, P.; Picard, J.; Eloff, J. N. *J. Ethnopharmacol.* **2005**, *99*, 301.

(19) Bowman, S. M.; Free, S. J. *BioEssays* **2006**, *28*, 799.

(20) Hossain, M. A.; Ghannoum, M. A. *Expert Opin. Investig. Drugs* **2000**, *9*, 1797.

(21) Pavan, F. R.; Von Poelhsitz, G.; do Nascimento, F. B.; Leite, S. R. A.; Batista, A. A.; Deflon, V. M.; Sato, D. N.; Franzblau, S. G.; Leite, C. Q. F. *Eur. j. Med. Chem.* **2010**, *45*, 598.

(22) Thangadurai, T. D.; Son-Ki, I. *Synth. React. Inorg. Met. -Org. Nano-metal Chem.* **2005**, *47*, 1352.

(23) Manimaran, A.; Jayabalakrishnan, C. *Appl. Organomet. Chem.* **2010**, *24*, 71.

(24) Allardyce, C. S.; Dorcier, A.; Scolaro, C.; Dyson, P. J. *Appl. Organomet. Chem.* **2005**, *19*, 1.

(25) Hartinger, C. G.; Zorbas-Seifried, S.; Jakupec, M. A.; Kynast, B.; Zorbas, H.; Keppler, B. K. *J. Inorg. Biochem.* **2006**, *100*, 891.

(26) Hartinger, C. G.; Jakupec, M. A.; Zorbas-Seifried, S.; Groessl, M.; Egger, A.; Berger, W.; Zorbas, H.; Dyson, P. J.; Keppler, B. K. *Chem. Biodivers.* **2008**, *5*, 2140.

(27) Allardyce, C. S.; Dyson, P. J. *Platinum Metals Rev.* **2001**, *45*, 62.

(28) Kostova, I. *Curr. Med. Chem.* **2006**, *13*, 1085.

(29) Dyson, P. J.; Sava, G. *Dalton Trans.* **2006**, *16*, 1929.

(30) Heffeter, P.; Boeck, K.; Atil, B.; Hoda, M. A. R.; Koemer, W.; Bartel, C.; Jungwirth, U.; Keppler, B. K.; Micksche, M.; Micheal, B.; Walter, B.; Gunda, K. *J. Biol. Inorg. Chem.* **2010**, *15*, 737.

(31) Rademaker-Lakhai, J. M.; Van den Bongard, D.; Pluim, D.; Beijnen, J. H.; Schellens, J. H. *Clin. Cancer Res.* **2004**, *10*, 3717.

(32) Chen, H.; Parkinson, J. A.; Parsons, S.; Coxall, R. A.; Gould, R. O.; Sadler, P. J. *J. Am. Chem. Soc.* **2002**, *124*, 3064.

(33) Chen, H.; Parkinson, J. A.; Morris, R. E.; Sadler, P. J. *J. Am. Chem. Soc.* **2003**, *125*, 173.

(34) Liu, H.-K.; Berners-Price, S. J.; Wang, F.; Parkinson, J. A.; Xu, J.; Bella, J.; Sadler, P. J. *Angew. Chem. Int. Ed.* **2006**, *45*, 8153.

(35) Saha, A.; Mohapatra, S.; Das, G.; Jana, B.; Ghosh, S.; Bhunia, D.; Ghosh, S. *ACS Applied Mat. Interfaces* **2016**, *ahead of print*.

(36) Collman, J. P.; Roper, W. R. *J. Am. Chem. Soc.* **1966**, *88*, 3504.

(37) Yang, C.; Yang, Q. O.; Kong, Q.-J.; Yuan, W.; Yang, Y.-P. O. *Cell. Physiol. Biochem.* **2016**, *40*, 146.

(38) Schweighoffer, T.; Schweighoffer, E.; Apati, A.; Antoni, F.; Molnar, G.; Lapis, K.; Banfalvi, G. *Histochemistry* **1991**, *96*, 93.

(39) Grollman, A. P. *J. Biol. Chem.* **1968**, *235*, 4089.

(40) Garcia, R. M. A.; Oliveira, M. A.; Barros, W. S. *Biochem. Syst. Ecol.* **2005**, *33*, 233.

(41) Dorcier, A.; Ang, W. H.; Bolano, S.; Gonsalvi, L.; Juillerat-Jeannerat, L.; Laurenczy, G.; Peruzzini, M.; Phillips, A. D.; Zanobini, F.; Dyson, P. J. *Organometallics* **2006**, *25*, 4090.

(42) Scolaro, C.; Hartinger, C. G.; Allardyce, C. S.; Keppler, B. K.; Dyson, P. J. *J. Inorg. Biochem.* **2008**, *102*, 1743.

(43) Gossens, C.; Dorcier, A.; Dyson, P. J.; Rothlisberger, U. *Organometallics* **2007**, *26*, 3969.

(44) Sivakami, M.; Natarajan, B.; Vijayachandrasekar *Chem. Sci. Trans.* **2014**, *3*, 1110.

Chapter 6

Experimental

6.1 General experimental details

Carbonylation reactions were carried out in a Berghof Bar 845 autoclave. After carbonylation further manipulations were carried out under an inert atmosphere of argon using standard Schlenk techniques. The microwave irradiation experiments were undertaken in a Monowave 900 microwave reactor using thick-walled 35 mL glass reaction vessel with Teflon-lined caps. All solvents used for microwave synthesis were used as received. The instrument used was programmed to reach the set temperature within a minute and maintain that temperature for the required time. In each case, the reactor was set to a maximum of 6 bar and high stirring rate was used. Caution was taken due to the toxic nature of metal carbonyl compounds. All manipulations were conducted under a highly efficient fume hood. The general cell culture technique and conditions for biochemical studies are as described in Section 6.4.Thin layer chromatography (TLC) was carried out on TLC Silica gel 60 F_{254} from Merck.

6.2 Solvents and reagents

Solvents were dried and distilled by standard literature procedures and stored in an atmosphere of argon. Dichloromethane and acetonitrile were distilled from calcium hydride. Methanol and 2-methoxyethanol were distilled from magnesium/iodine. Most chemicals were used as received, unless otherwise stated.

Potassium osmate $K_2[OsO_2(OH)_4]$ was obtained from Anglo Platinum Corporation. $(NH_4)_2[OsCl_6]$, $(NH_4)_2[OsBr_6]$ and $K_2[OsI_6]$ were prepared from $K_2[OsO_2(OH)_4]$ using the method reported by Chiririwa and Muzenda.[1] Triphenylphosphine ($P(C_6H_5)_3$), benzyldiphenylphosphine ($Ph_2P(CH_2C_6H_5)$, tribenzylphosphine ($P(CH_2C_6H_5)_3$), tricyclohexylphosphine ($P(C_6H_{11})_3$), 1,1-bis(diphenylphosphino)methane (dppm), 1,2-bis(diphenylphosphino)ethane (dppe), 1,3-bis(diphenylphosphino)propane (dppp), 1,4-bis(diphenylphosphino)butane (dppb) were purchased from Sigma-Aldrich and used as received.

6.3 Characterization techniques

Infrared spectra were recorded on a Bruker vertex 70 FT-IR spectrophotometer. All measurements were conducted between 4000 and 400 cm^{-1}. Spectra were recorded using dichloromethane as a solvent for cluster complexes (Chapter 4). Spectra was recorded in solid state (Chapter 2 and 3). Spectra obtained at spectral resolution of 4 cm^{-1}.

Raman studies were conducted on a Bruker vertex 70 FT-Raman spectrophotometer. All measurements were carried out between 4000 and 50 cm^{-1}. Spectra obtained from solids at spectral resolution of 4 cm^{-1}.

NMR spectroscopic studies were recorded on Agilent spectrophotometer (300 MHz for ^{1}H, 75 MHz for ^{13}C, 121 MHz for ^{31}P) and data reported using the chemical shift scale in units of ppm relative to the solvent resonance: ^{1}H $CDCl_3$ 7.24 ppm and ^{13}C $CDCl_3$ 77.00 ppm. Spectral measurements recorded at room temperature.

Thermal stability of the compounds was recorded on a Thermogravimetric Analysis SQ600 at temperatures ranges between 100 and 1300 °C at a heating rate of 10 °C/min.

Elemental analyses were carried out by Agricultural Research Council (ARC)-Institute for soil, climate and water

Data collection and structure determinations were done by Prof A. Lemmerer at the University of the Witwatersrand.

6.4 Biochemical studies

6.4.1 *In vitro* antibacterial studies

The *in vitro* antimicrobial screening was done at the College of Agriculture and Environmental Science (CAES) at UNISA.

6.4.1.1 Microorganism and reagents

E. coli (ATCC 35218), *P.aeruginosa* (ATCC 7700), *E. Faecalis* (ATCC 19433), *S. Aureus* (ATCC 25925), *C. Albicans* (ATCC 24433) and *C. Neoformans* (ATCC 14116) were obtained from Davis dianostics. Gentamicin, Amphotericin B, p-iodonitrotetrazolium violet (p-INT) and dimethylsulfoxide (DMSO) were purchased from Sigma-Aldrich. Muller-Hilton (MH) agar, MH broth, Sabouraud dextrose agar and Sabouraud dextrose broth were obtained from Sigma-Aldrich.

6.4.1.2 Antibacterial microdilution assay

To determine the minimum inhibitory concentration (MIC) values for the test compounds a serial microdilution assay developed by Eloff was used.[2] The test compounds were dissolved in an appropriate solvent (DMSO or acetone) to a concentration of 1 mg/mL and serially diluted up to 50% with water in a 96 well microtitre plate. The bacterial cultures were

maintained on Muller-Hilton (MH) agar at 4 °C and in MH broth at 37 °C. Growing bacterial organisms were transferred into a fresh MH broth and 100 μL of these cultures were added to each well. The plates were incubated overnight at 37 °C in 100% relative humidity. DMSO was used as negative control and Gentamicin was used as a reference antibiotic and a positive control. About 40 μL of 0.2 mg/mL INT was added to each well after incubation and the plates then incubated further at 37 °C for an additional 2 h.

6.4.1.3 Antifungal microdilution assay

For the antifungal assay a modified version of microdilution assay developed by Eloff and colleagues was used.[3] The fungal strains were maintained in Sabouraud dextrose agar and Sabouraud dextrose broth prior to inoculation. Two-fold serial dilutions of the test compound were prepared as described above for bacteria. Growing fungal organisms were transferred into Sabouraud dextrose broth and 100 μL of these cultures were added to each well. DMSO was used as neative control and Amphotericin-B was used as antifungal agent and positive control. 40 μL of 0.2 mg/mL INT was added to each well and the plates were incubated at 30 °C for 24 h. The MIC was determined at the lowest sample concentration of compounds at which fungal growth was inhibited.

6.4.2 Anticancer assay

6.4.2.1 Tumor cell lines for *in vitro* tests

The *in vitro* anticancer and cytotoxicity screening was done at the CSIR Biosciences Pharmacology division. The renal (TK-10), melanoma (UACC-62), breast (MCF-7) and Hela (ECACC) human cancer cell line were obtained from NCI (National Cancer Institute) and

maintained in Roswell Park Memorial Institute (RPMI) medium supplemented with 5% fetal bovine serum, 2 mM L-glutamine and 50 μg/ml gentamicin.

All cells were maintained in CO_2 incubator with 5% CO_2, 95% air and 100% relative humidity at 37 °C. Cell lines were routinely maintained as a monolayer cell.

6.4.2.2 Cell viability

Cells were inoculated on 96-well plates for 24 h before incubation with concentrations ranging from 100 - 0.01 μM concentration of the compounds. Analysis was performed after 24 h incubation period by Sulforhodamine B (SRB) viability test. The results are expressed as the concentrations inhibiting growth by 50% (IC_{50}) after a 2-day incubation period after exposure to the complexes. The complexes were dissolved in DMSO just before incubation with cancer cells. Cells without drug addition were used as a control for the experiment. The cells with only medium were used as blanks.

Drug induced cytotoxicity and cell proliferation was measured using the SRB assay developed by Skehan and collegues.[4] Adherent cells were fixed with 50% cold trichloroacetic acid (TCA). After fixation TCA was washed, dried and dyed with SRB. Unbound dye was removed and bound stain was dissolved in 10 mM tris base (tris-hydroxymethyl-aminomethane). Absorbance was read at 540 nm wavelength.

6.5 Preparation of complexes

6.5.1 General procedure for $[OsX_2(CO)_2(PR_3)_2]$

Complex **1a-c**, **2a-4b** were synthesized according to the general method given below. The procedure has two parts, the first part involves carbonylation under pressurized gas (CO). The

second part is done under inert gas using Schlenk tube techniques. An excess of tertiary phosphine was used in the synthesis.

Method:

Into a 100 mL Teflon reaction cup equipped with a magnetic stirrer were placed hexahalo osmate salt $[OsX_6]^{2-}$ (where X = Cl, Br, I) and alcohol solvent and inserted into an autoclave. The reaction mixture was purged with ca. 5 bar carbon monoxide while stirring and finally pressurised to 10 bar at 140 °C for 48 h. The pressurized gas was vented after cooling to room temperature. An excess of tertiary phosphine ligand was weighed into a Schlenk tube and the pale yellow solution from reaction cup added. The mixture was heated to reflux and solution was left to cool to room temperature before filtering off the crude product (white solid). More product was obtained from the filtrate, concentrated under reduced pressure. The product was washed thoroughly with hexane and dried in vacuum.

6.5.1.1 *cis,cis,trans*-$[OsCl_2(CO)_2(PPh_3)_2]$ (1a)

Reactants: $(NH_4)_2[OsCl_6]$ (0.20 g, 0.45 mmol), 2-methoxyethanol (50 mL) and PPh_3 (0.34 g, 1.30 mmol). Yield (0.25 g, 66%). Anal. Calc. For $C_{38}H_{30}Cl_2O_2OsP_2$: C, 54.22 %; H, 3.59%; Found: C, 53.74%; H, 3.58%. Solid IR (ν_{CO}): 2043(s), 1960(s) cm^{-1}. Raman ($\nu_{(Os\text{-}X)}$): 308(vs), 284(vs) cm^{-1}. ^1H NMR (300 MHz, $CDCl_3$): δ 7.87 (dt, $J_{(HH)}$ = 9.4, 5.3 Hz, 18H, H-aromatic), 7.40 (dd, $J_{(HP)}$ = 3.7, 2.3 Hz, 12H, H-aromatic) ppm. $^{13}C\{H\}$ NMR (75 MHz, $CDCl_3$): δ 172.88 (t, $J_{(PC)}$ = 7.1 Hz, carbonyl C), 134.35 (t, $J_{(PC)}$ = 5.2 Hz, *ortho C*, phenyl), 131.13 (d, $J_{(PC)}$ = 26.9 Hz, *ipso C*, phenyl), 130.63 (s, *para C*, pheny), 128.16 (t, $J_{(PC)}$ = 5.1 Hz, *meta C*, phenyl) ppm. $^{31}P\{H\}$ NMR (121 MHz, $CDCl_3$): δ -10.21 (s) ppm. TGA (on set of decomposition): 315 °C.

6.5.1.2 *cis,cis,trans*-$[OsBr_2(CO)_2(PPh_3)_2]$ (1b)

$(NH_4)_2[OsBr_6]$ (2.07 g, 2.93 mmol), 2-methoxyethanol (40 mL) and PPh_3 (2.07 g, 7.89 mmol). Yield (2.20 g ,81%). Anal. Calc. For $C_{38}H_{30}Br_2O_2OsP_2$: C, 49.04%; H, 3.25%; Found: C, 47.59%; H, 3.13%. Solid IR (ν_{CO}): 2041(s), 1960(s) cm^{-1}. Raman ($\nu_{(Os\text{-}X)}$): 229(vs), 210(s) cm^{-1}. ^1H NMR (300 MHz, $CDCl_3$): δ 7.89 (ddd, $J_{(HP)}$ = 9.8, 6.4, 3.4 Hz, 12H, H-aromatic), 7.48 – 7.30 (m, 18H, H-aromatic) ppm. $^{13}C\{H\}$NMR (75 MHz, $CDCl_3$): δ 171.66 (t, $J_{(PC)}$ = 7.1 Hz, C carbonyl), 134.90 (t, $J_{(PC)}$ = 5.0 Hz, *ortho C*, phenyl), 131.86 (t, $J_{(PC)}$ = 27.1 Hz, *ipso C*, phenyl), 130.72 (s, *para C*, phenyl), 127.82 (t, $J_{(PC)}$ = 5.2 Hz, *meta C*, phenyl) ppm. ^{31} P{H} NMR (121 MHz, $CDCl_3$): -17.15 (s) ppm. TGA (on set of decomposition): 313 °C.

6.5.1.3 *cis,cis,trans*-$[OsI_2(CO)_2(PPh_3)_2]$ (1c)

$K_2[OsI_6]$ (1.18 g, 1.14 mmol), 2-methoxyethanol (50 mL) and triphenylphosphine (0.89 g, 4.88 mmol). Yield (0.81 g, 69%).Solid IR (ν_{CO}): 2033(s), 1962(s) cm^{-1}. Raman ($\nu_{(Os\text{-}X)}$): 174(vs), 157(vs) cm^{-1}. ^1H NMR (300 MHz, $CDCl_3$): δ 8.00 – 7.67 (m, 12H, H-aromatic), 7.67 – 7.30 (m, 18H, H-aromatic) ppm. $^{13}C\{H\}$ NMR (75 MHz, $CDCl_3$): δ 169.93 (t, $J_{(PC)}$ = 6.7 Hz, C carbonyl), 134.90 (t, $J_{(PC)}$ = 4.8 Hz, *ortho C*, phenyl), 131.86 (t, $J_{(PC)}$ = 27.1 Hz, *ipso C*, phenyl), 130.72 (s, *para C*, phenyl), 127.82 (t, $J_{(PC)}$ = 5.2 Hz, *meta C*, benzyl) ppm. ^{31} P{H} NMR (121 MHz, $CDCl_3$): δ -28.44 (s) ppm. TGA (on set of decomposition): 299 °C

6.5.1.4 *cis,cis,trans*-$[OsCl_2(CO)_2\{Ph_2P(CH_2C_6H_5)\}_2]$ (2a)

$(NH_4)_2[OsCl_6]$ (0.20 g, 0.46 mmol), 2-methoxyethanol (40 mL) and benzyldiphenylphosphine (0.33 g, 1.19 mmol). Yield (0.25 g, 63%). Anal. Calc. For $C_{40}H_{34}Cl_2O_2OsP_2$: C, 55.24%; H, 3.94%; Found: C, 55.40%; H, 3.90%. Solid IR (ν_{CO}):

2036(s), 1962(s) cm^{-1}. Raman ($\nu_{(Os-X)}$): 312(s), 285(m) cm^{-1}. ^{1}H NMR (300 MHz, $CDCl_3$): δ 7.75 – 7.57 (m, 8H, H-aromatic), 7.49 – 7.18 (m, 12H, H-aromatic), 6.93 (dt, $J_{(HH)}$ = 25.2, 7.2 Hz, 6H, H-aromatic), 6.61 (d, $J_{(HH)}$ = 7.1 Hz, 4H, H-aromatic), 4.41 (t, $J_{(HP)}$ = 4.4 Hz, 4H, 2 × CH_2 benzyl) ppm. $^{13}C\{H\}$ NMR (75 MHz, $CDCl_3$): δ 172.52 (t, $J_{(PC)}$ = 6.8 Hz, C carbonyl), 133.55 (t, $J_{(PC)}$ = 5.7 Hz, *ipso C*, benzyl), 133.40 (t, $J_{(PC)}$ = 4.9 Hz, *ortho C*, phenyl), 130.73 (s, *para C*, phenyl), 130.45 (s, *ortho C*, benzyl), 129.14 (t, $J_{(PC)}$ = 25.5 Hz, *ipso C*, phenyl), 128.15 (t, $J_{(PC)}$ = 5.0 Hz, *meta C*, phenyl), 127.70 (s, *meta C*, benzyl), 126.12 (s, *para C*, benzyl), 29.14 (t, $J_{(PC)}$= 13.1 Hz, CH_2, benzyl) ppm. ^{31} P{H} NMR (121 MHz, $CDCl_3$): δ -3.80 (s) ppm. TGA (on set of decomposition): 330 °C.

6.4.1.5 *cis,cis,trans*-$[OsBr_2(CO)_2\{Ph_2P(CH_2C_6H_5)\}_2]$ (2b)

$(NH_4)_2[OsBr_6]$ (2.00 g, 2.83 mmol), 2-ethoxyethanol (70 mL) and benzyldiphenylphosphine (2.16 g, 7.82 mmol). Yield (1.50 g, 55%). Solid IR ($\nu_{(CO)}$): 2040(s), 1970(s) cm^{-1}. Raman ($\nu_{(Os-X)}$): 210(vs), 190(s). ^{1}H NMR (300 MHz, $CDCl_3$): δ 7.69 (dd, $J_{(HP)}$ = 6.7, 13.8 Hz, 8H, H- aromatic), 7.30 (dd, $J_{(HH)}$ = 24.0, 3.7 Hz, 12H, H-aromatic), 6.92 (dt, $J_{(HH)}$ = 15.0, 7.2 Hz, 6H, H-aromatic), 6.60 (d, $J_{(HH)}$ = 7.2 Hz, 4H, H-aromatic), 4.56 (t, $J_{(HP)}$ = 4.3 Hz, CH_2 benzyl) ppm. $^{13}C\{H\}$ NMR (75 MHz, $CDCl_3$): δ 171.45 (t, $J_{(PC)}$ = 6.8 Hz, C carbonyl), 134.10 (t, $J_{(PC)}$ = 5.4 Hz, *ipso C*, benzyl), 133.63 (t, $J_{(PC)}$ = 4.8 Hz, *ortho C*, phenyl), 130.70(s, *para C*, phenyl), 130.43 (s, *ortho C*, benzyl), 129.12 (t, $J_{(PC)}$ = 25.8 Hz, *ipso C*, phenyl), 128.01 (t, $J_{(PC)}$ = 4.9 Hz, *meta C*, phenyl), 127.70 (s, *meta C*, benzyl), 126.08 (s, *para C*, benzyl), 31.61 (t, $J_{(PC)}$ = 13.9 Hz, CH_2, benzyl) ppm. ^{31} P{H} NMR (121 MHz, $CDCl_3$): δ -11.04 (s) ppm. TGA (on set of decomposition): 197 °C.

6.4.1.6 *cis,cis,trans*-$[OsCl_2(CO)_2\{P(CH_2C_6H_5)_3\}_2]$ (3a)

$(NH_4)_2[OsCl_6]$ (0.20 g, 0.46 mmol), 2-methoxyethanol (40 mL) and tribenzylphosphine (0.38 g, 1.18 mmol) .Yield (0.43 g, 63%). Solid IR ($\nu_{(CO)}$): 2034(s), 1960(s) cm^{-1}. Raman ($\nu_{(Os-X)}$): 311(vs), 305(vs) cm^{-1}. ^1H NMR (300 MHz, $CDCl_3$): δ 7.46 – 7.15 (m, 18H, H-aromatic), 7.15 – 6.98 (m, 12H, H-aromatic), 3.61 (t, $J_{(HP)}$ = 3.8 Hz, 6H, $3CH_2$ benzyl) ppm. $^{13}C\{H\}$ NMR (75 MHz, $CDCl_3$): δ 172.52 (t, $J_{(PC)}$= 7.1 Hz, C carbonyl), 133.93 (t, $J_{(PC)}$= 2.9 Hz, *ipso C*, benzyl), 130.53 (t, $J_{(PC)}$ = 2.3 Hz, *ortho C*, benzyl), 128.81 (s, *meta C*, benzyl), 127.01 (s, *para C*, benzyl), 30.53 (t, $J_{(PC)}$ = 13.3 Hz, CH_2, benzyl) ppm. $^{31}P\{H\}$ NMR (121 MHz, $CDCl_3$): δ -12.97 (s) ppm. TGA (on set of decomposition): 332 °C.

6.5.1.7 *cis,cis,trans*-$[OsBr_2(CO)_2\{P(CH_2C_6H_5)_3\}_2]$ (3b)

$(NH_4)_2[OsBr_6]$ (0.41 g, 0.58 mmol), 30 mL 2-ethoxyethanol and tribenzylphosphine (0.44 g, 1.44 mmol). Yield (0.33 g,56%). Anal. Calcd for $C_{40}H_{34}Br_2O_2OsP_2$: C, 52.08%; H, 4.17; Found: C, 51.93%; H, 4.10%. Solid IR ($\nu_{(CO)}$): 2023(s), 1953(s) cm^{-1}. Raman ($\nu_{(Os-X)}$): 216(vs), 189(vs) cm^{-1}. ^1H NMR (300 MHz, $CDCl_3$): δ 7.24 (dd, $J_{(HH)}$ = 6.5, 3.6 Hz, 18H, H-aromatic), 7.08 – 6.93 (m, 12H, H-aromatic), 3.72 (t, $J_{(HP)}$= 3.8 Hz, 12H, $3CH_2$ benzyl) ppm. $^{13}C\{H\}$ NMR (75 MHz, $CDCl_3$): δ 171.74 (t, $J_{(PC)}$ = 7.1 Hz, C carbonyl), 134.27 (t, $J_{(PC)}$ = 3.0 Hz, *ipso C*, benzyl), 130.46 (t, $J_{(PC)}$ = 2.3 Hz, *ortho C*, benzyl), 128.81 (s, *meta C*, benzyl), 127.00 (s, *para C*, benzyl), 32.16 (t, $J_{(PC)}$ = 13.7 Hz, CH_2 benzyl) ppm. ^{31} $P\{H\}$ NMR (121 MHz, $CDCl_3$): δ -23.17 (s) ppm. TGA (on set of decomposition): 299 °C.

6.5.1.8 *cis,cis,trans*-$[OsCl_2(CO)_2(PCy_3)_2]$ (4a)

$(NH_4)_2[OsCl_6]$ (0.30 g, 0.68 mmol), 2-methoxyethanol (40 mL) and tricyclohexylphosphine (0.48 g, 1.71 mmol). Yield (0.49 g, 67%.) Solid IR ($\nu_{(CO)}$): 2010 (s), 1933 (s) cm^{-1}. Raman ($\nu_{(Os-X)}$): 305(s), 281(s) cm^{-1}. ^1H NMR (300 MHz, $CDCl_3$): δ 2.61 (s, 6H), 2.15 (d, $J_{(HH)}$ =

12.8 Hz, 12H), 1.80 – 1.36 (m, 32H), 1.31 (t, $J_{(HH)}$ = 8.6 Hz, 16H) ppm. $^{13}C\{H\}$ NMR (75 MHz, $CDCl_3$): δ 176.91 (t, *J* = 7.3 Hz, carbonyl), 33.98 (t, $J_{(PC)}$ = 11.7 Hz, virtual triplet), 29.32(s), 27.64 (t, $J_{(PC)}$ = 5.1 Hz, virtual triplet), 26.30 Hz (s) ppm. ^{31} P{H} NMR (121 MHz, $CDCl_3$): δ -2.63(s) ppm. TGA (on set of decomposition): 306 °C.

6.5.1.9 *cis,cis,trans*-$[OsBr_2(CO)_2(PCy_3)_2]$ (4b)

$(NH_4)_2[OsBr_6]$ (2.04 g, 2.89 mmol), 70 mL 2-ethoxyethanol and tricyclohexylphosphine (3.39 g, 12.1 mmol) . Yield (2.57 g, 92 %). Solid IR ($\nu_{(CO)}$): 2012(s), 1939(s) cm^{-1}. Raman ($\nu_{(Os-X)}$): 221(vs), 189(m) cm^{-1}. ^{1}H NMR (300 MHz, $CDCl_3$): δ 2.66 (d, $J_{(HP)}$ = 11.8 Hz, 6H), 2.19 (d, $J_{(HH)}$ = 11.8 Hz, 6H), 1.93 – 1.48 (m, 16H), 1.43 – 1.16 (m, 8H) ppm. $^{13}C\{H\}$ NMR (75 MHz, $CDCl_3$): δ 175.66 (t, $J_{(PC)}$ = 7.3 Hz, C carbonyl), 34.89 (t, $J_{(PC)}$ = 11.8 Hz, virtual triplet), 29.66(s), 27.55 (t, $J_{(PC)}$ = 5.1 Hz, virtual triplet), 26.30 Hz (s) ppm. ^{31} P{H} NMR (121 MHz, $CDCl_3$): δ -10.57 (s) ppm. TGA (on set decomposition): 286 °C.

6.5.2 General procedure for $[OsX_2(P–P)_2]$ using microwave mediated synthesis

Excess diphosphine ligand and the hexahaloosmate, $[OsX_6]^{2-}$ (X = Cl, Br, I) (1.0 mmol) were placed in a 35 mL reaction vessel equipped with a magnetic stirrer bar. To this mixture 2-methoxyethanol (10 mL) was added and the reaction vessel was irradiated with microwaves at constant power of 200 W. A temperature of 80 °C was maintained for 15 min. A brown-yellow solution was filtered to remove any unreacted solid starting material. The solvent was removed under reduced pressure and the residue was washed with hexane. The product was obtained as a yellow product.

6.5.2.1 *cis*-$[OsCl_2(dppm)_2]$ (5a)

$(NH_4)_2[OsCl_6]$ (0.20 g, 0.46 mmol) and dppm (0.71 g, 1.87 mmol). Yield (0.19 g, 40%). Solid IR (cm^{-1}): 3055 (ν_{PhH}), 2913 (ν_{CH}), 1572 ($\nu_{C=C}$), 1090 (ν_{P-Ar}). ^{1}H NMR (300 MHz,

$CDCl_3$): δ 8.12 (s, 4H, H-aromatic), 7.69 (s, 2H, H-aromatic), 7.40 (d, $J_{(HH)}$ = 5.2 Hz, 6H, H-aromatic), 7.25 – 6.81 (m, 18H, H-aromatic), 6.72 (s, 4H, H-aromatic), 6.47 (s, 6H, H-aromatic), 5.90 (s, 2H, -CH_2-), 4.40 (s, 2H, -CH_2-). TGA (on set of decomposition): 370 °C.

6.5.2.2. *cis*-[$OsBr_2(dppm)_2$] (5b)

$(NH_4)_2[OsBr_6]$ (0.20 g, 0.28 mmol) and dppm (0.45 g, 1.17 mmol). Yield (0.10g, 91%). Solid IR (cm^{-1}): 3070 (ν_{PhH}), 2984 (ν_{CH}), 1572 ($\nu_{C=C}$), 1093 ($\nu_{P\text{-}Ar}$). ^{1}H NMR (300 MHz, $CDCl_3$): δ 8.22 (dd, $J_{(HH)}$ = 12.2, 5.3 Hz, 4H, H-aromatic), 7.94 (dd, $J_{(HH)}$ = 11.6, 5.7 Hz, 4H, H-aromatic), 7.48 – 6.92 (m, 20H, H-aromatic), 6.80 (dt, $J_{(HH)}$ = 14.0, 8.3 Hz, 8H), 6.68 – 6.56 (m, 4H, H-aromatic), 6.02 – 5.85 (m, 2H, -CH_2-), 4.87 – 4.69 (m, 2H, -CH_2-) ppm. ^{31}P{H} NMR (121 MHz, $CDCl_3$): -57.9 (t, $J_{(PP)}$ = 23.1 Hz), -72.8 (t, $J_{(PP)}$ = 23.1 Hz) ppm. TGA (on set of decomposition): 376 °C.

6.5.2.3 *cis*-[$OsI_2(dppm)_2$] (5c)

$K_2[OsI_6]$ (0.21 g, 0.20 mmol) and dppm (0.33 g, 0.86 mmol). Yield (0.17 g, 68%). Solid IR (cm^{-1}): 3045 (ν_{PhH}), 2913 (ν_{CH}), 1584 ($\nu_{C=C}$), 1090 ($\nu_{P\text{-}Ar}$). ^{1}H NMR (300 MHz, $CDCl_3$): δ 8.20 (dd, $J_{(HH)}$ = 12.2, 5.3 Hz, 4H, H-aromatic), 8.03 (dd, $J_{(HH)}$ = 8.2, 4.6 Hz, 4H, H-aromatic), 7.45 – 6.81 (m, 24H, H-aromatic), 6.70 (dt, $J_{(HH)}$ = 17.7, 7.4 Hz, 8H, H-aromatic), 6.19 – 6.02 (m, 2H, -CH_2-), 4.99 – 4.84 (m, 2H, -CH_2-) ppm. ^{31}P{H} NMR (121 MHz, $CDCl_3$): -64.4 (t, $J_{(PP)}$ = 2.3 Hz), - 83.5 (t, $J_{(PP)}$ = 22.3 Hz) ppm. TGA (on set of decomposition): 340 °C.

6.5.2.4 *trans*-[$OsCl_2(dppe)_2$] (6a)

$(NH_4)_2[OsCl_6]$ (0.21 g, 0.48 mmol) and dppe (0.77 g, 1.93 mmol). Yield (0.24 g, 48%). Solid IR (cm^{-1}): 3052 (ν_{PhH}), 2917 (ν_{CH}), 1585 ($\nu_{C=C}$), 1090 ($\nu_{P\text{-}Ar}$). ^{1}H NMR (300 MHz, $CDCl_3$):

δ 7.65 – 6.72 (m, 40H, H-aromatic), 2.29 (s, 8H, 2×-CH_2CH_2-). TGA (on set of decomposition): 347 °C.

6.5.2.5 *trans*-[$OsBr_2(dppe)_2$] (6b)

$(NH_4)_2[OsBr_6]$ (0.20 g, 0.28 mmol) and dppe (0.47 g, 1.18 mmol). Yield (0.27 g, 82%), Solid IR (cm^{-1}): 3071 (ν_{PhH}), 2922 (ν_{CH}), 1585 ($\nu_{C=C}$), 1088 ($\nu_{P\text{-}Ar}$). ^{1}H NMR (300 MHz, $CDCl_3$): δ 7.53 – 7.13 (m, 8H, H-aromatic), 7.10 (d, $J_{(HH)}$ = 28.5 Hz, 32H, H-aromatic), 2.30 (d, $J_{(HH)}$ = 64.1 Hz, 8H, 2 × -CH_2CH_2-) ppm. ^{31}P{H} NMR (121 MHz, $CDCl_3$): 29.5 (s) ppm. TGA (on set of decomposition): 325 °C.

6.5.2.6 *trans*-[$OsI_2(dppe)_2$] (6c)

$K_2[OsI_6]$ (0.21 g, 0.20 mmol) and dppe (0.34 g, 0.85 mmol). Yield (0.21 g, 81%). Solid IR (cm^{-1}): 3050 (ν_{PhH}), 2950 (ν_{CH}), 1583 ($\nu_{C=C}$), 1087 ($\nu_{P\text{-}Ar}$). ^{1}H NMR (300 MHz, $CDCl_3$): δ 7.35 – 7.16 (m, 12H, H-aromatic), 7.11 (d, $J_{(HH)}$ = 7.5 Hz, 12H, H- aromatic), 6.99 (dt, $J_{(HH)}$ = 14.9, 7.6 Hz, 16H, H-aromatic), 2.67 (s, 4H, -CH_2CH_2-), 2.12 (s, 4H, -CH_2CH_2-). ^{31}P{H} NMR (121 MHz, $CDCl_3$): δ 26.5 (s). TGA (on set of decomposition): 336 °C.

6.5.2.7 *trans*-[$OsCl_2(dppp)_2$] (7a)

$(NH_4)_2[OsCl_6]$ (0.20 g, 0.45 mmol) and dppp (0.77 g, 1.87 mmol). Yield (0.22, 44%). Solid IR (cm^{-1}): 3046 (ν_{PhH}), 2925 (ν_{CH}), 1588 ($\nu_{C=C}$), 1090 ($\nu_{P\text{-}Ar}$). ^{1}H NMR (300 MHz, $CDCl_3$): 7.64 – 7.50 (m, 15H, H-aromatic), 7.30 – 7.19 (m, 15H, H-aromatic), 7.14 (s, 18H, H-aromatic), 7.00 (s,12H, H-aromatic), 3.55 (s, 12H, -CH_2-) ppm. TGA (on set of decomposition): 289 °C.

6.5.2.8 *trans*-[$OsBr_2(dppp)_2$] (7b)

$(NH_4)_2[OsBr_6]$ (0.20 g, 0.28 mmol) and dppp (0.48 g, 1.16 mmol). Yield (0.14 g, 52%). Solid IR (cm^{-1}): 3047 (ν_{PhH}), 2912 (ν_{CH}), 1585 ($\nu_{C=C}$), 1091 ($\nu_{P\text{-}Ar}$). ^1H NMR (300 MHz, $CDCl_3$): δ 7.42 – 7.23 (m, 15H, H-aromatic), 7.08 (tt, $J_{(HH)}$ = 20.2, 7.2 Hz, 15H, H-aromatic), 6.88 (t, $J_{(HH)}$ = 7.6 Hz, 10H, H-aromatic), 3.16 – 2.99 (m, 6H, 3-CH_2-), 2.45 – 2.30 (m, 6H, 3-CH_2-) ppm. $^{31}P\{H\}$ NMR (121 MHz, $CDCl_3$): δ -25.3 (s) ppm. TGA (on set of decomposition): 279 °C.

6.5.2.9 *trans*-[$OsI_2(dppp)_2$] (7c)

$K_2[OsI_6]$ (0.20 g, 0.19 mmol) and dppp (0.32 g, 0.77 mmol). Yield (0.10 g, 42%). Solid IR (cm^{-1}): 3071 (ν_{PhH}), 2940 (ν_{CH}), 1585 ($\nu_{C=C}$), 1089 ($\nu_{P\text{-}Ar}$). ^1H NMR (300 MHz, $CDCl_3$): 7.48 – 7.15 (m, 10H, H-aromatic), 7.1 (d, $J_{(HH)}$ = 7.5, 15H, H-aromatic), 6.99 (dt, $J_{(HH)}$ = 14.9, 7.6 Hz, 15H), 2.67 (s, 6H, -CH_2-), 2.12 (s, 6H, -CH_2-) ppm. $^{31}P\{^1H\}$ NMR (121 MHz, $CDCl_3$): δ 32.4(s) ppm. TGA (on set of decomposition): 263 °C.

6.5.3 Preparation of triosmium clusters and phosphine substituted derivatives

6.5.3.1 Preparation of [$Os_3(CO)_{12}$] (9)

$(NH_4)_2[OsCl_6]$ (2.03 g, 4.62 mmol) and zinc (4.62 g, 88.37 mmol) were placed in an autoclave Teflon cup. Dry methanol (30 mL) was added and placed in the autoclave. The reaction mixture was purged three times with ca. 10 bar CO while stirring. Finally pressurized to 55 bar at 50 °C. After 24 h the autoclave was switched off and cooled to room temperature before venting the pressurized gas. Yellow crystalline material was filtered and washed with acetone. Yield (0.89 g, 64%). Anal Calc for $C_{12}O_{12}Os_3$: C, 15.89%; Found: C, 15.90%. IR (CH_2Cl_2) $\nu_{(CO)}$: 2067, 2037, 2015, 1995 cm^{-1}. Raman $\nu_{(CO)}$: 2127, 2068, 2025, 2002 cm^{-1}

6.5.3.2 Preparation of $Os_3(CO)_{12-n}(PR_3)_n$ ($PR_3 = PPh_3$, n = 2-3) via microwave.

A sample of $Os_3(CO)_{12}$ (0.20 g, 0.22 mmol) and triphenylphosphine (0.23 g 0.88 mmol) were placed in a 35 mL reaction vessel equipped with a magnetic stirrer bar . Acetonitrile (20 mL) was added and reaction mixture irradiated with microwaves at a constant power of 200 W and high stirring rate. A reaction temperature of 80 °C was maintained for 2 min. Upon cooling the crude product precipitated as an orange-red solid. TLC was performed with an eluent of 1.7:1 hexane: CH_2Cl_2 to give 0.20 g (67.0%) of orange $[Os_3(CO)_{10}(PPh_3)_2]$ (**11)**, Rf = 0.71, and 0.12 g (33.0%) of orange-red $[Os_3(CO)_9(PPh_3)_3]$ (**10)**, R_f = 0.44. The IR (CH_2Cl_2), ^1H NMR and $^{31}P\{H\}$ NMR of complex **9** were identical to those previously published.[5] Spectral data for **9**: IR (CH_2Cl_2) $\nu_{(CO)}$: 2084 (w), 2055(m), 2029(m), 1996(s), 1968(mw) cm^{-1}. Solid Raman $\nu_{(CO)}$: 2077(vs), 2029(w), 2020(m), 1991(s), 1967(s), 1959(s) cm^{-1}. ^1H NMR (300 MHz, $CDCl_3$): 7.51 – 7.27 (m, 30H, H-aromatic) ppm. $^{31}P\{H\}$ NMR (121 MHz, $CDCl_3$): δ -1.76 (s) ppm. Spectral data for **10:** IR (CH_2Cl_2) $\nu_{(CO)}$: 2067(w), 2049(w), 2023(m), 2019(m), 1996(m), 1987(mw), 1969(mw) cm^{-1}. Solid Raman $\nu_{(CO)}$: 2050 (s), 1989(vs), 1967 (vs), 1950 (m), 1924 (m), 1918 (mw) cm^{-1}. ^1H NMR (300 MHz, $CDCl_3$): 7.45 – 7.31 (m, 45H, H-aromatic) ppm. $^{31}P\{H\}$ NMR (121 MHz, $CDCl_3$): δ -2.29 (s) ppm.

6.5.3.2 Preparation of $[Os_3(CO)_{11}(dppm)]$ (12)

A sample of $[Os_3(CO)_{12}]$ (0.11 g, 0.12 mmol) and dppm (0.10 g, 0.26 mmol) were placed in a 35 mL glass reaction vessel equipped with magnetic stirrer bar. MeCN (10 mL) was added and the reaction mixture was irradiated with microwaves at constant power of 850 W. A temperature of 80 °C was maintained for 2 min. The yellow solution was obtained. The solvent was removed under reduced pressure and residue washed with hexane 3 × 10 mL. Yield (0.09 g, 60%). IR (CH_2Cl_2) $\nu_{(CO)}$: 2074(w), 2069(mw), 2057(m), 2020(m), 1999(m), 1974(w) cm^{-1}. ^1H NMR (300 MHz, $CDCl_3$): 7.90 – 6.60 (m, 20H, H-aromatic), 4.82 (d, *J* =

7.8 Hz, 2H, -CH_2-) ppm. $^{31}P\{H\}$ NMR (121 MHz, $CDCl_3$): δ -20.25 (dd, J_{PC} =49.1 Hz), -23.60 (dd, J_{PC} = 49.1 Hz) ppm.

6.6 References

(1) Chirariwa, H.; Muzenda In *Int'l Conf. on Chemical Engineering and Advanced Computational Technologies* Pretoria (South Africa), 2014, p 31.

(2) Eloff, J. N. *Planta. Medica.* **1998**, *64*, 711.

(3) Masoko, P.; Picard, J.; Eloff, J. N. *J. Ethnopharmacol.* **2005**, *99*, 301.

(4) Skehan, P.; Soreng, R.; Scudiero, D.; Monks, A.; McMahon, J.; Vistica, D.; Warren, J. T.; Bokesch, H.; Kennet, S.; Boyd, M. R. *J. Natl. Cancer Inst.* **1990**, *82*, 1107.

(5) Leadbeater, N. E. *J. Org. Chem.* **1999**, *573*, 211.